การผลิตไบโอดีเซลโดยปฏิกิริยาไฮโดรโพรเซสซิงจากน้ำมันปาล์มที่ใช้แล้วโดยใช้ตัวเร่งปฏิกิริยานิกเกิลโมลิบดินัมและโคบอลต์โมลิบดินัมคาร์ไบด์บนอะลูมินา

นายชัยยศ คงวัฒนกุล

วิทยานิพนธ์นี้เป็นส่วนหนึ่งของการศึกษาตามหลักสูตรปริญญาวิศวกรรมศาสตรมหาบัณฑิต

สาขาวิชาวิศวกรรมเคมี ภาควิชาวิศวกรรมเคมี

คณะวิศวกรรมศาสตร์ จุฬาลงกรณ์มหาวิทยาลัย

ปีการศึกษา 2553

BIODIESEL PRODUCTION WITH HYDROPROCESSING PROCESS FROM WASTE COOKING PALM OIL OVER Ni-Mo/Al_2O_3 AND Co-Mo/Al_2O_3 CARBIDES CATALYSTS

Mr. Chaiyod Kongwattanakul

A Thesis Submitted in Partial Fulfillment of the Requirements

for the Degree of Master of Engineering Program in Chemical Engineering

Department of Chemical Engineering

Faculty of Engineering

Chulalongkorn University

Academic Year 2010

Thesis Title	BIODIESEL PRODUCTION WITH HYDROPROCESSING PROCESS FROM WASTE COOKING PALM OIL OVER Ni-Mo/Al_2O_3 AND Co-Mo/Al_2O_3 CARBIDES CATALYSTS
By	Mr. Chaiyod Kongwattanakul
Field of Study	Chemical Engineering
Thesis Advisor	Professor Suttichai Assabumrungrat, Ph.D.
Thesis Co-advisor	Assistant Professor Worapon Kiatkittipong, D.Eng.

Accepted by the Faculty of Engineering, Chulalongkorn University in Partial Fulfillment of the Requirements for the Master's Degree

…… Dean of the Faculty of Engineering
(Associate Professor Boonsom Lerdhirunwong, Dr.Ing.)

THESIS COMMITTEE

……Chairman
(Associate Professor Muenduen Phisalaphong, Ph.D.)

……Thesis Advisor
(Professor Suttichai Assabumrungrat, Ph.D.)

……Thesis Co-Advisor
(Assistant Professor Worapon Kiatkittipong, D.Eng.)

……Examiner
(Associate Professor Bunjerd Jongsomjit, Ph.D.)

……External Examiner
(Peangpit Wongmaneenil, D.Eng.)

ชัยยศ คงวัฒนกุล : การผลิตไบโอดีเซลโดยปฏิกิริยาไฮโดรโพรเซสซิงจากน้ำมันปาล์มที่ใช้แล้วโดยใช้ตัวเร่งปฏิกิริยานิกเกิลโมลิบดินัมและโคบอลต์โมลิดิบนัมคาร์ไบด์บนอะลูมินา (BIODIESEL PRODUCTION WITH HYDROPROCESSING PROCESS FROM WASTE COOKING PALM OIL OVER Ni-Mo/Al_2O_3 AND Co-Mo/Al_2O_3 CARBIDES CATALYSTS) อ. ที่ปรึกษาวิทยานิพนธ์หลัก: ศ.ดร. สุทธิชัย อัสสะบำรุงรัตน์, อ. ที่ปรึกษาวิทยานิพนธ์ร่วม: ผศ.ดร.วรพล เกียรติกิตติพงษ์, 113 หน้า.

ไฮโดรโพรเซสซิงของน้ำมันพืชเป็นกระบวนการสำหรับการผลิตไบโอดีเซลแทนที่ปฏิกิริยาทรานเอสเทอร์ริฟิเคชัน ในงานวิจัยนี้ น้ำมันปาล์มที่ผ่านการใช้แล้วถูกใช้เป็นสารตั้งต้นเพื่อลดราคาของวัตถุดิบ นิกเกิลโมลิบดินัมและโคบอลต์โมลิดิบนัมบนอะลูมินาเตรียมด้วยวิธีเคลือบฝังร่วม เตรียมการซัลไฟต์เดชันหรือคาร์บูไรเซชัน ดำเนินการที่อุณหภูมิ 380 องศาเซลเซียส ความดันไฮโดรเจน 50 บาร์และเวลาในการทำปฏิกิริยา 6 ชั่วโมงพบว่าเหมาะสมที่ให้ร้อยละผลได้ดีเซลสูงสุด ร้อยละผลได้ของดีเซลสูงสุดคือ 71.8% สามารถพบได้โดยใช้ตัวเร่งปฏิกิริยานิเกิลโมลิบดินัมบนอะลูมินาซัลไฟต์ ตัวเร่งปฏิกิริยาซัลไฟต์แสดงร้อยละผลได้ของดีเซลสูงกว่าตัวเร่งปฏิกิริยาคาร์ไบด์เล็กน้อย อย่างไรก็ตาม ตัวเร่งปฏิกิริยาคาร์ไบด์ดีกว่าตัวเร่งปฏิกิริยาซัลไฟต์เนื่องจากสามารถนำกลับมาใช้ใหม่ได้หลังจากการบำบัดขั้นต้น ตัวเร่งปฏิกิริยาคาร์ไบด์ที่ใช้แล้ว ประสิทธิภาพของตัวเร่งปฏิกิริยาที่ผ่านการบำบัดขั้นต้นใกล้เคียงกับตัวเร่งปฏิกิริยาคาร์ไบด์ใหม่ ในขณะที่ตัวเร่งปฏิกิริยาซัลไฟต์ที่ผ่านการบำบัดขั้นต้นได้สูญเสียความว่องไว ผลิตภัณฑ์ของเหลวและแก๊สถูกพบโดยแสดงสิ่งนั้นด้วยเส้นทางปฏิกิริยาไฮโดรดีคาบอกซีเลชันและปฏิกิริยาไฮโดรดีคาบอนิซีเลชันเหนือกว่าปฏิกิริยาไฮโดรดีออกซีจิเนชัน

ภาควิชา .....วิศวกรรมเคมี.....	ลายมือชื่อนิสิต .....
สาขาวิชา .....วิศวกรรมเคมี.....	ลายมือชื่อ อ. ที่ปรึกษาวิทยานิพนธ์หลัก .....
ปีการศึกษา .....2553.....	ลายมือชื่อ อ.ที่ปรึกษาวิทยานิพนธ์ร่วม ……

5270268021: MAJOR CHEMICAL ENGINEERING

KEYWORDS: HYDROPROCESSING / WASTE COOKING PALM OIL / SULPHIDATION / CABURIZATION

CHAIYOD KONGWATTANAKUL: BIODIESEL PRODUCTION WITH HYDROPROCESSING PROCESS FROM WASTE COOKING PALM OIL OVER Ni-Mo/Al_2O_3 AND Co-Mo/Al_2O_3 CARBIDES CATALYSTS. ADVISOR: PROF. SUTTICHAI ASSABUMRUNGRAT, Ph.D., CO-ADVISOR: ASST. PROF. WORAPON KIATKITTIPONG, D.Eng., 113 pp.

Hydroprocessing of vegetable oil has been known as a process for biodiesel production to replace trans-esterification. In this research, waste cooking palm oil (WCPO) is used as a starting feedstock to reduce a cost of raw-material. Ni- and Co-Mo/Al_2O_3 prepared by co-impregnation method were pretreated by sulphidation or carburization. The operating temperature of 380°C, hydrogen pressure of 50 bar and reaction time of 6 h was found suitable to maximize the diesel range yield. The highest yield of 71.8% can be obtained by Ni-Mo/Al_2O_3 sulphided catalyst. Sulphided catalyst shows slightly higher diesel yield than that of carbide catalyst; however, the strong beneficial of carbide catalyst over sulphided catalyst are higher reusability. After pretreatment the used carbide catalyst, the catalytic performance becomes comparable to the fresh carbide catalyst while the regenerated sulphided catalysts are still suffered from activity loss. The liquid and gas product distribution shows a conform results which indicated that hydrodecarboxylation and hydrodecarbonylation reaction pathways are dominated over hydrodeoxygenation.

Department : ……Chemical Engineering……	Student's Signature ……
Field of Study : ……Chemical Engineering……	Advisor's Signature ……
Academic Year : ……2010……	Co-advisor's Signature ……...

ACKNOWLEDGEMENTS

First of all, the author would like to express my sincere and deepest appreciation to my advisor and co-advisor, Professor Suttichai Assabumrungrat and Assistant Professor Worapon Kiatkittipong for their invaluable suggestions, support, encouragement, and help during the course of my graduate study. Without the continuous guidance and comments from Professor Piyasan Praserthdam, this work would never have been achieved. In additional, the author would also be grateful to Associate Professor Muenduen Phisalaphong, as the chairman, Associate Professor Bunjerd Jongsomjit, and Dr. Peangpit Wongmaneenil as the members of the thesis committee.

Most of all, the author would like to express his highest gratitude to his parents who always pay attention to him all the times for their suggestions and have provided support and encouragements. The most success of graduation is devoted to his parents.

Moreover, the author wishes to thank the members of the Center of Excellence on Catalysis and Catalytic Reaction Engineering, Department of Chemical Engineering, Faculty of Engineering, Chulalongkorn University and the member of Chemical Engineering Laboratory for their friendship, assistance and special thank Mr. Watcharapong Khaodee, Mr. Jakrapan Janlamool and Mr. Natpakan Srisawad. To the many others, not specifically named, who have provided his with support and encouragement, please be assured that he thinks of you.

Finally, the author would like to thank the Thailand Research Fund (TRF), as well as the Graduate School of Chulalongkorn University for their financial supports.

CONTENTS

Page

CHAPTER

Page

CHAPTER

Page

CHAPTER

LIST OF TABLES

TABLE Page

LIST OF FIGURES

FIGURE Page

FIGURE Page

CHAPTER I

INTRODUCTION

1.1Rationale

Presently, the production of renewable fuels has been expanding worldwide for energy and environmental securities. Biodiesel is a promising alternative in renewable fuels production because it decreases amounts of carbon dioxide; moreover, decrease dependence on fossil fuels, and improved the rural economics and so on (Donnis et al., 2009; Huber et al., 2010; Meng et al., 2008). A conventional method for producing biodiesel is trans-esterification of vegetable oils. Triglycerides of vegetable oils are reacted with an alcohol mostly methanol (or ethanol), from which fatty acid methyl esters (FAME) is obtained as a main product while glycerol is obtained as a by-product. However, the obtained glycerol is in excess of demand thus alternative ways to utilize glycerol have been recently suggested (Kiatkittipong et al., 2010). However, the stability and cetane number of FAME has been mainly an obstacle for being mixed with fossil diesel fuels (Donnis et al., 2009). In generally, limitation of FAME for blending in fossil diesel fuel is at 7 wt% because the car manufactures observed filter plugging from the tank to the engine (Mikulec et al., 2010; Simacek et at., 2010). Therefore the use of FAME as "1st generation biodiesel" still has a limitation to substitute fossil diesel.

Recently, hydroprocessing of vegetable oil has been known as a process for biodiesel production to replace FAME from trans-esterification, it is so called "2nd generation biodiesel". The primary advantages of this biodiesel production over 1st generation biodiesel technology are: the obtained hydrocarbon fuels are similar to fossil diesel fuel, the propane by-product is preferable over glycerol by-product, the cetane number is greater, and capital costs and operating costs are lower (Walendziewski et al., 2009; Guzman et al., 2010).

Palm oil, the most potential feedstock in Thailand, was considered in this study. The lower cost of raw material leads to the lower cost of biodiesel

production. Therefore, in this study, waste cooking palm oil (WCPO) is used as a starting feedstock instead of fresh palm oil (FPO) in order to reduce cost of raw-material and environmental burden to treat it.

The conventional hydrodesulfurization catalysts i.e. $NiMo/Al_2O_3$ and $CoMo/Al_2O_3$ are presently employed as a catalyst for hydroprocessing of vegetable oil for 2nd genenation biodiesel production. It is worthy to note that the WCPO contained higher concentrations of sulfur and nitrogen than those of FPO (Bezergianni and Kalogianni, 2009).

In addition, $NiMo/Al_2O_3$, $CoMo/Al_2O_3$ carbide catalyst showed higher activites per surface area in hydrodenitrogenation (HDN) and hydrodesulfurization (HDS) reactions than that of $NiMo/Al_2O_3$ and $CoMo/Al_2O_3$ sulphided catalysts (Diaz et al., 2003; Izhar et al., 2006; Ramanathan and Oyama 1995; Schwartz et al., 2000; Sundaramurthy et al., 2007). Therefore, we will also investigate the possibility of using $NiMo/Al_2O_3$, $CoMo/Al_2O_3$ carbide catalyst comparing with conventional sulphided catalyst for hydroprocessing of WCPO. In the United States estimated that around 100 million gallons of waste cooking oil is produced per day (Radich, 2006). The estimated amount of waste cooking oil in Europe is about 700,000–1,000,000 tons/year (Supple et al., 2002). We expected that the knowledge obtained from this study e.g. pre-treatment of WCPO, the suitable catalyst and operating condition of hydroprocessing of WCPO could be adaptable or applicable for hydroprocessing of others waste cooking oil.

In this study, hydroprocessing of WCPO was performed in a shaking batch reactor under operating temperature of 360, 380, 400 and 420 ˚C, hydrogen pressure of 50 bar, reaction time 2-8 h catalyzed by $NiMo/Al_2O_3$, $CoMo/Al_2O_3$ sulphided catalysts and $NiMo/Al_2O_3$, $CoMo/Al_2O_3$ carbide in-house prepared catalysts. Liquid reaction products are hydrocarbons whose main components were identified as C_{15} - C_{18} alkanes. The yield of diesel (range 250 – 380 ˚C) is calculated from simulated distillation following by ASTM-2887-D86 procedure. It can be concluded that the products are suitable for diesel fuel blending. Influence of operating condition and catalyst on the product compositions in the case of WCPO as starting materials is also discussed (Filho et al., 1993).

1.2 Objective

To find suitable catalyst and appropriated operating condition for biodiesel production via hydroprocessing of waste cooking palm oil (WCPO).

1.3 Research scopes

1. Prepared bimetallic $NiMo/Al_2O_3$, $CoMo/Al_2O_3$ sulphided catalysts and Ni-Mo/Al_2O_3, Co-Mo/Al_2O_3 carbides catalysts with characterization including Brunauer-Emmett-Teller (BET) surface area analysis, X-ray diffraction (XRD), carbon monoxide chemisorptions (CO-Chemisorptions), temperature-programmed reduction of hydrogen (H_2-TPR) and thermal gravimetric analysis (TGA).

2. Perform the experiment of hydroprocessing of WCPO in a shaking batch reactor under operating temperature of 360, 380, 400 and 420 ˚C, hydrogen pressure of 50 bar, reaction time of 2-8 h catalyzed by $NiMo/Al_2O_3$, $CoMo/Al_2O_3$ sulphided and $NiMo/Al_2O_3$, $CoMo/Al_2O_3$ carbide in-house prepared catalysts.

3. The product composition was analyzed by using gas chromatography with thermal conductivity detector (TCD), flame ionization detector (FID) and yield of diesel range is calculated form simulated distillation following by ASTM-2887-D86.

1.4 Research Methodology

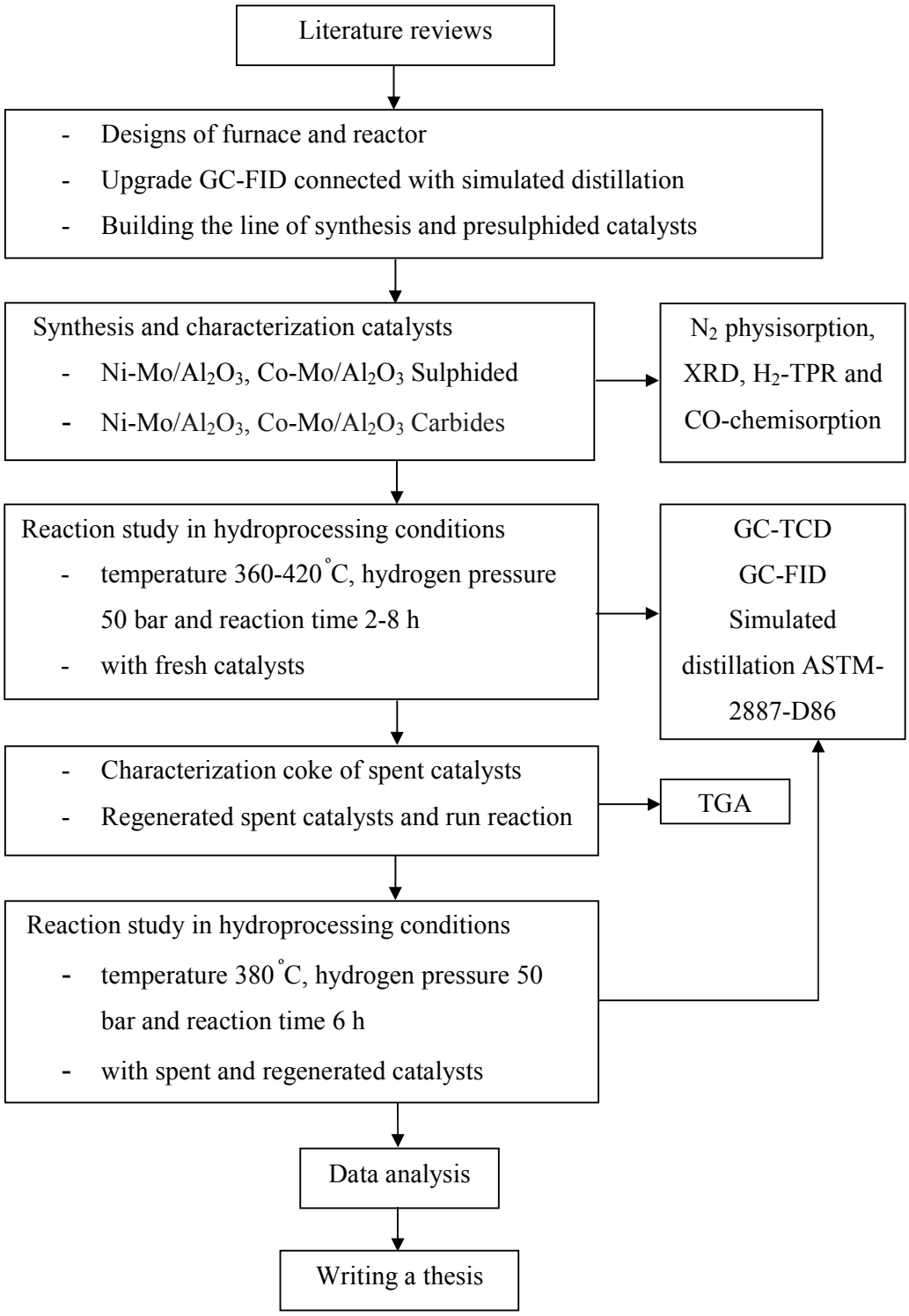

CHAPTER II

THEORY

This chapter presents background information of hydroprocessing of vegetable oil mechanism, raw-material for biodiesel production, properties of diesel production, simulated distillation method and metal carbides and nitrides catalysts.

2.1 Mechanism of hydroprocessing

Hydroprocessing involves several simultaneous reactions, such as hydrodenitrogenation (HDN), hydrodesulfurization (HDS), hydrodeoxygenation (HDO), hydrogenation (HYD) and hydrodemetallization (HDM). Mutual effects of these reactions depend on the origin of feed, operating conditions and the type of catalyst (Furimsky 2003).

The overall reaction pathway for conversion of triglycerides into alkanes is shown in Figure 2.1 In the first step of this reaction pathway, double bonds of triglycerides is

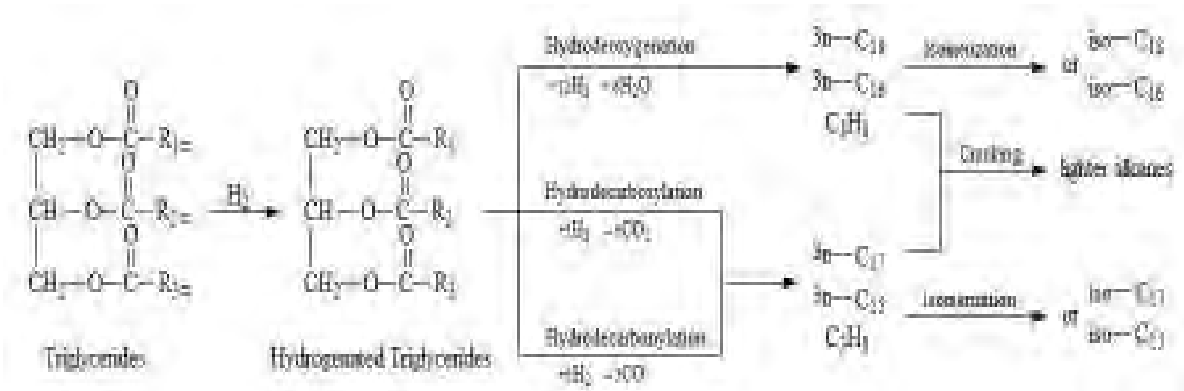

Figure 2.1 The reaction pathway overall of triglycerides to alkanes.

hydrogenated and preceded by other reactions which are broken down into various intermediates by hydroprocessing process. During this process the unsaturated chains of fatty acids are hydrogenated and become saturated while the structure of triglycerides remains unchanged (Simacek et al., 2010). In the second step, the list is not exhaustive; rather, it represents the dominant reactions for the final products because this reaction is very complex.

There are mainly three pathways for hydroprocessing of triglycerides (Huber et al., 2007; Mikulec et al., 2010) including hydrodeoxygenation (hydrogenation/dehydration), decarboxylation, and decarbonylation. The other reactions which involve this process are water gas shift and methanization as well as isomerization and cracking that can be described as follows

2.1.1 Hydrodeoxygenation (hydrogenation/dehydration)

Hydrodeoxygenation (HDO) is a hydrogenolysis process that remove oxygenated compounds from the organic molecule in reaction with hydrogen froming water using commercial hydrotreating catalysts. There is commonly used Ni-Mo or Co-Mo on γ-Al_2O_3, zeolites (ZSM-5), Pd or Pt on carbon as well as alumina. Ni-Mo sites for hydrogenation reactions and acid catalytic sites for dehydration reactions. The summarized reactions are showed as follows in Figure 2.2.

The carboxylic acids as a reactant which is hydrogenated can be converted into Aldehyde and water. The aldehyde compound is enolized because α-hydrogen can be isomerized to the enol from, which is the reactive intermediate. On the contrary, compounds

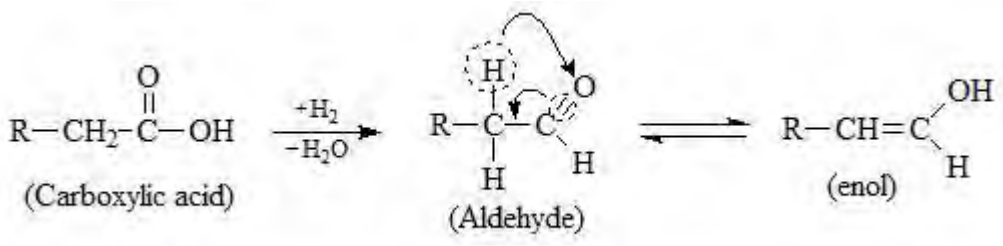

Figure 2.2 Reaction pathway of carboxylic acid to enol form.

lacking α-hydrogen cannot be isomerized to the enol form (Donnis et al., 2009).

In Figure 2.3 shown the enol form could either be hydrogenated over the catalyst at the highly reactive oxygen, at the C=C double forming alcohol or forming 1-alkene and water. The alcohol which is dehydrated can be converted into alkane and water. The alkene which is hydrogenated at C=C double can be converted to alkane (Donnis et al., 2009).

If the triglycerides which have no double bond are converted by the hydrodeoxygenation route. The products for this mechanism are water, propane and three normal alkanes of the full length of fatty acid chains in Figure 2.4. By this reaction, one mole of triglyceride reacts with 12 moles of hydrogen. The products are forms one mole of propane, six moles of water, and three moles of a normal alkanes of the full length of fatty acid (Donnis et al., 2009; Mikulec et al., 2010).

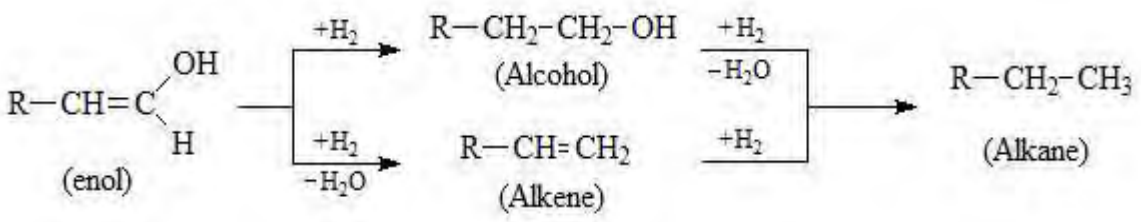

Figure 2.3 Reaction pathway of enol from to alkane.

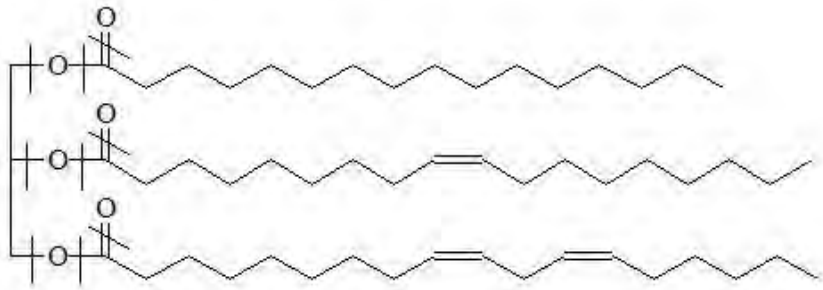

Figure 2.4 Mechanism of the hydrodeoxygenation reaction pathway for the removal of triglyceride oxygen.

2.1.2 Hydrodecarboxylation

The decarboxylation is a chemical reaction which releases carbon dioxide (CO_2). Generally, decarboxylation refers to a reaction of carboxylic acids, removing a carbon atom from a carbon chain and no hydrogen required to convert a carboxylic acid group to an alkane.

If the triglycerides which have no double bond are converted by the decarboxylation route. The products of this mechanism are carbon dioxide, propane and three normal alkanes with carbon numbers one less than fatty acid chains in Figure 2.5. By this reaction, one mole of triglyceride reacts with 3 moles of hydrogen. The products are forms one mole of propane, three moles of carbon dioxide and three moles of a normal alkanes one carbon atom shorter than the full length of fatty acid (Donnis et al., 2009; Mikulec et al., 2010).

2.1.3 Hydrodecarbonylation

The decarbonylation is chemical reaction which the carboxylic group is reacted with hydrogen for removal one or more carbonyl groups from a molecule to produce a methyl group, carbon monoxide and water.

If the triglycerides which have no double bond are converted by the decarbonylation route. The products for this mechanism are carbon monoxide, water, propane and three normal alkanes with carbon numbers one less than fatty acid chains in Figure 2.6. By this reaction, one mole of triglyceride reacts with 6 moles of hydrogen.

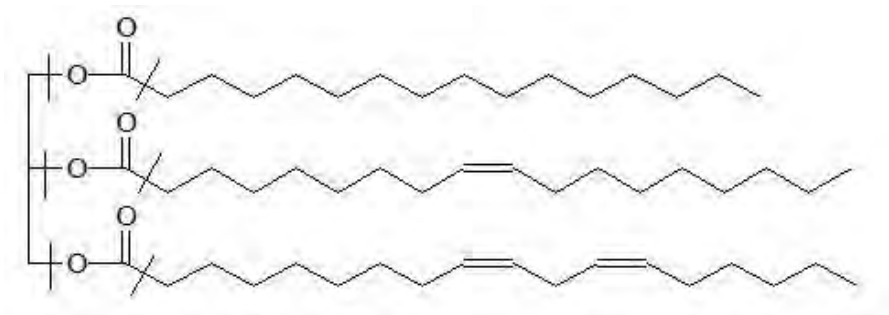

Figure 2.5 Mechanism of the hydrodecarboxylation reaction pathway for the removal of triglyceride oxygen.

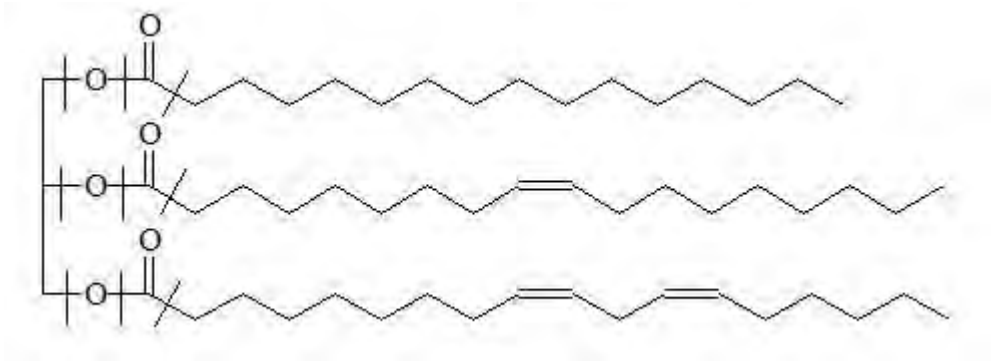

Figure 2.6 Mechanism of the hydrodecarbonylation reaction pathway for the removal of triglyceride oxygen.

The products are forms one mole of propane, three moles of carbon monoxide, three moles of water and three moles of a normal alkanes one carbon atom shorter than the full length of fatty acid (Donnis et al., 2009; Mikulec et al., 2010).

2.1.4 Isomerization and cracking

The normal alkanes produced from triglyceride can undergo isomerization and cracking to produce isomerized and lighter alkanes, respectively. The normal alkanes have a high cetane number, which is a good for diesel production. If the normal alkanes are desired then the isomerization and cracking reactions should be minimized (Huber et al., 2007).

2.1.5 Water gas shift and Methanization

$$CO_2 + H_2 \longleftrightarrow CO + H_2O \qquad (2.1)$$

$$CO + 3H_2 \longrightarrow CH_4 + H_2O \qquad (2.2)$$

The carbon monoxide and carbon dioxide are formed, there are two additional reactions. These are water gas shift and methanization. The water gas shift is a chemical reaction in which carbon dioxide reacts with hydrogen to form carbon monoxide and water vapor as shown in Eq. 2.1. The methanization is converted carbon monoxide from water gas reaction reacting with hydrogen into methane and water vapor as shown in Eq. 2.2. The both reactions are influence the hydrogen consumption and product yields (Mikulec et al., 2010).

2.1.6 Hydrodesulfurization

Hydrodesulfurization is catalytic hydrogenation processes which remove sulfur in petroleum. The hydrodesulfurization process had been developed in the 1960s to remove high concentration of sulfur in fuel (Kabe, 1999). The main aims of hydrodesulfurization are to prevent poisoning of sulfur-sensitive metal catalysts used in subsequent reactions and the catalytic converter in an automobile, to remove the unpleasant odor, to minimize the amount of sulfur oxides introduced into the atmosphere (contribution to acid rain) by combustion of petroleum-based fuels in catalytic cracking to meet environmental restrictions and to reduce corrosion problem in the refining process.

The hydrodesulfurization reaction generally proceeds through two parallel pathways. The first assumes that hydrogenation of the unsaturated heterocycle to a saturated (or partially saturated) species is followed by hydrogenolysis, while the second postulates that hydrogenolysis occurs first and that the product moieties are hydrogenated in subsequent steps.

Two reactions which occurred in hydrodesulfurization process are:

(I) hydrogenation of unsaturated compounds that occurs during hydrodesulfurization, and the reaction rates are significant compared with those of hydrodesulfurization;

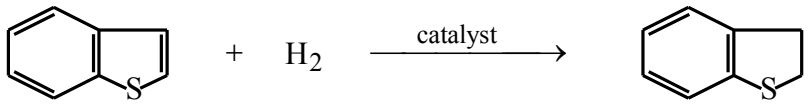

(II) hydrogenolysis which results in cleavage of a C-S bond;

$$R-SH + H_2 \longrightarrow RH + H_2S$$

Under industrial reaction conditions, hydrogenolysis reaction resulting in breaking of C-C bonds also occurs, e.g., the hydrocracking reaction.

The hydrodesulfurization reactions are virtually irreversible at temperatures and pressures ordinarily applied, roughly 300 to 450°C and up to 200 atm. The reactions are exothermic with heats of reaction of the order of 10 to 20 kcal/mol of hydrogen consumed. Coking reactions occur as well in hydrodesulfurization. Coke not only poisons catalyst surfaces but also contributes to blocking of catalyst pores and fixed-bed interstices (Gates, 1979).

2.1.6.1 Dibenzothiophene

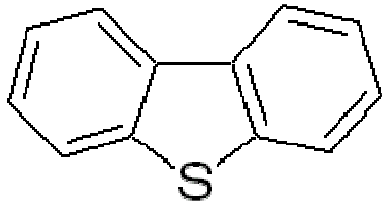

Dibenzothiophene (DBT; $C_{12}H_8S$) is a sulfur-containing high molecular weight polycyclic hydrocarbon (PAH) and colourless crystals. Its molecular weight, density, melting and boiling points are 184.26 g/mol, 1.252 g/cm^3, 97-99°C and 332-333°C, respectively.

DBT is a very persistent compound as compared to most PAHs and other aromatic hydrocarbons. It can be found after 10 years in sediment polluted with crude oil, long after most aromatics had disappeared. In some cases, crude oil may contain significant amounts of DBT and homologous series of its alkylated forms. Over 200 sulfur-containing organic compounds, classified as thiols, sulfides, thiophenes and

substituted benzothiophenes and DBT (Williams, 1986; Collier, 1995). In Texas oils, up to 70% of the organic sulfur is present as DBTs, whereas up to 40% of the organic sulfur present in the Middle East oils is the alkyl-substituted benzothiophenes and DBT. DBT can be formed in the catalytic reforming process for benzene and diesel oil production. Therefore, removal of elemental sulfur and sulfur compounds from crude oil prior to the refinery can be an advantage. In general, PAHs are associated with chronic risks. Acute toxicity of DBT has been rarely reported in human, fish or wildlife as a result of exposure to low levels of a single PAH compound (Yanik, 2003; Shemer, 2007).

2.1.6.2 Reaction pathways for dibenzothiophene

Two major pathways to desulfurized products have been proposed, the first one is called direct desulfurization (DDS) and the second one is usually referred to as the hydrogenation route (HYD). In the DDS pathway, the sulfur atom is removed from the structure and replaced by hydrogen, without hydrogenation of any of the other carbon–carbon double bonds. On the other hand, in the HYD route, also shown in Figure 2.7, it is assumed that at least one aromatic ring is hydrogenated before the sulfur atom is removed. Desulfurization of DBT yielded three organic products: biphenyl (BP), product of direct desulfurization route, cyclohexylbenzene (CHB) and bicyclohexane (BCH), products of hydrogenation route.

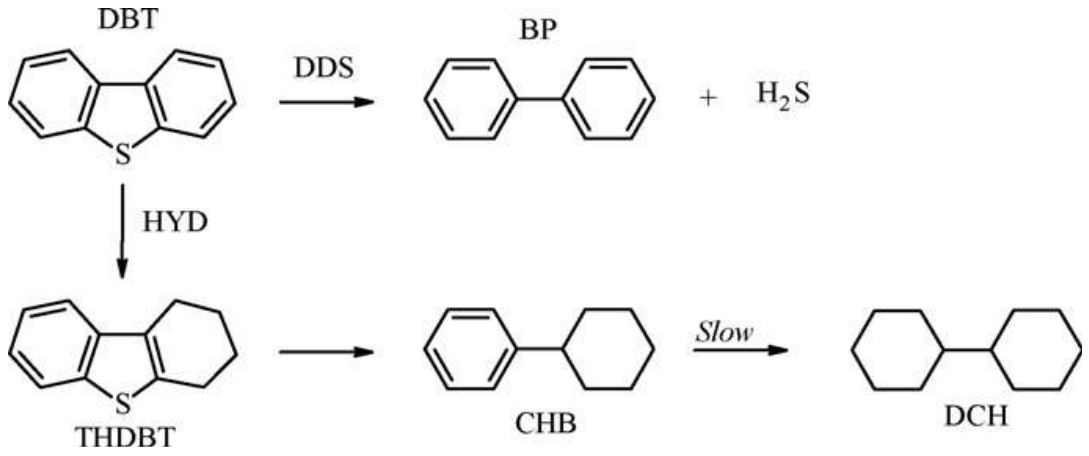

Figure 2.7 Reaction scheme for DBT. (Isidoro, 2008)

2.2 Raw-material

Triglycerides present in vegetable oils or animal fats are suitable as the raw material for producing high quality engine fuel. It has high molecular weight and low volatility (Mikulec et al., 2010). Vegetable oil is mostly use in the cooking process at present with various types available such as rapeseed oil, palm oil, sunflower oil, soybean oil, tall oil, and so on. Palm oil is most readily used so the majority amount of waste oil is palm oil. This oil is a good renewable resource for producing biodiesel fuel. However, the waste palm oil from cooking contains some impurities such a food particles, phospholipids, grease, wax and water (Meng et al., 2008), which are required to be removed before the hydroprocessing process (Banerjee and Chakraborty, 2009). Both fresh vegetable oil and waste vegetable oil have the triglycerides or fatty acids which are used to produce straight chain alkanes ranging from n-C_{15}-n-C_{18}. The fatty acids ranging from C_{16}-C_{18} may be is suitable for producing diesel fuel. The fatty acids compositions in vegetable oils are shown in Table 2.1.

2.2.1 Heteroatom compounds in waste cooking palm oil

Waste cooking palm oil (WCPO) feedstocks contain amounts of sulfur, nitrogen, and oxygen, which form to heteroatom compounds. Sulfur can be found in a variety of food, including kale, cabbage, cauliflower, horseradish, cranberries, meat, nuts, seeds, milk, fish, egg yolks, onion, garlic, as well as condiments including mustard power according to Healthyeatingclub.com. A sulfur compounds found in petroleum or synthetic oils are generally classified into two types: nonheterocycles and heterocycles. The former comprises thiols, sulfides and disulfides. The heterocycles are mainly composed of thiophenes, benzothiophenes and dibenzothiophenes. Petroleum fuels, especially diesel fuel contain a high level of various heterocyclic-organosulfur compounds.

Sulfur is the heteroatom most frequently formed in crude oils. Sulfur concentrations can range from 0.1 to more than 3 weight percent. Moreover, this content is correlated with the gravity of the crude oil, its quality (light or heavy) and its sources.

Table 2.1 Fatty acids compositions of vegetable oils (100 wt% basis).
(J.Mikulec et al. 2010; Sebos et al., 2009)

Fatty acid	Rapeseed oil, refined	Sunflower oil, refined	Crude palm oil	Rapeseed (Canola)	Coconut	Cotton seed oil	Lard
C 8: 0	-	-	-	-	-	-	-
C 10: 0	-	-	-	-	-	-	-
C 12: 0	-	-	-	-	-	-	-
C 14: 0	0.06	-	1.1	-	-	-	1.5
C 14: 1	-	-	-	-	-	-	-
C 16: 0	4.64	9	43.5	4.7	91	22.96	31.2
C 16: 1	0.24	-	-	-	-	0.9	-
C 18: 0	11.96	6	4.3	1.8	-	2.3	16.5
C 18: 1	63.47	26	39.8	63.0	6	16.7	42
C 18: 2	20.01	50	9.3	20	3	55.42	6.6
C 18: 3	6.97	7	0.5	8.6	-	0.2	-
C 20: 0	0.6	-	-	-	-	-	-
C 20: 1	1.18	-	-	1.9	-	-	-
C 22: 0	0.15	-	-	-	-	-	-
C 22: 1	0.07	-	-	-	-	-	-
C 24: 0	0.13	-	-	-	-	-	-
C 24: 1	0.14	-	-	-	-	-	-

The sulfur compounds found in petroleum or synthetic oils are generally classified into one of two types: heterocycles and nonheterocycles. The latter comprises thiols, sulfides and disulfides. Heterocycles are mainly composed of thiophenes with one to several rings and their alkyl or aryl substituents. Examples of sulfur compounds are shown in Table 2.2

Table 2.2 Examples of the sulfur compounds found in petroleum. (Kabe, 1999)

Compound class	**Structure**
Thiols (mercaptane)	RSH
Disulfides	RSSR’
Sulfides	RSR’
Thiophene	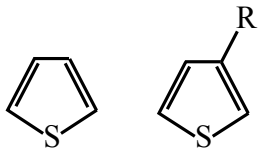 etc.
Benzothiophene	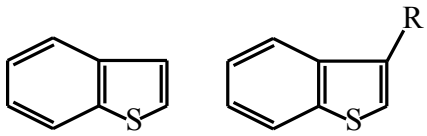 etc.
Dibenzothiophene	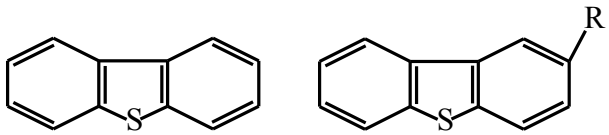 etc.

Nitrogen compounds included in the feedstocks are divided to two types: heterocycles and nonheterocycles. Some of those are shown in Figure 2.8 Heterocyclic nitrogen compounds can be divided into basic compounds and nonbasic compounds. Basic nitrogen compounds include six-membered ring heterocycles such as pyridine, quinoline and acridine. Nonbasic nitrogen compounds include five-membered ring heterocycles such as pyrrole, indole and carbazole (Kabe, 1999).

Crude oil is passed through several operations designed to separate it into fractions, to convert the certain fractions from the primary distillation (usually material of high molecular weight) to products of greater market and to purify the products, especially to remove the sulfur compounds. Many of the products made by the process of separation and conversion need further treatment by hydrotreating, before they can be distributed for use. Not only is good technical performance in an appliance needed but color, smell, stability on storage are all important and the removal, or limitation, of constituents harmful in use is also desirable (Macrae, 1966).

Basic nitrogen compounds

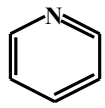

Pyridine

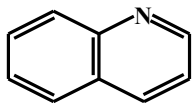

Quinoline

Non-basic nitrogen compounds

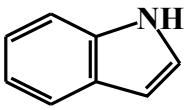

Indole

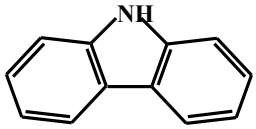

Carbazole

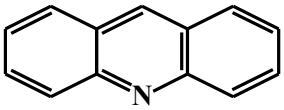

Acridine

Pyrrole

Figure 2.8 Nitrogen-containing compounds in petroleum. (Bozenko, 2008)

The most common method of desulfurization of fuels is hydrodesulfurization, in which the fuel is reacted with hydrogen gas at elevated temperature and high pressure in the presence of a costly catalyst.

2.2.2 Regulations on sulfur content in petroleum products

According to the environmental effects of sulfur oxides, strict regulation on sulfur emissions and the sulfur content of refined fuels have been adopted in many countries. The requirements for the sulfur content of diesel fuels have been gradually stiffened as shown in Table 2.3. In mid-2006, a maximum level of 15 ppm was introduced in the USA, and 80% of the oil refineries in this country are ready to produce so-called

ultralow-sulfur diesel (ULSD) and 20% will convert to manufacture of ULSD by 2010. Beginning in 2009, the sulfur content in diesel fuel in all European countries will be set at a maximum of 10 ppm and in 2010, the entire diesel automobile fleet will be converted to fuel with near-zero sulfur content. These severe standards are not only imposed on fuels for high-speed automobile diesel engines, but similar requirements are also beginning to spread to diesel fuels for offroad machinery (Krylov, 2005). It is expected that similar regulations will be adopted in other countries.

In Thailand the maximum sulfur content in diesel fuel was enacted. The following years were proposed for the stepwise sulfur reduction: 500 ppm on July 1998; 350 ppm on January 2004; and 50 ppm for the year 2010 (Knowledge Management on Air-Quality).

Table 2.3 Sulfur Levels in Diesel in Asia the European Union and the United States (Knowledge Management on Air-Quality).

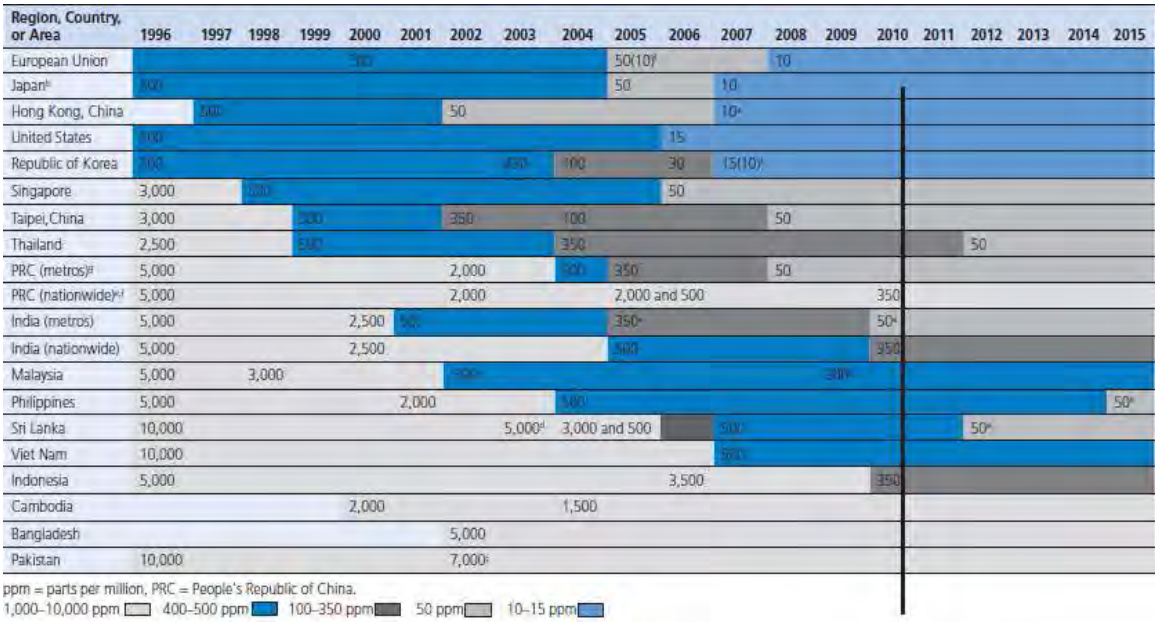

2.3 Diesel product properties

After the reaction run, aqueous and organic liquid phase were physically separated and, analyzed using several gas-chromatography methods. Gas products (carbon monoxide, carbon dioxide, methane, and propane) were analyzed by gas-chromatography thermal conductivity detector (GC-TCD). Organic liquid products were analyzed by gas-chromatography with flame ionization detector (GC-FID). The physiochemical properties of the organic liquid products are shown in Table 2.4.

Table 2.4 Standard test physiochemical properties of the organic liquid products. (Walendziewski et al., 2009; Guzman et al., 2010)

Properties	Solution	Method	
		European diesel fuel standard (EN)	ASTM
Density (15°C)	aerometer	EN ISO 3675, EN ISO 12185	ASTM D-4052
Kinematical viscosity (40 °C)	Ubbelohde viscosimeter	EN ISO 3104	ASTM D-445
Fractional composition		EN ISO 3405	
Flash point	Pensky-Martens-closed cup	EN ISO2719	ASTM D-93
Cloud point			ASTM D-2500
Pour point			ASTM D-97
Corrosion			ASTM D-130
Color			ASTM D-1500
Cold filter plugging point (CFPP)		EN 116	
Bromine number	PN-68/C-04520		ASTM D-1159

Properties	Solution	Method	
		European diesel fuel standard (EN)	ASTM
Total acid number (TAN)	titration of the sample with KOH solution PN 85/C-04066		ASTM D-664 ASTMD974
Carbon and hydrogen Cetane index Thermal stability Simulated distillation			ASTM D-5291 ASTM D-4737 ASTM D-6468 ASTM D-7213 ASTM-2887-D86
Contents o f ester bonds, aromatic compounds and carboxylic groups in hydrorefined products	FTIR method		

The physiochemical properties of the organic liquid products can be comparison with European diesel fuel standard EN590, NExBTL biodiesel, GTL diesel and FAME shown in Table 2.5 and cetane number in Table 2.6.

Table 2.5 The physiochemical properties standard of the organic liquid products from hydroprocessing. (Technical Research centre of Finland 2005)

Fuel properties	**NExBTL biodiesel**	**GTL diesel**	**FAME**	**EN590/2005**
density @ 15°C (kg/m^3)	775-785	770-785	≈ 885	≈ 835
viscosity @ 40°C (mm^2/s)	2.9-3.5	3.2-4.5	≈ 4.5	≈ 3.5
Cetane index	84-99	73-81	≈ 51	≈ 53
Distillation 10 vol% (°C)	260-270	≈ 260	≈ 340	≈ 200
Distillation 90 vol% (°C)	295-300	325-330	≈ 355	≈ 350
Cloud point (°C)	-5…-30	0…-25	≈ -5	≈ -5
Lower heating value (MJ/kg)	≈ 44	≈ 43	≈ 38	≈ 43
Lower heating value (MJ/litres)	≈ 34	≈ 34	≈ 34	≈ 36
Polyaromatics (wt%)	0	0	0	≈ 4
Oxygen (wt%)	0	0	≈ 11	0
Sulfur (mg/kg)	≈ 0	< 10	< 10	< 10

Table 2.6 Cetane number of normal and iso-paraffins. (Santana et al., 2006)

N-PARAFFINS	CN	ISO-PARAFFINS	CN
n-Butane	22	2-Methylpentane	33
n-Pentane	30	3-Methylpentane	30
n-Hexane	45	2,3-Dimethylpentane	22
n-Heptane	54	2,4-Dimethylpentane	29
n-Octane	64	2,2,4-Trimethylpentane	14
n-Nonane	72	2,2,5-Trimethylhexane	24
n-Decane	77	2,2-Dimethyloctane	59
n-Undecane	81	2,2,4,6,6-Pentamethylheptane	9
n-Dodecane	87	3-Ethyldecane	47
n-Tridecane	90	4,5-Diehtyloctane	20
n-Tetradecane	95	4-Propyldecane	39
n-Pentadecane	96	2,5-Dimethylundecane	58
n-Hexadecane	100	5-Butylnonane	53
n-Heptadecane	105	2,7-Dimethyl-4,5-diethyloctane	39
n-Octadecane	106	5-Butyldodecane	45
n-Nonadecane	110	7,8-Dimethyltetradecane	40
n-Eicosane	110	7-Butyltridecane	70
		7,8-Diethyltetradecane	67
		8-Propylpentadecane	48
		9-Methylheptadecane	66
		5,6-Dibutyldecane	30
		9,10-Dimethyloctadecane	60
		7-Hexylpentadecane	83
		2,9-Dimethyl-5,6-diisopentyldecane	48
		10,13-Dimethyldocosane	56
		9-Heptylheptadecane	88
		9,10-Dipropyloctadecane	47

2.4 Simulated distillation

Simulated distillation (SimDist) is a gas chromatography (GC) technique which separates individual hydrocarbon components in the order of their boiling points, and is used to simulate the time-consuming laboratory-scale physical distillation procedure known as true boiling point (TBP) distillation. The separation is accomplished with a non polar chromatography column using a gas chromatograph equipped with an oven and injector that can be temperature programmed. A flame ionization detector (FID) is used for detection and measurement of the hydrocarbon analytes. The result of SimDist analysis provides a quantitative percent mass yield as a function of boiling point of the hydrocarbon components of the sample. The chromatographic elution times of the hydrocarbons are calibrated to the atmospheric equivalent boiling point (AEBP) of the paraffins reference material. The SimDist method ASTM (American Society for Testing and Materials) D2887 covers the boiling range 55–538°C (100–1000°F) which covers the n-alkanes (n-paraffins) of chain length about C_5–C_{44}. The high-temperature simulated distillation (HTSD) method covers the boiling range 36–750°C (97–1382 °F) which covers the n-alkane range of about C_5–C_{120}. A key difference between ASTMD-2887 and HTSD is the ability of the latter technique to handle residue-containing samples (i.e. material boiling > 538°C, 1000°F). SimDist and laboratory-scale physical distillation procedures are routinely used for determining boiling ranges of petroleum crude oils and refined products, which include crude oil bottoms and residue processing characterization. The boiling points with yield profile data of these materials are used in operational decisions made by refinery engineers to improve product yields and product quality. Data from SimDists are valuable for computer modeling of refining processes for improvements in design and process optimization. Precise yield correlations between HTSD and crude assay distillation (methods ASTM D2892 and D5236) have allowed HTSD to be successfully used in place of physical distillation procedures. This has given the refiner the ability to rapidly evaluate crude oils for selection of those with economic advantages and more favorable refining margins. SimDist methods are becoming more widely used in environmental applications. HTSD is useful for characterizing

hydrocarbons which can be present as soil and water contaminants; for example, to map and follow hydrocarbon removal processes.

SimDist became an ASTM standard method in 1973, with the designation D2887, ‘‘Boiling Range Distribution of Petroleum Fractions by GC’’. The current edition is designated D2887-97. This method covers the determination of the boiling range distribution of petroleum products and fractions having a final boiling point (FBP) of 538°C (1000°F) or lower at atmospheric pressure. HTSD is a relatively recent method which extends ASTM D2887 determination of the boiling range distribution of hydrocarbons to a FBP of about 750°C (1382°F). Technological advances in capillary GC columns and stationary phases together with either programmed temperature vaporization (PTV) or on-column injection techniques, provide adequate separation from C_5 to C_{120} normal paraffins and allows the characterization of petroleum products from about 36–750°C (97–1382°F). Under the special conditions of HTSD, elution of materials from the GC column occurs at up to 260–316°C (500–600°F) below their AEBP. For instance, the elution of C_{110} (AEBP of 735°C or 1355°F) occurs at a column temperature of about 427°C (800°F). Also under these conditions, little or no evidence of cracking is normally seen in HTSD (Villalanti et al., 2000).

2.4.1 Measurement of boiling point distribution using the total area method

A linear temperature programming method is applied to the analysis using a gas chromatograph with a non-polar liquid phase column, the hydrocarbons will be eluted in the order of boiling point. Since the elution time is more or less directly proportional to the boiling point, a calibration curve of the retention time and boiling point can be created, as shown in Figure 2.9. In other words, the retention time can be converted into the boiling point. Therefore, by working out the relationship between the retention time and the boiling point before through the analysis of a hydrocarbon mixture with a known boiling point (with the gas chromatograph analysis conditions kept constant), it becomes possible to convert the retention time of an unknown sample into the boiling point. Furthermore, the total area of the gas chromatogram obtained is divided into fixed time intervals, and the smaller areas comprised by each time period are calculated. Since the

time interval can be converted into the boiling point interval, this in effect calculates the gas chromatogram area for the fraction of a particular boiling point (Shimadzu, 2011: online).

In this study, used calibration mixture 1%wt/wt -An accurately weighed mixture of approximately equal mass quantities of n-hydrocarbons dissolved in carbon disulfide (CS_2) The mixture shall cover the boiling range from n-C_5 to n-C_{44}, but does not need to include every carbon number shown in Table 2.7 and Figure 2.10.

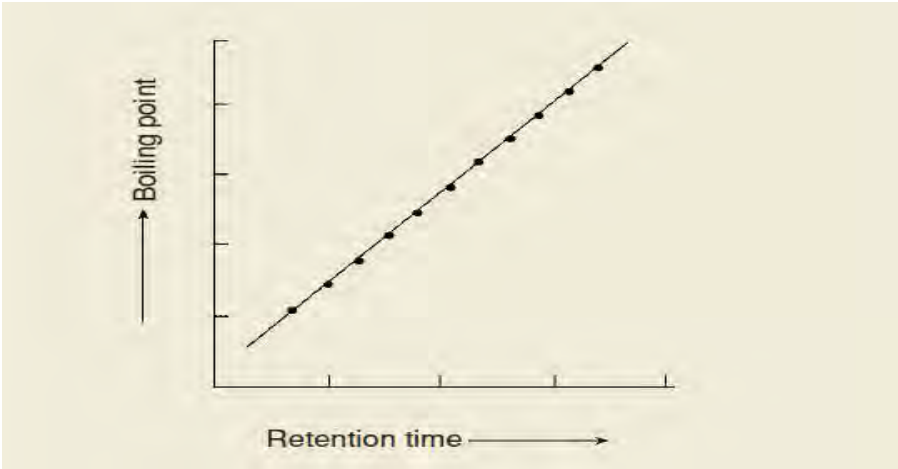

Figure 2.9 Calibration curve of the retention time and boiling point.
(Shimadzu, 2011: online)

Table 2.7 Component of n-C_5 to n-C_{44} alkanes in calibration mixture. (Restek, 2011: online)

Elution order	Compound	CAS#	Percent Purity	Concentration (weight/weight%)
1	n-Pentane (C5)	109-66-0	99%	0.9995 wt./wt.%
2	n-Hexane (C6)	110-54-3	99%	0.9995 wt./wt.%
3	n-Heptane (C7)	142-82-5	99%	0.9995 wt./wt.%
4	n-Octane (C8)	111-65-9	99%	0.9995 wt./wt.%
5	n-Nonane (C9)	111-84-2	99%	0.9995 wt./wt.%
6	n-Decane (C10)	124-18-5	99%	0.9995 wt./wt.%
7	n-Undecane (C11)	1120-21-4	99%	0.9995 wt./wt.%
8	n-Dodecane (C12)	112-40-3	99%	0.9995 wt./wt.%
9	n-Tetradecane (C14)	629-59-4	99%	0.9995 wt./wt.%
10	n-Pentadecane (C15)	629-62-9	99%	0.9995 wt./wt.%
11	n-Hexadecane (C16)	544-76-3	99%	0.9995 wt./wt.%
12	n-Heptadecane (C17)	629-78-7	99%	0.9995 wt./wt.%
13	n-Octadecane (C18)	593-45-3	99%	0.9995 wt./wt.%
14	n-Eicosane (C20)	112-95-8	99%	0.9995 wt./wt.%
15	n-Tetracosane (C24)	646-31-1	99%	0.9995 wt./wt.%
16	n-Octacosane (C28)	630-02-4	99%	0.9995 wt./wt.%
17	n-Dotriacontane (C32)	544-85-4	98%	0.9991 wt./wt.%
18	n-Hexatriacontane (C36)	630-06-8	99%	0.9995 wt./wt.%
19	n-Tetracontane (C40)	4181-95-7	97%	0.9986 wt./wt.%
20	n-Tetratetracontane (C44)	7098-22-8	99%	0.9995 wt./wt.%
Solvent	Carbon Disulfide	75-15-0	99%	

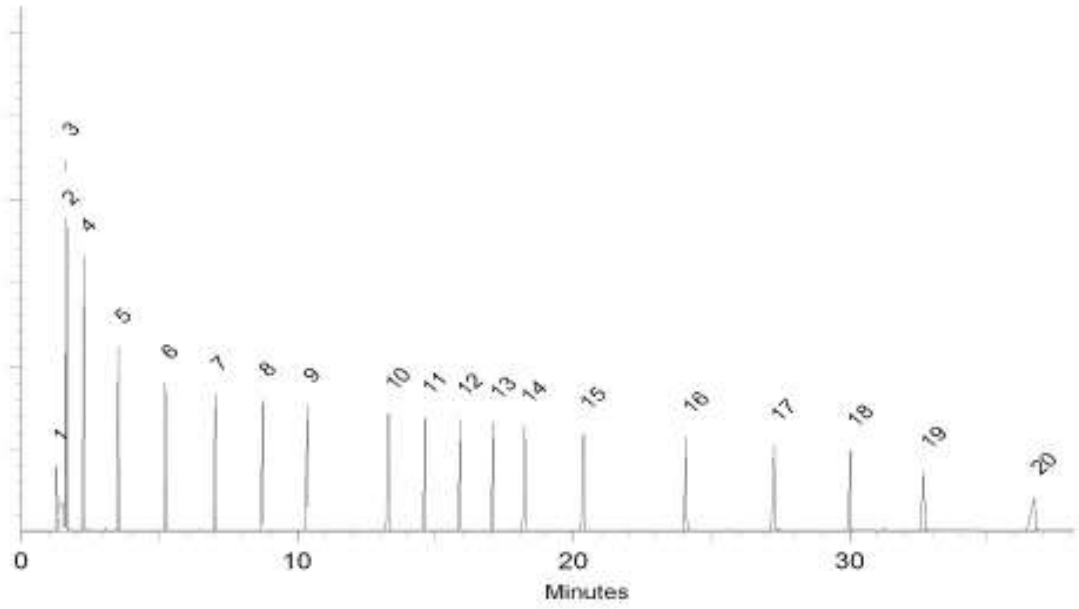

Figure 2.10 Graph of n-C_5 to n-C_{44} alkanes at various times in calibration mixture. (Restek, 2011: online)

In addition, by obtaining the cumulative area through the addition of all the small areas from the start point onwards, and expressing it as a ratio of the area of the entire gas chromatogram, the elution amount up to that time will have been calculated. In Figure 2.11 for example, the cumulative area up to 'n' consists of 'S1', 'S2', 'Sn-1', 'Sn'. By figuring out the ratio with respect to the total area 'St', the elution amount at 'tn' is obtained. The data in Figure 2.12 is an example of the elution amount (corresponds to the amount of distillate). This method is applied to samples where all the components of the sample are eluted from the column during high temperature analysis using GC, such as the oil fractions of gasoline, kerosene, and light oil (Shimadzu, 2011: online).

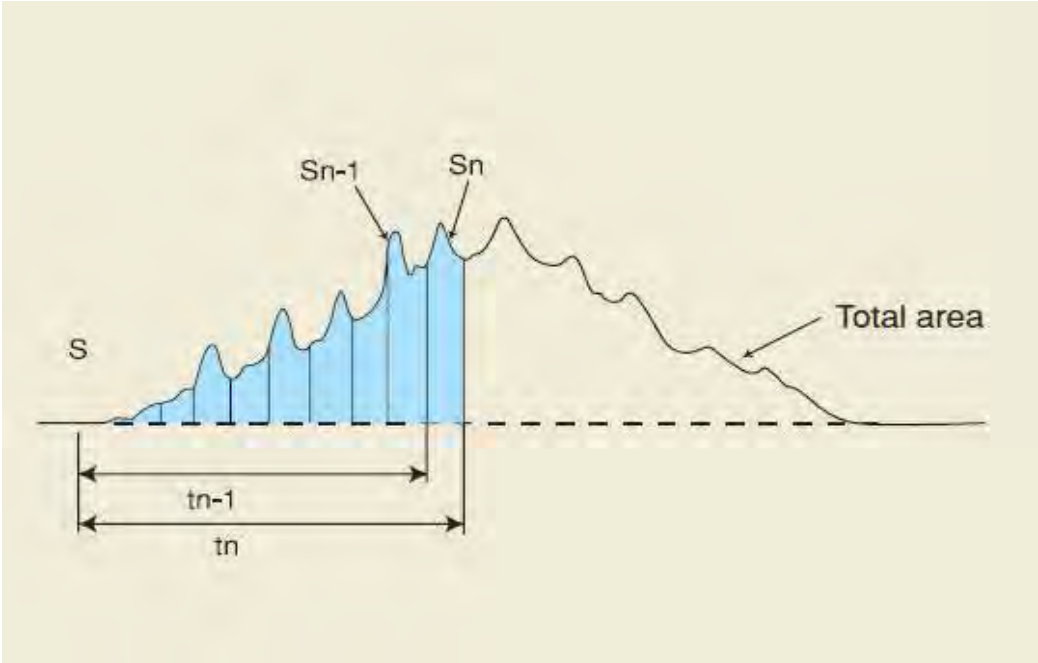

Figure 2.11 Calculating the elution amount. (Shimadzu, 2011: online)

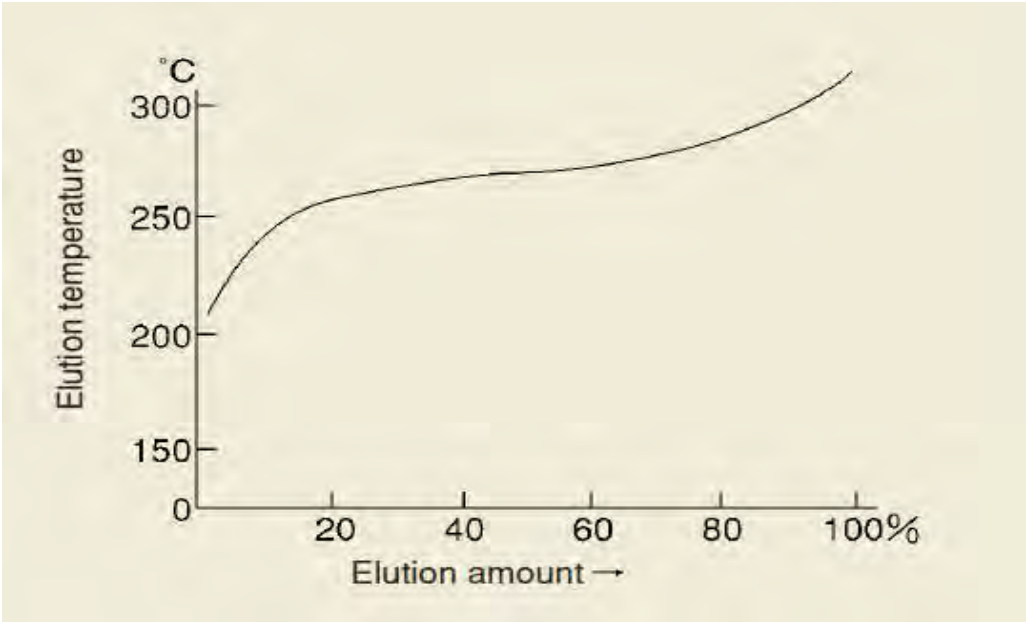

Figure 2.12 Distillation characteristics curve. (Shimadzu, 2011: online)

In this study, we used simulated distillation to analyze the temperature range of products following by ASTM-2887-D86 procedure. It was found, at temperature range of 250-380°C is a suitable for diesel range (n-C_{15}-n-C_{18}) shown in Table 2.8. It can be concluded that the products are suitable for diesel fuel blending (Huber et al., 2007).

Table 2.8 Distillation data in specified temperature range. (Huber et al., 2007)

The straight chain alkanes	**Range of temperature (°C)**
Lighter alkanes	-50 to 65
Alkanes C_5-C_8	65-150
Alkanes C_9-C_{14}	150-250
Alkanes C_{15}-C_{18}	250-380
Intermediates and the alkanes < C_{20}	380-520
The tri-glycerides and fatty acids	520-1000

2.5 Catalysts

2.5.1 Nickel (Wikipedia, 2011: online)

Nickel, a transition series metallic element having atomic number 28, is a silvery-white lustrous metal with a slight golden tinge. Nickel is used in many industrial and consumer products, including stainless steel, magnets, coinage, rechargeable batteries, electric guitar strings and special alloys. It is also used for plating and as a green tint in glass. Nickel is pre-eminently an alloy metal, and its chief use is in the nickel steels and nickel cast irons, of which there are many varieties. It is also widely used in many other alloys, such as nickel brasses and bronzes, and alloys with copper, chromium, aluminium, lead, cobalt, silver, and gold.

2.5.1.1 Physical properties of nickel

The electronic structure of nickel is [Ar] $3d^8 4s^2$. The physical properties of nickel are listed in Table 2.9.

Table 2.9 Physical properties of nickel. (Wikipedia, 2011: online)

Property	Value
atomic number	28
atomic weight	58.69
melting point, ^oC	1453
latent heat of fusion, ΔH_{fus} kJ/mol[a]	17.48
boiling point, ^oC	2732
latent heat of vaporization at bp, ΔH_{vap} kJ/mol[a]	377.5
specific heat, kJ/(mol.K)[a] 25^oC	26.07
coefficient of thermal expansion, oC^{-1}	13.4 $\mu m \cdot m^{-1} \cdot K^{-1}$
thermal conductivity at 27 ^oC, W/(m.K)	90.9
Curie temperature, ^oC	355
Young's modulus, Gpac	200

2.5.2 Cobalt (Young, 1960; Othmer, 1991)

Cobalt, a transition series metallic element having atomic number 27, is similar to silver in appearance. Cobalt and cobalt compounds have expended from use colorants in glasses and ground coat fits for pottery to drying agents in paints and lacquers, animal and human nutrients, electroplating materials, high temperature alloys, hard facing alloys, high speed tools, magnetic alloys, alloys used for prosthetics, and used in radiology. Cobalt is also as a catalyst for hydrocarbon refining from crude oil for the synthesis of heating fuel.

2.5.2.1 Physical properties of cobalt

The electronic structure of cobalt is [Ar]$3d^7 4s^2$. At room temperature the crystalline structure of the α (or ε) form, is close-packed hexagonal (cph) and lattice parameters are a = 0.2501 nm and c = 0.4066 nm. Above approximately 417°C, a face-centered cubic (fcc) allotrope, the γ (or β) form, having a lattice parameter a = 0.3554 nm, becomes the stable crystalline form.

The scale formed on unalloyed cobalt during exposure to air or oxygen at high temperature is double-layered. In the range of 300 to 900°C, the scale consists of a thin layer of mixed cobalt oxide, Co_3O_4, on the outside and cobalt (II) oxide, CoO, layer next to metal. Cobalt (III) oxide, Co_2O_3, may be formed at temperatures below 300°C. Above 900°C, Co_3O_4 decomposes and both layers, although of different appearance, are composed of CoO only. Scales formed below 600°C and above 750°C appear to be stable to cracking on cooling, whereas those produced at 600-750°C crack and flake off the surface.

Cobalt forms numerous compounds and complexes of industrial importance. Cobalt, atomic weight 58.933, is one of the first transition series of Group 8 (VIIIB). There are thirteen know isotope, but only three are significant: ^{59}Co is the only stable and naturally occurring isotope; ^{60}Co has a half-life of 5.3 years and is a common source of γ-source for MÖssbauer spectroscopy.

Cobalt exists in the +2 or +3 valance states for the major of its compounds and complexes. A multitude of complexes of the cobalt (III) ion exists, but few stable simple salt are know. Octahedral stereochemistries are the most common for cobalt (II) ion as well as for cobalt (III). Cobalt (II) forms numerous simple compounds and complexes, most of which are octahedral or tetrahedral in nature; cobalt (II) forms more tetrahedral complex than other transition-metal ions. Because of the small stability difference between octahedral and tetrahedral complexes of cobalt (II), both can be found equilibrium for a number of complexes. Typically, octahedral cobalt (II) salts and complexes are pink to brownish red; most of the tetrahedral Co (II) species are blue.

Table 2.10 Physical properties of cobalt. (Othmer, 1991)

Property	Value
Atomic number	27
Atomic weight	58.93
Heat of transformation, J/g[a]	251
Melting point, ^{o}C	1493
Latent heat of fusion, ΔH_{fus} J/g[a]	395
Boiling point, ^{o}C	3100
Latent heat of vaporization at bp, ΔH_{vap} kJ/g[a]	6276
Specific heat, J/(g·^{o}C)[a]	
15-100°C	0.442
molten metal	0.560
Coefficient of thermalexpansion, $^{o}C^{-1}$	
cph at room temperature	12.5
fcc at 417°C	14.2
Thermal conductivity at 25 ^{o}C, W/(m·K)	69.16
Curie temperature, ^{o}C	1121
Young's modulus, Gpac	211

2.5.3 Molybdenum (Wikipedia, 2011: online)

Molybdenum, a transition series metallic element having atomic number 42, the metal is silvery white, very hard transition metal. Nonetheless, it is softer and more ductile than tungsten. It has a high elastic modulus, and only tungsten and tantalum, of the more readily available metals, have higher melting points. It has one of the highest melting points of all pure elements. Molybdenum is attacked slowly by acids.

Molybdenum is a valuable alloying agent, as it contributes to the hardenability and toughness of quenched and tempered steels. It is also improves the strength of steel at high temperatures. In addition, molybdenum was used in alloys, electrodes and catalysts

in the refining of petroleum. It has found applications as a filament material in electronic and electrical applications. It is also possible that molybdenum powders are used in circuit inks for circuit boards, and in microwaves devices and heat sinks for solid-state devices.

2.5.3.1 Physical Properties

The electronic structure of molybdenum is [Kr] $4d^5 5s^1$. The physical properties of molybdenum are listed in Table 2.11.

Table 2.11 Physical properties of molybdenum. (Wikipedia, 2011: online)

Property	Value
atomic number	42
atomic weight	95.96
melting point, ^{o}C	2610
latent heat of fusion, ΔH_{fus} kJ/mol	37.48
boiling point, ^{o}C	4825
latent heat of vaporization at bp, ΔH_{vap} kJ/mol	598
specific heat, J/(mol·K)	
25°C	24.06
coefficient of thermal expansion, $^{o}C^{-1}$	4.8 $\mu m \cdot m^{-1} \cdot K^{-1}$
thermal conductivity at 27 ^{o}C, W/(m·K)	138
Young's modulus, GPa	329

2.5.4 Aluminium oxides or alumina (Al_2O_3)

It is well known that alumina is a term of alumina compounds. Also, alumina has a number of crystalline phases, in generally, alumina can exist in many metastable phase before transforming to the stable form of alumina in which the stable form of alumina was well known as α-alumina form or corundum from. There are six principle phase designated by the Greek letters, composed that chi (χ), kappa (κ), eta (η), theta (θ), delta (δ), and gamma (γ). The nature of the product obtained depending on many factors such as calcination temperature, heating environment, as one can so-called heat treatment conditions. In addition, starting hydroxide such as gibbsite, boehmite and others could be affecting to the nature of the product, which can be illustrated in Figure 2.13, which shows thermal transformation scheme of different types of starting material. As can be seen, among the various crystalline phases of alumina, γ-Al_2O_3 is probably the most important inorganic oxide refractory of widespread technological importance in the field of catalysis, also used as catalyst support. In addition, γ-Al_2O_3 is an exceptionally good choice for catalytic applications because of a defect spinel crystal lattice that imparts to it a structure that is both open and capable of high surface area (Yang et al., 2007).

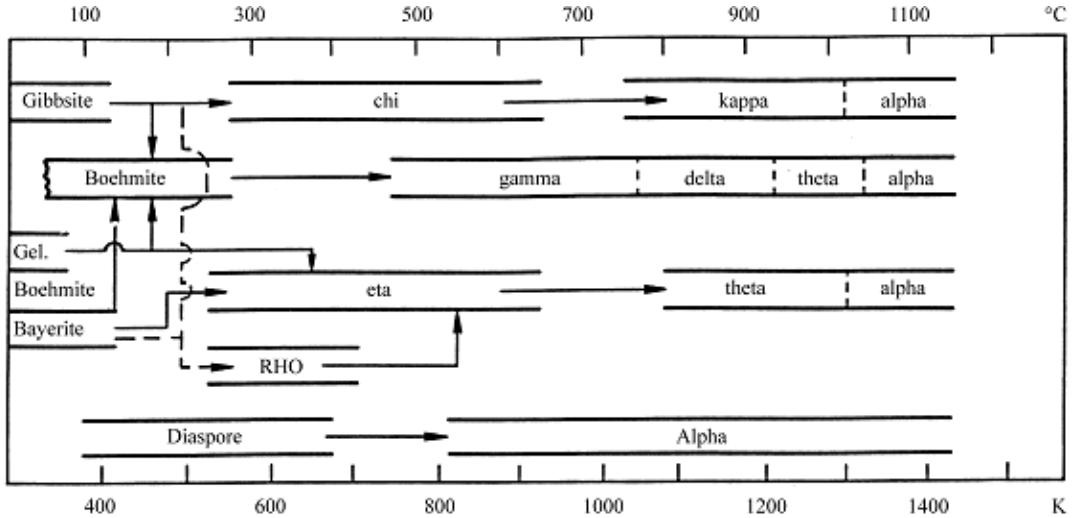

Figure 2.13 Thermal transformations of different types of starting material.
(Santos et al., 2000)

2.6 Metal carbides and nitrides catalysts

Catalysts for hydrotreating reactions have traditionally been sulfides of molybdenum with cobalt and nickel promoter. In recent year, petroleum refining industry has been facing significant challenges because of the continuously decreasing allowable amount of emissions, such as SO_x, NO_x and aromatics from the combustion of fuels. With the currently used technology, the quality of fuels prescribed by the new environmental regulations can be attained by the significant modifications of refining operations (Furimsky 2003). Later, efforts have been to develop such catalysts for hydroprocessing. Carbides and nitrides of molybdenum have been identified as the excellent potential for use in hydrodenitrodenation (HDN) and hydrodesulfurization (HDS) reactions catalysts

The information on the structure and properties is available for Mo carbides and nitrides. Figure 2.14 illustrates fundamental difference between the structures of Mo carbide and nitride compared with that of Mo sulfide. These materials differ substantially from the previous molybdenum compounds in being metallic interstitial alloys of carbon and nitrogen, and not insulating layered compounds. Molybdenum carbides and nitrides are characterized by the hexagonal close-packed and body-centered cubic crystal structure, respectively (Sajkowski and Oyama, 1996).

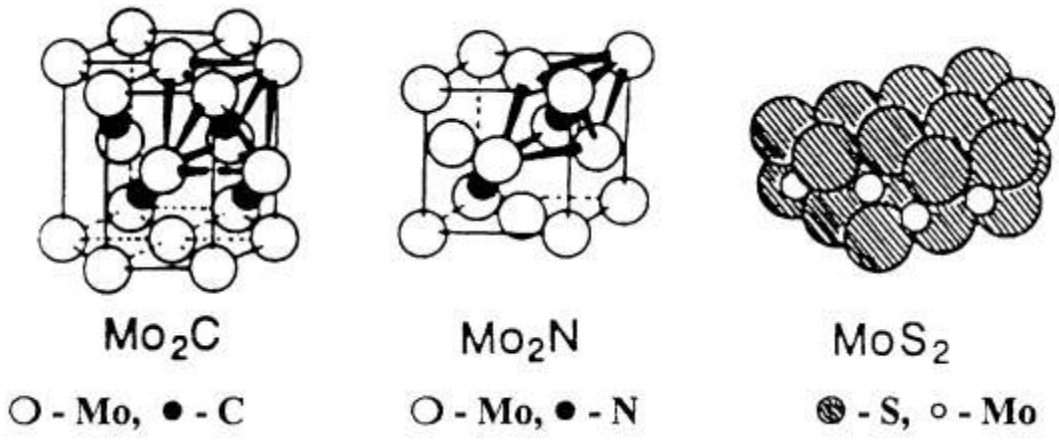

Figure 2.14 Crystallographic structure of Mo_2C, Mo_2N and MoS_2.
(Sajkowski and Oyama, 1996)

The carbon and nitrogen deficiency in such crystals can be supplemented by oxygen, which yields oxycarbides and oxynitrides respectively. The elementary theory of these compounds suggests that the introduction of carbon or nitrogen into the lattice of the early transition metals results in an increase of the lattice parameter a_0. This leads to an increase in the d-electron density. After carburization or nitridation, the early transition metals exhibit the noble metals-like behavior. Because of their small atomic radius, carbon and nitrogen can nest in the interstices of the lattice. Therefore, some row 2 metals (Mo, Nb and Ze) and row 3 metals (Re, W, Hf and Ta) are called the interstitial carbides and nitrides, whereas row 1 metals (Ti, V, Cr, Mn, Fe, Ni and Co) are called the intermediate carbides and nitrides. Apparently, the stability of the row 1 metal carbides and nitrides is limited (Colling and Thompson, 1994).

The electronegativity (EN) of Mo and W on one hand and that of carbon and nitrogen on the other suggests that the bonding is partly covalent and ionic but mostly metallic. Thus, the EN values obtained by subtracting the EN of Mo from either C or N are 0.7 and 1.2, respectively compared with 0.8 and 1.3 for the W carbide and nitride, respectively. The extensive metal–metal bonding, particularly in the carbides and nitrides possessing a high metal/carbon (nitrogen) ratio explains why the interstitial carbides and nitrides resemble metals (Pierson, 1996). Thus, their electrical and thermal conductivity are high. Also, they have high melting point and hardness.

The thermodynamic properties of metal carbides and nitrides showed that Group VI metal carbides and nitrides are more resistant to recarburization than the Group V metal carbides and nitrides because they more closely resemble noble metals (Brungs, 1997; Oyama et al., 1997). Figure 2.15 shows the heat of formation decreases from the Group IV towards Group VIII. Similar information for the noble metal carbides and nitrides is not available. Figure 2.16 shows that the catalyst activity for HDN increases with the decreasing heat of formation (Ramanathan and Oyama, 1995).

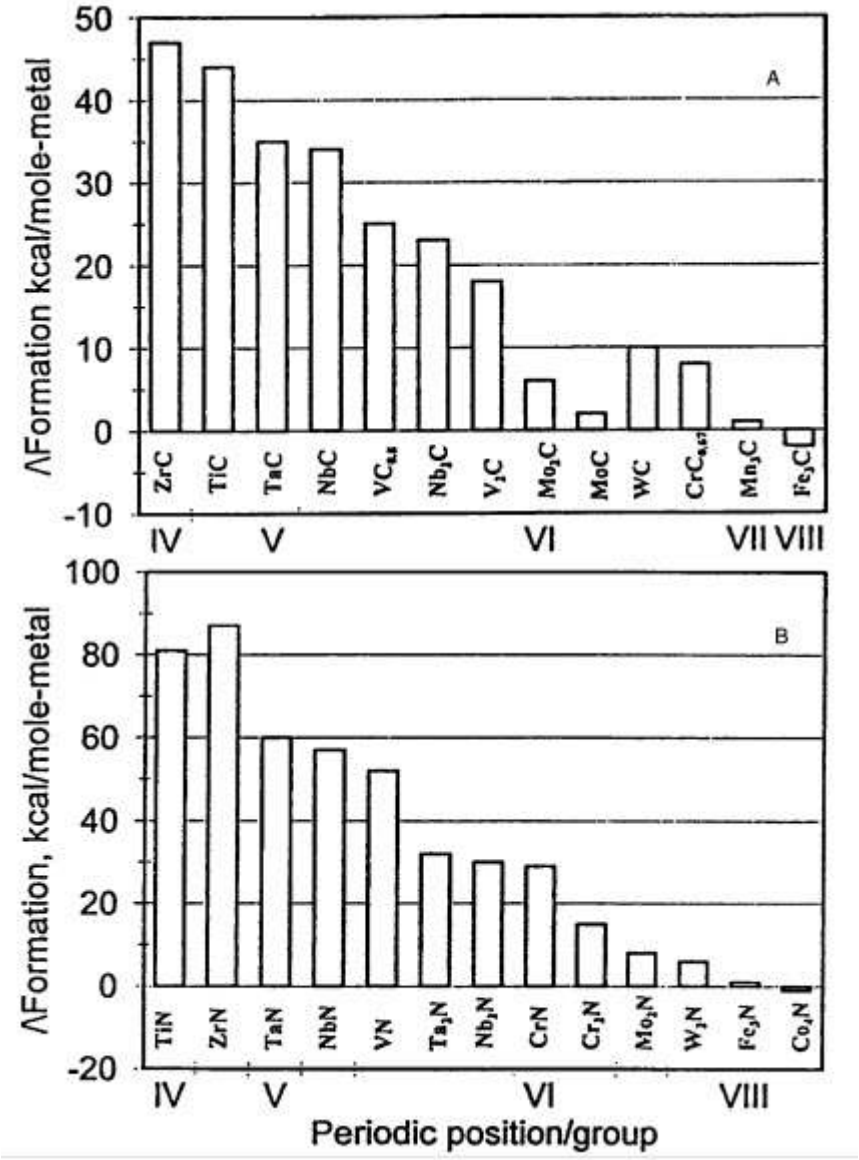

Figure 2.15 Heat of formation vs. periodic position for (A) metal carbides and (B) metal nitrides. (Oyama et al., 1997; Brungs, 1997)

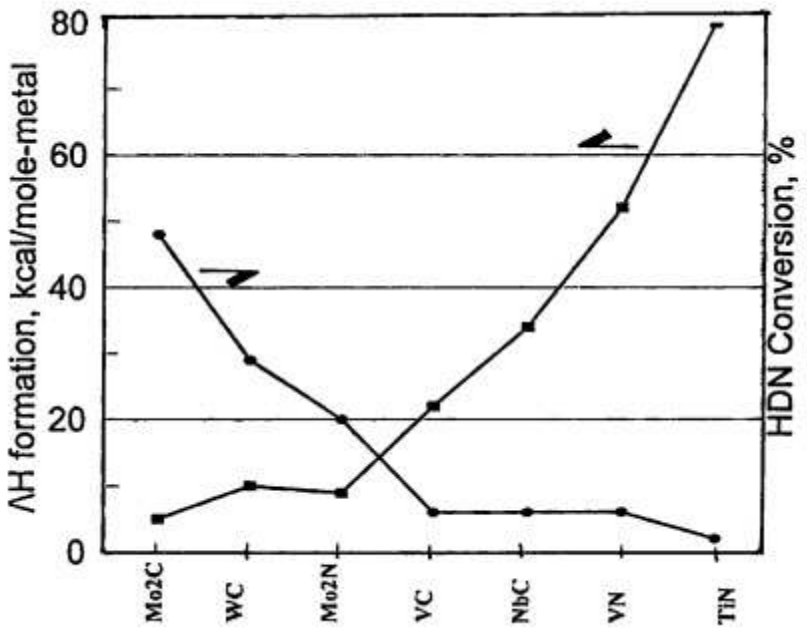

Figure 2.16 Effect of heat of formation on activity for HDN for various metal carbides and nitrides. (Ramanathan and Oyama, 1995)

CHAPTER III

LITERATURE REVIEWS

This section consists of the research reviews which is related to biodiesel producing on aspect of reaction of hydroprocessing with various suitable operating conditions, catalyst selection, methods for analysis properties of products, advantages and drawback of their strategies.

3.1 Raw-material

The properties of the waste cooking oils (WCOs) are somewhat different from fresh vegetable oils because of the physical and chemical changes mainly due to oxidative and hydrolytic reactions that take place during frying (Cvengros and Cvengrosova, 2004; Tomasevic and Siler-Marinkovic, 2003). It has been reported that WCO have acid value (Banerjee and Chakraborty, 2009) because that contains large amount of free fatty acids (Patil et al., 2010).

Edible vegetable oils such as palm, soybean, corn, canola and sunflower have been used for biodiesel production, which is due to the higher cost of edible oil. Waste cooking oil is a promising alternative to reduce cost of raw-material and environmental. The waste cooking oil had amount of heteroatom (Sulfur and Nitrogen) in restaurants and fast food higher than domestic (Bezergianni and Kalogianni, 2009), which given in Table 3.1.

3.2 Reaction condition of hydroprocessing process

The hydrogenation reaction is quite similar to those of hydrodesulfurization (HDS), which is convert sulfur-containing molecules into H_2S. Therefore, the hydrogenation of oils and fats can take place desulfurization unit. Donnis et al., 2009 studied mechanism of overall reaction for the hydrogenation between triglycerides and hydrogen.

Table 3.1 Heteroatoms of different sources of used waste cooking oil.

Heteroatom	Domistic	Restaurants	Fast food
S (wppm)	0.00	187.70	26.30
N (wppm)	0.4	49.10	61.90
H (wt%)	11.56	11.52	11.58
C (wt%)	77.24	76.53	76.32
O (wt%)	11.20	11.92	12.09

This study describes the three carboxylic acids are stepwise liberated and hydrogenated into straight chain alkanes of the same length or one carbon atom shorter. Then the backbone of the triglycerides is converted into propane, water, carbon monoxide, carbon dioxide and methane. These products will be considerable due to appropriated conditions and suitable catalyst. The proposed reaction mechanism, which can be explained the path way of these products, involve at least three reaction pathways as hydrodeoxygenation, decarboxylation and decarbonylation.

One mechanism is hydrodeoxygenation (HDO) reaction (see the unbroken red lines in Figure 3.1), which occurs via the absorbed enol intermediate. The products for this mechanism are water, propane and three normal alkanes of the full length of fatty acid chains. The others mechanism, which are called decarboxylation and decarbonylation (see the broken blue lines in Figure 3.1). The triglycerides are broken down the products, which are propane, carbon monoxide and/or carbon dioxide and three normal alkanes with carbon numbers one less than fatty acid chains (Filho et al., 1993).

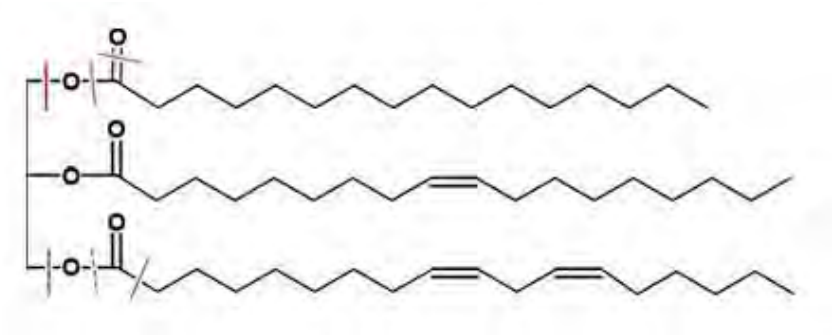

Figure 3.1 Schematic representation of the different reaction pathways for the removal of triglyceride oxygen by hydrodeoxygenation (--) and decarboxylation (--)

3.3 Effect of operating condition

Temperatures, hydrogen pressure, time of stream and catalysts have been identified as a key parameter for catalyst effectiveness and catalyst life. Increasing temperature increases catalyst activity and increasing catalyst activity causes a faster decay of catalyst life.

Sebos et al., 2009 were tested the hydrodeoxygenation of mixture of 10 wt% cottonseed oil in diesel used in conventional hydrodesulphurization units of refinery plants. The product of renewable diesel has almost the same behavior as desulphurized diesel. Tailleur et al., 2006 studied SHP technology, which is developing diesel hydrotreating unit in a conventional diesel hydroreactor (HDT). It was found that low sulfur low aromatics diesel and enhancing selectivity toward to light parafin and napthene formation can obtain for this process.Moreover, the lower emission of pollution including No_x and PM as well as the better in cetane number were observed. Finally, rate of reaction with respect to the lump of 11 gas and liquid phase reaction for hydroprocessing process was determined by the simpled of kinetic model in order to optimize the investment cost of this catalytic system.

Donnis et al., 2009 were conducted the hydroprocessing by feed 0, 15 and 25 vol% rapeseed oil in light gas oil (LGO) with reaction temperature 350ºC and under hydrogen pressure of 45 bar. A commercial TK-565 (Ni-Mo based) catalyst was used. The products obtain 100% conversion from repeseed oil and the same final boiling point (FBP) of all three products were analzed by the simulated distillation curves, which is also the FBP of the LGO feed. The HDO route and the decarboxylation route can be calculated from the yields of CO, CO_2, and CH_4. The triglycerides reacted via the decarboxylation rate about 66-74%. Increased rapeseed oil mixed in LGO, properties of the diesel product were a low density and a high cetane index. The cloud point is important because the car manufactures observed filter plugging from the tank to the engine when operated at low temperatures. Therefore, the production of rapeseed oil will be improved product properties as concern cloud and pour point.

Walendziewski et al., 2009 studied hydroprocessing of 10 and 20 wt.% of rape oil and 90 and 80 wt.% of LGO fraction mixtures in continuous reactor with the same

parameter sets, temperature 320, 350 and 380ºC as well as under hydrogen pressure 3 and 5 MPa. A commercial $NiMo/Al_2O_3$ catalyst was used. As the result of process the temperature range 350-380ºC and hydrogen pressure 5 MPa are good efficiency. In comparision to the product yields for hydrotreating of vegetable oil (sunflower oil) used simulated distillation to analyze with the same as catalyst, temperature and pressure. It was obtained the maximum theoretical products carbon yields and carbon yields of C_{15}-C_{18} are 95% and 75%, respectively. The yields of gaseous (propane, carbon monoxide and carbon dioxide), isomerized and cracked products are minimum at the same temperature (Huber et al., 2007). The obtained liquid product was approximately 95 wt% yields of all products and 5 wt% of gaseous light hydrocarbons. Hydrogenation of unsaturated hydrocarbons and hydrogenolysis reactions of ester and carboxyl acid bonds results in fatty acid chains were converted to saturated linear hydrocarbon (paraffins), which are higher melting temperatures. It leads to undesirable increasing in boiling point, cloud point and CFPP. Bromine number decreased but acid number increased because ester bonds in fatty acids was hydrogenolized giving carboxylic group, which is loss because of hydrogenation of the carbonyl group (Filho et al., 1993). Then partial hydrocracking of paraffins hydrocarbons were transformed to light hydrocarbons whose flash point, density and kinematics viscosity are lower. There are improvement by the separation and removal of low boiling hydrocarbons from the product distillation.

The product yields for hydrotreating of vegetable oil used the simulated distillation to analyze. If at temperature less than 350ºC was observed in products which contained small amounts of reaction intermediate and reactant. It was obtained that temperature at 350ºC is suitable due to no oxygenated compounds and achieved 100% conversion (Simacek et al., 2010), the maximum theoretical products carbon yields and carbon yields of C_{15}-C_{18} are 95% and 75%, respectively. The yields of gaseous (propane, carbon monoxide and carbon dioxide), isomerized and cracked products are minimum (Huber et al., 2007). It was observed by GC-MS when pressure is decreased to15 bar, product yields from n-C16 to n-C18 was increased due to increasing number of products and cannot specified exactly products like octadecenes, octadecanol, n-hexadecanoic acid, actadecanal and hexa-actadecyl hexadecanoate so there are several intermediates of

this reactions. On the other hand, when pressure is increased (90 bar), decreasing number of products can be indentified because intermediates were not found and fatty acids is reduced as well. Subsequently, pressure effect and hydrogen consumption were tested via simulated in Aspen plus. It was found that the hydrodeoxygenation reaction is better than decarboxylation and decarbonylation when pressure increased and increasing hydrogen consumption. Moreover, time analysis was obtained by simulated distillation curves, the best diesel yields (95.3 %vol) was observed at 4 hours (Guzman et al., 2010).

Simacek et al., 2009 studied hydroprocessing of rapeseed oil various at temperatures 260-340ºC and under hydrogen pressure of 7 MPa. Three NiMo/alumina hydrorefining catalysts were used. Reaction products contained water, hydrogen-rich gas and organic liquid product (OLP). At low reaction temperature (260-300ºC), the OLP contained also reactant and intermediates (mainly triglycerides and free fatty acids). At reaction temperature higher than 310ºC, the OLP contained mostly hydrocarbon (n-$C_{17}$and n-C_{18}). The reaction temperature is increased the content of n-C_{17} increases and n-C_{18} decreases. The OLP contained amount of i-alkanes (up to 40 wt.%) in the case of catalyst B (NiO 2.6 wt.% and MoO_3 15.7 wt.%). It could improve low-tempurature properties of the product. Simacek and Kubicka, 2010 studied hydrocracking of pure petroleum vacuum distillalate and the same fraction containing 5 wt% of rapeseed oil at temperatures 400 and 420ºC and under hydrogen pressure of 18 MPa over commercial Ni-Mo. At 400ºC the product of co-processing contained larger amount of n-C_{17} and n-C_{18} than the product from rapeseed-oil-free raw material. The high concentration of n-alkane resulted in worse low-tempurature properties. On the other hand larger formation of i-alkane at 420ºC decreased the content of n-C_{17} and n-C_{18}. The low-tempurature properties of product were improved (Cloud point and CFPP).

Simacek et al., 2010 studied hydroprocessing of rapeseed oil under reaction conditions at temperatures 310 and 360ºC and under hydrogen pressure 7 and 15 MPa. A commercial hydrotreating NiMo/alumina catalyst was used. The conversion of rapeseed oil was > 99% at 310ºC because of observed in products contained small amounts of reaction intermedia (mainly stearic acid) and reactant. Trace on n-octadecanol, another reaction intermediate. At 360ºC contained no oxygenated compounds, conversion was

achieved 100%. Reaction products yields contained organic liquid product (OLP) -83 wt%, water-11 wt% and gaseous hydrocarbon- 6 wt%, the reaction gas contained propane, carbon dioxide, carbon monoxide and methane. The main of OLP are n-heptadecane and n-octadecane more than 75 wt% of all OLP. Beside other n-alkanes, iso-alkanes and cycloalkanes. Formation of i-alkanes was increased when increasing reaction temperature and hydrogen pressure. Approximately 80% of all four products distilled at a boiling point of about 300-310ºC were analzed by the simulated distillation curves, which is falling into the diesel fuel distillation range. The kinematics viscosity was acceptable but the density was a little lower than diesel fuel. The cetane number can exceed the value of 100. Acid number increased at 310ºC due to carboxylic group content. The parameters (Cloud point, pour point and CFPP) are main disadvantage of OLPs at low-tempurature properties, which can prevent by utilization.

The hydrodecarboxylation (HDC) reaction is favored by lower hydrogen pressure 35-55 bar and by higher temperature (330-350ºC). At higher hydrogen pressure prefer the hydrodeoxygenation (HDO) reaction (Mikulec et al., 2010), the formation o f fatty acids and other oxygenated compounds is reduced and therefore high molecular esters are not observed in the reaction products (Guzman et al., 2010).

Bezergianni and Kalogianni, 2009 studied effect of temperature at 350, 370 and 390ºC, the conversion and product yields are estimated from the simulated distillation data of the total liquid product at the each temperature. The produced liquid biofuels (gasoline and diesel) increase. This is expected as hydrocracking activity rises with increasing temperature. Furthermore gasoline yield increases monotonically with temperature, while diesel yield is smaller at the middle temperature (370ºC). The minimum diesel yield observed at 370ºC is attributed to the fact that increasing temperature. The cracking reactions favored by increasing temperature. These hydrocracking reactions convert heavier molecules including some diesel molecules into lighter gasoline molecules (Bezergianni et al., 2010). Bezergianni et al., 2010 was observed that as the temperature increases the amount of paraffins decrease, while the amount of iso-paraffins increases. The decrease of n-paraffins vs. the increase of iso-paraffins indicate that isomerization reactions are favored by hydrotreating temperature,

which is expected as higher temperatures because hydrocracking type of reactions (which include isomerization and cracking).

The Liquid Hourly Space Velocity (LHSV) is an important operating parameter for regulating catalyst effectiveness and also catalyst life expectancy. Bezergianni and Kalogianni, 2009 studied effect of LHSV at five different LHSVs, i.e. 0.5, 1, 1.5, 2 and 2.5 h^{-1}. The conversion and product yield of diesel decreasing with increasing LHSV from 0.5 to 2.5 h^{-1}. The conversion and overall biofuels yield is favored by decreasing LHSV (at 0.5 h^{-1}).

A small percentage of DMDS (di-methyl-di-sulfide) and TBA (tetra-butyl-amine) is added in the feedstock. Heteroatom removal (mainly sulfur, nitrogen and oxygen) is expressed as the percentage of the sulfur (27,200 wppm), nitrogen (219.8 wppm) and oxygen (3.9 wt%) contained in the feed which has been removed during hydrotreatment reactions at operating temperature 330, 350, 370, 385 and 398ºC. As the result, Sulfur and nitrogen is most effectively removed by over 99.4% for all cases. Furthermore, the most difficult element to remove is oxygen. In low temperatures the oxygen removal is low (78.3%). However, by increasing the temperature, the oxygen removal gradually reaches over 99%. it is evident that higher temperatures favor all heteroatom removal from the final products (Bezergianni and Kalogianni, 2009; Bezergianni et al., 2010).

3.4 Thermodynamic balance

Smejkal et al., 2009 studied the thermodynamic model was derived for the total hydrogenation and its predictions were compared with the experimental of rape-seed oil transformation into hydrocarbons. Tristearate was chosen as a model compound to represent vegetable oils in the calculations. As the thermodynamic data for tristearate were not available in literature, their values were estimated by using the Joback's contribution method. Based on the comparison to a relevant known system (butyl stearate) it was concluded that the chosen method is suitable for the assessment of thermodynamic data of triglycerides. The Joback's contribution method has been demonstrated to estimate accurately the thermodynamic data of tristearate (ΔH_{f° = -2176.9 kJ/mol and ΔG_{f° = -504.5 kJ/mol) from Aspen plus. A thermodynamic model for

the total hydrogenation of tristearate was derived for temperatures between 250-450 C and hydrogen pressures ranging from 7 to 70 bar. The reaction was assumed to enable isothermal reaction conditions. Phase equilibrium liquid-gas was considered in the model, too (Peng–Robinson and Ideal EOS = Equation of State).The basic reaction mechanism of the proposed catalytic transformation is summarised and consists of two main reactions: hydrodeoxygenation and hydrodecarboxylation, completed by water-gas-shift reaction and CO formation. The thermodynamic balance of the system was used to predict the composition of the liquid phase, namely to predict the distribution of C_{17} and C_{18} hydrocarbons. The predictions suggest that C_{18} hydrocarbons are the main reaction products and that their concentration is affected by temperature and particularly by pressure. Moreover, the model predictions were found to be in good agreement with experimental data. The estimations suggested that the reaction were limited by hydrogen and triglyceride diffusivity through the liquid film on catalyst particles (Guzman et al., 2010).

Guzman et al., 2010 studied hydroprocessing of crude palm oil (CPO) using conventional hydrotreating with NiMo/γAl_2O_3 catalyst. The obtained products were characteristic by GC-MS. It was found when pressure is decreased (15 bar), product yields from n-C16 to n-C18 increased due to increasing number of products and cannot specified exactly products like octadecenes, octadecanol, n-hexadecanoic acid, actadecanal and hexa-actadecyl hexadecanoate.There are the intermediates of reactions. On the other hand, pressure is increased (90 bar), decreasing number of products can be indentified because intermediates were not found and fatty acids is reduced as well. Subsequently, test pressure effect and hydrogen consumption via simulated in Aspen plus. It was found that. The hydrodeoxygenation reaction is better than decarboxylation and decarbonylation when pressure increased (10-100 bar) and increasing hydrogen consumption. Moreover, time analysis was obtained by simulated distillation curves, the best diesel yields (95.3 %vol) was observed at 4 hours.

3.5 Catalyst selection

Kubicka and Kaluza, 2010 focuses on investigation of Mo, Ni and NiMo sulfide catalysts prepared by impregnation of commercial Al_2O_3 support having specific surface

area equal to 344 m^2/g. The experiments were carried out in a fixed-bed reactor at 260–280˚C, hydrogen pressure 3.5 MPa and LHSV 0.25–4 h^{-1}. Organic- liquid-phase analysis provided evidence of the differences in reaction pathways over the studied catalysts. The activity of catalyst, rate of triglycerides and oxygen disappearance increased in the order Ni/Al_2O_3 < Mo/Al_2O_3 < $NiMo/Al_2O_3$. Ni/Al_2O_3 was found to catalyze selectively decarboxylation of fatty acids while Mo/Al_2O_3 was found to catalyze selectively hydrodeoxygenation, on the other hand, there were only minor concentrations of decarboxylation products and consequently the hydrogenation (hydrodeoxygenation) pathway was nearly the exclusive one. $NiMo/Al_2O_3$ catalyst yielded both hydrogenation and decarboxylation products. It is know the optimum metal ratio Ni/(Ni + Mo) for desulfurization and highest conversion are about 0.3 and 0.2 respectively. Application of selecting catalysts gets along well with reaction. The hydrogenation is suitable for sulfide catalyst, which was active in unsaturated compounds (Filho et al., 1993) and hydrogenolysis is suitable for reduced catalyst. So we have to find the compatible catalyst with hydroprocessing process. (Walendziewski et al., 2009)

Simakova et al., 2009 had studied on the four difference of palladium on synthetic carbon support by precipitation method with varying pH of palladium hydroxide solution which explain where else to obtain the various metal dispersion and then characterized as well as tested in deoxygenation of steric acid and palmitic acid mixture. It was found that an optimum Pd dispersion that obtained the highest activity was the sample B and sample C resulting from their high surface concentration of Pd active sites. Piqueras et al., 2008 studied $Pd/\gamma\text{-}Al_2O_3$ catalysts of different metallic particle sizes and modified with 2-chloro-butane as well as the use of supercritical propane because they have information about the sizes of metal and supercrical fluid has an effect on reaction selectivity and specific activity of triglyceride. In adddition, they studied reaction pathway by DFT calculation and FTIR measurement. It is due to the electronic properties of paladium cluster that influence on adsorption properties. It was found that the catalyst with small Pd particles which modified with chloride having lower amount of isomerization product as well as increasing saturated fatty acid chains in the same time.

3.6 Bimetallic carbide and nitride catalysts

Several researchers have tried to develop new catalysts for hydroprocessing because waste cooking crude oil feedstocks contain amounts of sulfur, nitrogen, and oxygen, which form to heteroatom compounds. Most work has been carried out with sulfides such as Ni-Mo-S/Al_2O_3 and Co-Mo-S/Al_2O_3. Recently, in metallic oxycarbide and oxynitride-supported system, especially, transition metal carbides and nitrides have demonstrated to improved performance over the original catalysts, which have shown excellent performance for use in hydrodenitrogenation (HDN), hydrodesulfurization (HDS) and hydrodeoxygenation (HDO) reactions.

Metal carbides and nitrides were prefer label sulfur resistant since the structure of the active catalytic surface of alumina-supported molydenum carbide and nitride, which were found superior HDS activities when compared to sulfided Mo catalysts. It was found that the carbide was more active than the nitride, Sajkowski and Oyama 1996 studied Mo_2C/Al_2O_3 had activity over two times greater than commercial sulfides Mo-Ni-S/Al_2O_3 catalyst. Oyama et al., 1997 were found the bimetallic compounds showed activity and stability compared with the corresponding monometallic carbides.

The supported bimetallic oxycarbide was synthesized by temperature-programmed reaction (TPR). The catalysts were characterized by CO chemisorption, BET surface area measurement, X-ray diffraction (XRD), X-ray photoelectron spectroscopy (XPS), near-edge X-ray absorption fine structure (NEXAFS). The supported bimetallic materials were tested in HDN of quinoline and HDS of dibenzothiophene. As the result, The HDN and HDS activity were higher activities than the monometallic, the bulk bimetallic and the commercial sulfided Ni-Mo/Al_2O_3 compared on basis of active sites. The HDS activity increases with higher amounts of molybdenum metal ratio, HDS conversion increase with the concentration of carbidic carbon on the surface observed from NEXAFS. The catalysts did not deactivate with time on stream because amount of sulfur occupies small fraction on the surface in from metal sulfide after the hydroprocessing reaction. Moreover, the electronic properties of the oxycarbide were modified by the interaction with the Al_2O_3 support (Schwartz et al., 2000).

3.7 Properties of production

Physiochemical properties of the organic liquid products and mixed fuels were determined using standard test procedures designated for diesel fuel or petroleum products.

Simacek et al., 2010; Walendziewski et al., 2009 studied physical properties of products, which was blend onto mineral diesel fuel in several concentration levels ranging from 5 to 30 wt%. The product obtained by hydroprocessing of rapeseed oil at 360˚C and hydrogen pressure of 70 bar was chosen for mixing with diesel fuel from 5 to 30 wt%. As the result, the cetane number increased from 52 (pure mineral diesel) up to 66 (mixed with fuel containing 30 wt%). On the other hand, the addition of product worsened the low-temperature properties of mixed fuels in comparison with the basic mineral diesel, cloud point and pour point as well as cold filter plugging point (CFPP) were worse. Flash points of mixed fuels were comparable or slightly higher than mineral diesel fuel. It will be necessary to remove light hydrocarbons in order to increase its ignition temperature (Walendziewski et al., 2009).

CHAPTER IV

EXPERIMENTAL

4.1 Catalyst Preparation

4.1.1 Preparation of bimetallic oxide supported on γ-Al_2O_3

The γ-Al_2O_3 with a surface area of 113.8 m^2/g was used as support. The metal salts used to provide the required metals including ammonium heptamolybdate $(NH_4)_6Mo_7O_{24}.4H_2O$ (99.99%, March), nickel nitrate hexahydrate $Ni(NO_3)_2.6H_2O$ (99.99%, Aldrich) and cobalt nitrate hexahydrate $Co(NO_3)_2.6H_2O$ (99.99%, Aldrich), corresponding to the atomic ratio [x/(x+Mo)] = 0.3 by symbol x was cobalt or nickel. A heated deionized water at 100°C mixed with $(NH_4)_6Mo_7O_{24}.4H_2O$ and $Ni(NO_3)_2.6H_2O$ (9.4 wt% Mo and 2.45 wt% Ni) or $Co(NO_3)_2.6H_2O$ (9.71 wt% Mo and 2.54 wt% Co). Then, the aqueous solution was added dropwise to γ-Al_2O_3 support (Vallejo et al., 2005). The incipient wetness co-impregnation was carried out in three steps with intermediate drying and calcination in order to avoid precipitation of the mixture. The 40%, 35% and 25% of total amount of precursor was impregnated in the first step, second step, and third step, respectively. Normally, 1 ml of liquid precursor were applied to 2 g γ-Al_2O_3 for a batch of catalyst preparation. After precursor dropped in each impregnation, the material were dried at 120°C for 5 h and then calcined at 500°C (ramp rate 3°C /min) for 5 h in air. After calcination, the NiMo/Al_2O_3 and CoMo/Al_2O_3 oxide catalysts were activated either presulphidation or pre carburization.

4.1.2 Presulphidation process

The $NiMo/Al_2O_3$ and $CoMo/Al_2O_3$ oxide catalysts were presulphided using a mixture of H_2S/H_2 (5 vol%H_2S) at a gas flow rate of 50 ml/min and 400°C for 2 h before used in reaction The flow diagram of sulphided catalysts is shown in Figure 4.1.

4.1.3 Precarburization process

The metal oxide catalysts were converted into carbide in a reactive gas flow of 20% CH_4/ H_2.

The flow diagram of synthesis metal carbide catalysts is shown in Figure 4.1. The supported oxycarbide were prepared by passing a 20% CH_4/H_2 (v/v) gas mixture over approximately 0.2 g of the solid precursor. The synthesis was carried out in a tubular reactor of 8 mm o.d. (6 mm i.d.) placed in a furnace controlled by a temperature controller. First the sample was heated to 400˚C at heating rate of 3°C/min under He (with flow rate of 50 cm^3/min). When the temperature approach 400°C, He was switched to 20% CH_4/H_2 (v/v) gas mixture at flow rate of 50 cm^3/min, and then the temperature was ramped at heating rate of 1°C/min from 400 to 700°C. The carburization of sample was monitored by analyzing the consumption of methane and the formation of CO and CO_2 using gas chromatography with thermal conductivity detector (GC-8A). The 20% CH_4/H_2 (v/v) gas mixture passed through the sample until no CO and CO_2 were detected in the exhausted gas. Then the gas flow was switched from CH_4/H_2 to He, and the sample was cooled down to room temperature. After cooling, the He gas was switched to a gas mixture containing 1% O_2 in He (v/v) stream for 16 h to form a protective oxide layer that prevented bulk oxidation. Before used in reaction, catalysts were reduced at 400°C in H_2 flow for 2 h to remove and protective oxide layer. (Schwartz et al., 2000)

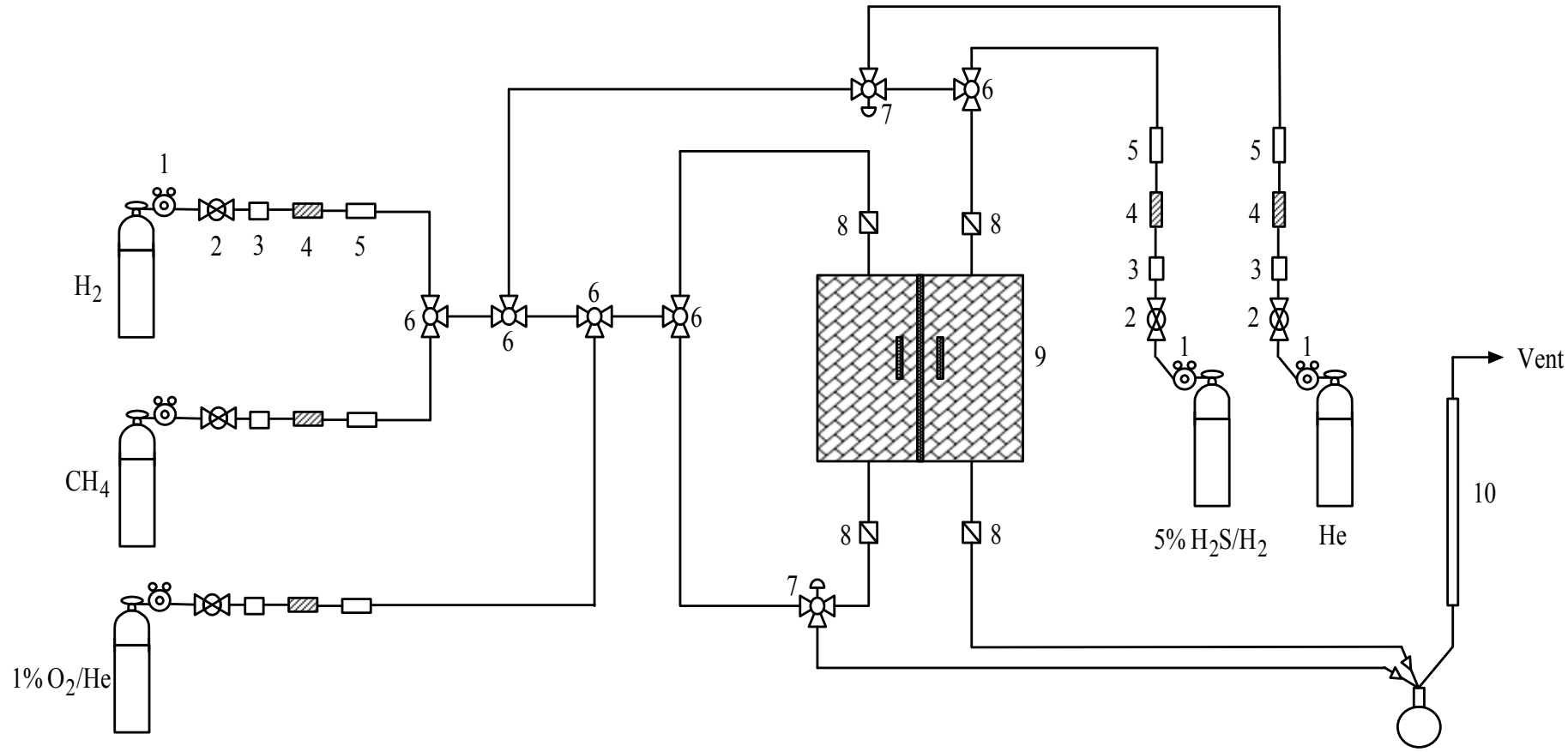

1. Pressure Regulator
2. On-Off Value
3. Gas Filter
4. Mass Flow Meter
5. Check Valve
6. 3-way
7. 3-way Valve
8. Sampling point
9. Furnace
10. Bubble Flow Meter

Figure 4.1 Flow diagram of synthesis metal carbide and sulphided catalysts.

4.2 Catalyst Characterization

4.2.1 X-ray diffraction (XRD)

XRD was be performed to determine the bulk phase of catalysts by SIEMENS D 5000 X-ray diffractometer connected to a computer with Diffract ZT programs version 3.3 for fully control of the XRD analyzer. The experiments were carried out by using CuK_{α} radiation with Ni filter in the 2θ range of 20–80 degrees resolution 0.04°. The crystallite size was estimated from line broadening according to the Scherrer's equation.

4.2.2 Nitrogen physisorption (BET surface area)

The BET apparatus for the multiple point method consisted of two feed lines for helium and nitrogen (Micromeritics ASAP 2020). The flow rate of the gas will be adjusted by means of fine-metering valve on the gas chromatograph. The sample cell made from pyrex glass. The mixture gases of helium and nitrogen will flow through the system at the nitrogen relative in the range of $0.05 < P/P_0 < 0.35$. The catalyst sample (ca. 0.05 g) will be placed in the sample cell, which will be then heated up to 150°C and will hold at this temperature for 3 h. After the catalyst sample was cooled down to room temperature, nitrogen uptakes will be measure as follows.

- Adsorption step: The sample that set in the sample cell will be dipped into liquid nitrogen. Nitrogen gas which flow through the system will be adsorbed on the surface of the sample until equilibrium reached.
- Desorption step: The sample cell with nitrogen gas-adsorption catalyst sample will dip into the water at room temperature. The adsorbed nitrogen gas will be desorbed from the surface of the sample. This step will be completed when the indicator line will be in the position of base line.
- Calibration step: 1 ml of nitrogen gas at atmospheric pressure will be injected through the calibration port of the gas chromatograph and the area will be measured. The area will be the calibration peak.

4.2.3 Temperature-programmed reduction (TPR)

TPR was used to determine the reduction behaviors of the samples using a Micrometritics Chemisorb 2750.

- The catalyst sample of 0.05 g was placed in the sample cell.
- Prior to operation, the catalysts were heated up to 150°C in flowing nitrogen and held at this temperature for 1 h.
- After the catalyst sample was cooled down to room temperature, the 5% H_2 in Ar (30 cm^3/min) carrier gas was fed with ramping temperature from 35 to 800°C at 10°C/min.
- A cold trap was placed before the detector to remove water produced during the reaction.
- A thermal conductivity detector (TCD) was used to determine the amount of hydrogen consumption during TPR.

4.2.4 Carbon monoxide chemisorption

Static CO chemisorption at room temperature on the reduce catalysts will be used to determine the number of reduce surface molybdenum, nickel or cobalt metal atoms. The total CO chemisorption will be calculated from the number of injection of a known volume. CO chemisorption will be carried out following the procedure using a Micrometritics Pulse Chemisorb 2750 instrument at the Analysis Center of Department of Chemical Engineering, Faculty of Engineering, Chulalongkorn University. In an experiment, about 0.05 g of the catalyst sample was placed in a glass tube. Prior to chemisorption, the catalysts will be reduced at 400°C for 2 hour after ramping up at a rate of 10°C/min. After that, 30 µl of carbon monoxide was inject to catalyst and repeat until desorption peak constant. Amount of carbon monoxide adsorption on catalyst was relative amount of active site.

4.2.5 Thermal gravimetric analysis (TGA)

The spent Ni-Mo/Al_2O_3, Co-Mo/Al_2O_3 sulphided and carbide catalysts were subjected to the thermogravimetric and differential thermal analysis (Diamond Thermogravimetric and Differential Analyzer, TA Instruments SDT Q600) to determine the carbon content in the spent catalysts, as well as their thermal behaviors in the range of 30-800°C. The analysis was performed at a heating rate of 10°C /min in 400 ml/min flow of air.

4.3 Experimental Setup

Six cylindrical batch reactor (90 mmID, 95 mm in lengh with a volume of 5 cm^3) were placed in a furnace with temperature controller as shown in Figure 4.2. The position of the second to the fifth do not the temperature gradient but the position of the first and the last do not match with temperature controller. Hence, we can put the four reactor into the furnace per one at a time.

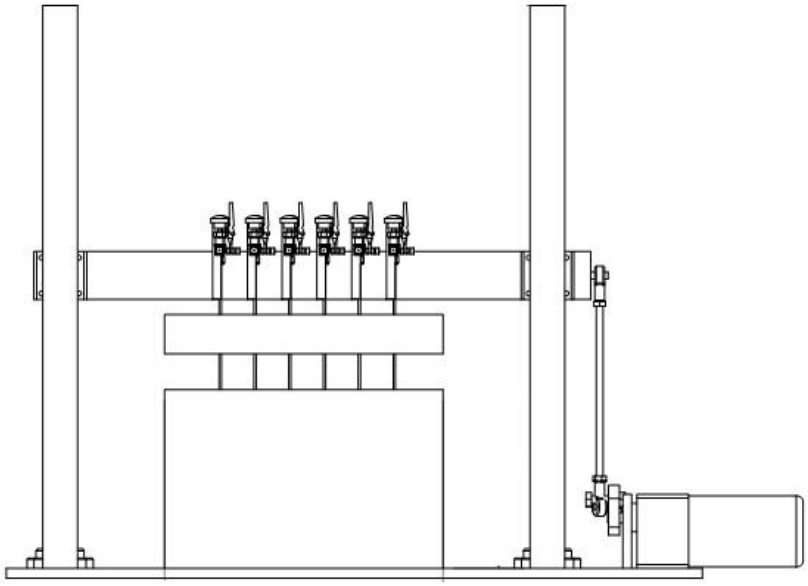

Figure 4.2 Illustrated of shaking batch reactor.

4.4 Experimental Procedure

4.4.1 Pretreatment of Feed Stock

The waste cooking palm oil (WCPO) was obtained from Sarmyarn restaurant in Bangkok. The WCPO contains some food particles, phospholipids, grease, and wax etc. The general process of pretreatment consists of two steps including filtration and dehydration. Initially, suspended solid impurity was removed by filtration and then the WCPO was repeatedly water washed and shaken for extraction of water soluble impurities as well as phospholipids. After that the waste cooking palm oil was heated to above 105˚C for 1 h to get rid of the water by evaporation (Banerjee and Chakraborty, 2009; Meng et al., 2008; Patil et al., 2010).

In addition, to study the effect of sulfur on the hydroprocessing performance, WCPO was added with dibenzothiophene upto 1000 ppm of sulfur (0.1 wt%). The sulfur and coke formation can deactivate the catalysts (Senol et al., 2007). Therefore, we can study sulfur content in feed has effect in the each type of catalysts.

4.4.2 Reaction Performance Testing

The WCPO and catalyst were loading into a tubular reactor. The reaction condition for hydroprocessing experiments were follows in Table 4.1.

Before the reaction was performed, the reactor was purged with He for 3 times to remove air in the reactor. After that, the reactor was compressed hydrogen pressure of 50 bar. The reactor was put into the furnace by shacking 30 rpm. When complete the reaction, the reactor was put out of the furnace dip into water for stop the reaction.

Table 4.1 Operating condition for hydroprocessing

Variable	Condition
Amount of WCPO	2 ml
Temperature	360, 380, 400 and 420°C
Hydrogen pressure	50 bar
Reaction time	2, 4, 6 and 8 h
Catalyst type	Ni-Mo/Al_2O_3 and Co-Mo/Al_2O_3 sulphided
	Ni-Mo/Al_2O_3 and Co-Mo/Al_2O_3 carbide
Amount of catalyst	0.01 and 0.1 g

4.5 Feed Stock and Product Characterization

After the reaction run, organic product liquid, gas product and spent catalysts were physically separated and analyzed using several gas-chromatography methods.

4.5.1 Product Liquid Characterization

The compositions of WCPO analyzed by gas chromatography with mass spectrometry (GC-MS). The method was used as reference standard mixture containing 10 mg/ml of the WCPO in methylene chloride (CH_2Cl_2). For the quantification of reaction products, the samples analyzed by GC–MS system included an Agilent 5973 N mass-selective detector (MSD) and an Agilent 6890 gas Chromatograph, equipped with a capillary column (HP-5, 5% phenyl methyl siloxane 30 m 250 µm 0.25 µm nominal). One microliter of the sample was injected into the column. The injection was performed in splitless mode. Helium was used as a carrier gas. The oven temperature program

involved the following steps: starting temperature at 100°C with increments of 10°C/min up to 250°C and a holding time of 5 min at 250°C (Patil et al., 2010).

Organic liquid products were analyzed by gas-chromatography equipped with flame ionization detector (GC-14B, Shimadzu). In addition, distillation temperature were determined by simulated distillation according to the ASTM-2887-D86 procedure. The operating condition for gas chromatograph equipped with flame ionization detector and Operating condition temperature program is shown in the Table 4.2

Table 4.2 Operating condition for gas chromatograph equipped with flame ionization detector.

Gas Chromagraph	SHIMADZU GC-14B
Detector	FID
Column	Capillary DB-2887
	(Agilent J&W GC Columns)
- Column material	Silica
- Length	10 m
- Outer diameter	0.53 mm
- Film thickness	3 µm
Spilt flow rate	30 ml/min
Purge flow rate	4 ml/min
Carrier gas	He (99.999%)
Carrier gas flow	70 kPa
Hydrogen gas flow	60 kPa

Table 4.2 Operating condition for gas chromatograph equipped with flame ionization detector (cont.)

Gas Chromagraph	SHIMADZU GC-14B
Air gas flow	50 kPa
Primary gas flow	500 kPa
Make up flow	60 kPa
Temperature limits (^oC)	-60 - 350
Injector temperature (^oC)	250
Column oven temperature program	
- initial column temperature (^oC)	40
- ramp rate (^oC/min)	10
- final column temperature (^oC)	330
Detector temperature (^oC)	340
Analysed liquids	Hydrocarbon normal C_5-C_{44} alkanes

The program simulated distillation curve was determined according to the ASTM-2887-D86 procedure. The products in the temperature range of 250-380°C is a suitable for diesel range (nC_{15}-nC_{18}) as shown in Table 4.3.

Table 4.3 Specified temperature range in program. (Huber et al., 2007)

The straight chain alkanes	Range of temperature (°C)
Lighter alkanes	-50 to 65
Alkanes C_5-C_8	65-150
Alkanes C_9-C_{14}	150-250
Alkanes C_{15}-C_{18}	250-380
Intermediates and the alkanes < C_{20}	380-520
The tri-glycerides and fatty acids	520-1000

4.5.2 Product Gas Characterization

Gas products were analyzed by gas-chromatography with 2 m molecular sieve 5A and a 2 m porapak Q column equipped thermal conductivity detector (GC-8A, Shimadzu). Operating condition for gas chromatograph equipped thermal conductivity detector is shown in the Table 4.4.

Table 4.4 Operating condition for gas chromatograph equipped thermal conductivity detector.

Gas Chromagraph	SHIMADZU GC-8A	SHIMADZU GC-8A
Detector	TCD	TCD
Column	Molecular sieve 5A	porapak Q
- Column material	Stainless steel	Stainless steel
- Length	2 m	2 m
- Outer diameter	4 mm	4 mm
- Inner diameter	3 mm	3 mm
- Mesh range	60/80	50/80
- Maximum temperature (^oC)	350 ^oC	350 ^oC
Carrier gas	He (99.999%)	He (99.999%)
Carrier gas flow	75 cm^3/min	75 cm^3/min
Column temperature		
- Initial column (^oC)	60	60
- Final column (^oC)	60	60
- Injector (^oC)	100	100
- Detector (^oC)	100	100
Current (mA)	80	80
Analysed gas	CO and CH_4	CO_2 and C_3H_8

CHAPTER V

RESULTS AND DISCUSSIONS

This chapter is divided into four sections. The first section described about the characteristics and the catalytic properties of $NiMo/Al_2O_3$, $CoMo/Al_2O_3$ sulphided catalysts and $NiMo/Al_2O_3$, $CoMo/Al_2O_3$ carbide catalysts by using several techniques such as XRD, BET surface area, H_2-TPR and CO-chemisorption. The second section reported the reaction performance of the catalysts with their corresponding product distribution. The third section reported coke formation of the spent catalysts. Finally, fourth section showed activity of fresh, spent and regenerated catalysts in reaction.

5.1 characterizations of catalysts

5.1.1 X-ray diffraction (XRD)

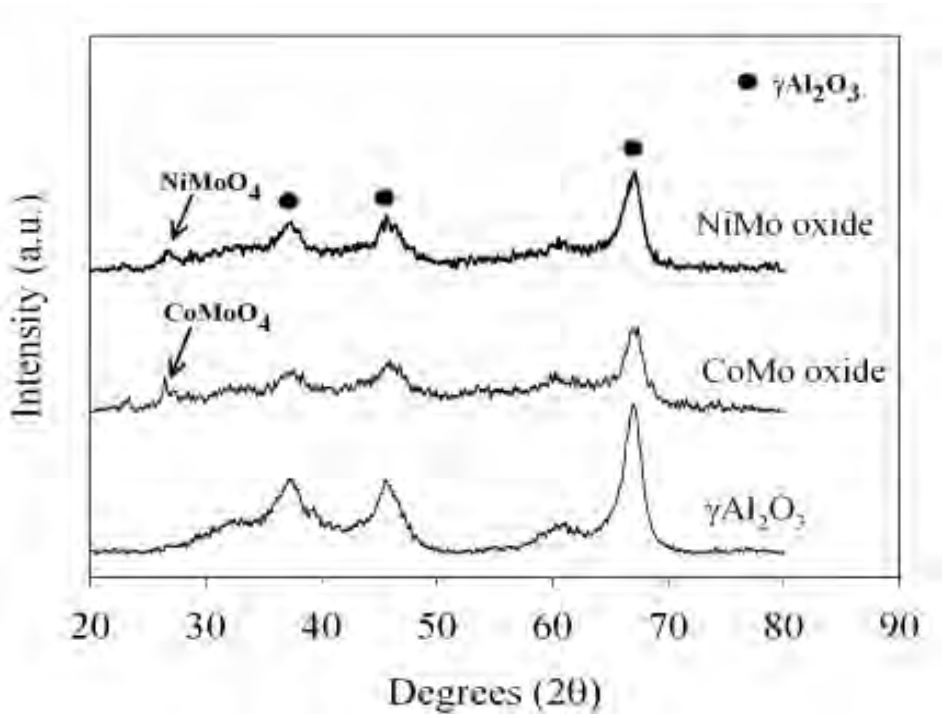

Figure 5.1 XRD patterns of γ-Al_2O_3 supports, $CoMo/Al_2O_3$ oxide and $NiMo/Al_2O_3$ oxide catalysts.

The XRD spectra for γ-Al_2O_3 supports, $CoMo/Al_2O_3$ oxide and $NiMo/Al_2O_3$ oxide catalysts are shown in Figure 5.1. Three peaks at 38°, 46° and 67° were observed for all catalysts. These three peaks were assigned to the γ-Al_2O_3 phase (Monteiro-Gezork et al., 2007; Sundaramurthy et al., 2008). For the oxide catalysts, the $CoMo/Al_2O_3$ and $NiMo/Al_2O_3$ oxide catalysts exhibits slight diffraction peak located at 26.48 and 26.56 respectively. This can be assigned the XRD peak of $CoMoO_4$ and $NiMoO_4$ which corresponding with Vallejo et at., 2005. In contrast, the characteristic peak of cobalt oxide (Co_3O_4 at 31°, 37°, 45°, 59°, and 65°), nickel oxide (37.3°, 43.3°, 62.8° and 75.5°) and molybdenum oxide (MoO_4 at 27°, 34°, 49°, 53°, and 55°) (Rojanapipatkul et al., 2008) are not appearance in our sample. The absence was due to the XRD pattern of γ-Al_2O_3 overlap with in the 2θ interval.

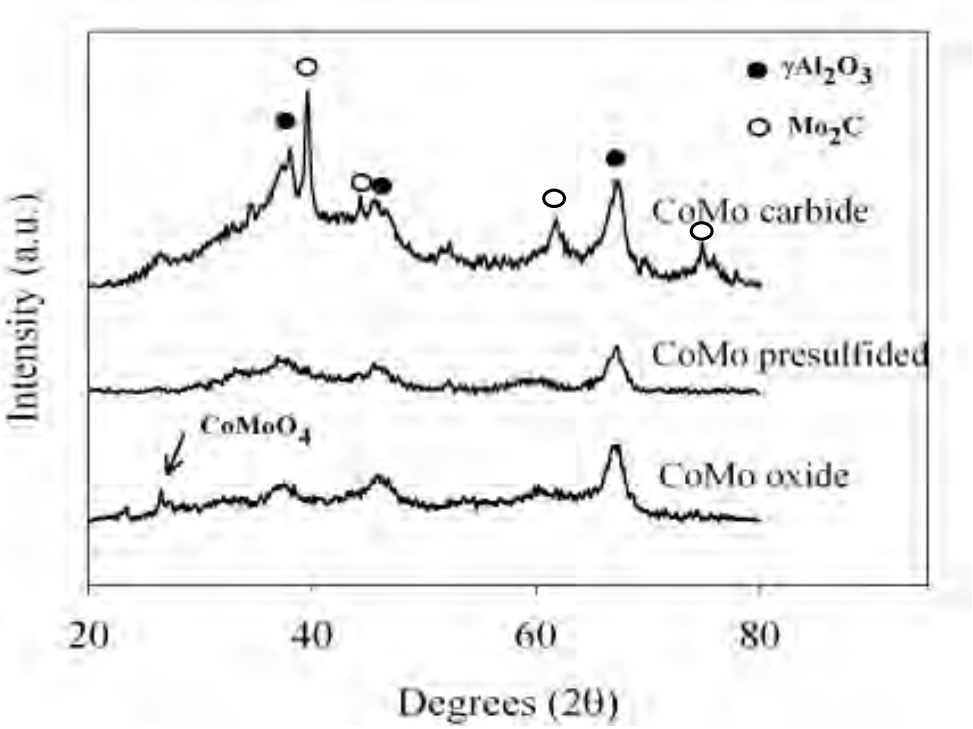

Figure 5.2 XRD patterns of $CoMo/Al_2O_3$ oxide, sulphided and carbide catalysts.

A clear difference can be found by comparing the XRD curves for the $CoMo/Al_2O_3$ oxide, sulphided and carbide forms as shown in Figure 5.2. The $CoMo/Al_2O_3$ oxide catalyst was sulphided using a mixture of H_2S/H_2 (5 vol%H_2S). The $CoMo/Al_2O_3$ sulphided catalyst do not show any MoS_2 phases peaks (33°, 59°) indicating that the MoS_2 phases are highly dispersed over the support and their particle sizes are below the detection limit of XRD technique or the formed MoS_2 amorphous phases (Sundaramurthy et al., 2008). It is only at high metal contents that some peaks become clearly outlined. The $CoMo/Al_2O_3$ oxide catalyst was converted into carbide in a reactive gas flow of 20% CH_4/ H_2. The molybdenum carbide phase has a structure with hexagonal symmetry. The typical β-Mo_2C crystals were observed at 38.9°, 44°, 64.5° and 74.3° (Sundaramurthy et al., 2006; Vallejo et al., 2005).

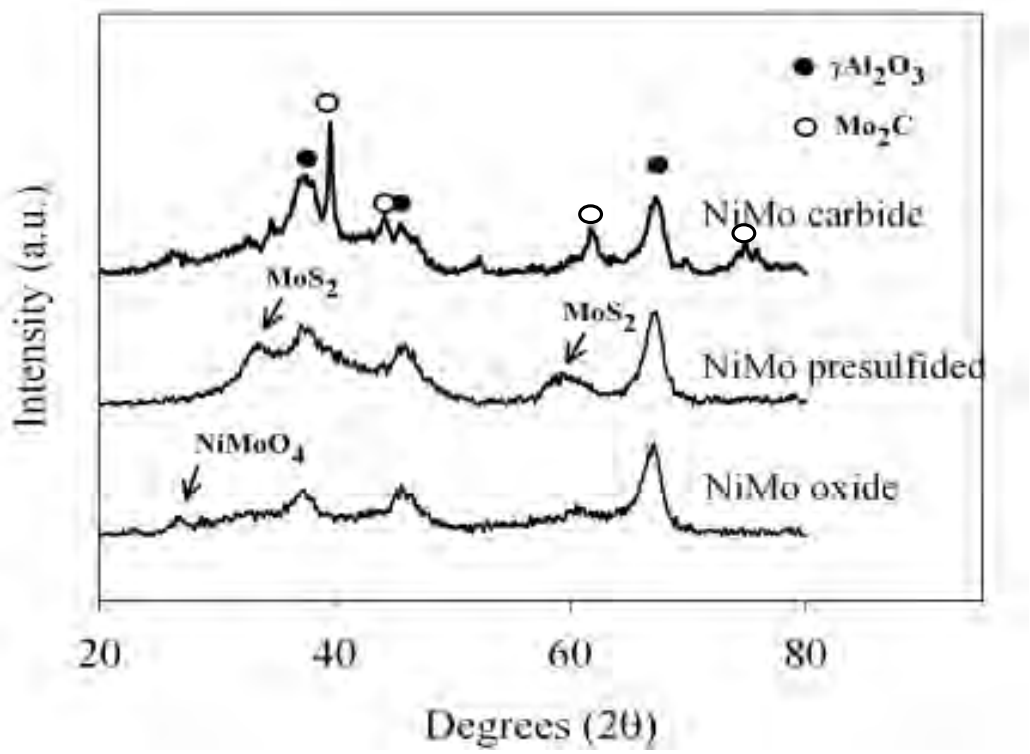

Figure 5.3 XRD patterns of $NiMo/Al_2O_3$ oxide, sulphided and carbide catalysts.

From the results, it can be observed the similar XRD patterns of $CoMo/Al_2O_3$ oxide and $CoMo/Al_2O_3$ sulphided catalysts. The XRD patterns of $NiMo/Al_2O_3$ oxide, sulphided and carbide catalysts are present in Figure 5.3. The attractive XRD peak at 26.58° can be attributed that the XRD peak of $NiMoO_4$. After sulphidation, two peaks at 33° and 59° were observed for the sulphided catalyst such as MoS_2, Ni_3S_2, NiS and $NiMo_2S_4$ (Monteiro-Gezork et al., 2007). Puello-polo et al., 2008 reported Mo^{4+} species could be the active center for converted to MoS_2. The XRD patterns did not exhibit significant peaks of Ni since its low loading. The XRD peak of identical β-Mo_2C crystals was observed at 38.9°, 44°, 64.5° and 74.3° (Sundaramurthy et al., 2006; Vallejo et al., 2005).

5.1.2 BET surface area

Table 5.1 The BET surface area, pore volume and pore diameter of support and various catalysts.

Catalyst	A_{BET} (m^2/g)	V_p (cm^3/g)	D_{BJH} (nm)
γ-Al_2O_3 support	113.8	0.2382	5.20
NiMo/Al_2O_3 oxide	97.24	0.1770	5.11
CoMo/Al_2O_3 oxide	94.10	0.1740	5.25
NiMo/Al_2O_3 carbide	70.62	0.1863	5.87
CoMo/Al_2O_3 carbide	73.32	0.1750	5.86

The BET surface area, pore volume and diameter of all catalyst samples are given in Table 5.1. The oxide phase catalysts can be represent similar surface area and pore structure to that of sulphided catalysts (Kubicka and Kaluza, 2010), therefore, we measure these physical properties of oxided catalyst to prevent the damage which might be occurred in the strument. After incorporation of NiMo and CoMo on γ-Al_2O_3, the surface area of NiMo/Al_2O_3 oxide and CoMo/Al_2O_3 oxide catalysts decreased from 113.8 to 97.24 and 94.10 m^2/g respectively. This is due to pore blockage of γ-Al_2O_3 support by the Co or Ni and Mo species (Sundaramurthy et al., 2006).

The BET surface area further decreased when NiMo/Al_2O_3 oxide and CoMo/Al_2O_3 oxide catalysts were converted into NiMo/Al_2O_3 and CoMo/Al_2O_3 carbide catalysts. Nevertheless, decrease in surface area sustained by supported carbides can be attributed to the increase of the metallic concentration in the form of carbon fiber on the surface (Vallejo et al., 2005). The presence of carbon fiber in prepared NiMo/Al_2O_3 and CoMo/Al_2O_3 carbide are illustrated by H_2-TPR which will be discussed later. The properties of the carbide catalysts were changed from slab structure to the hexagonal close-packed structure (Furimsky, 2003). Moreover, the pore volume and pore diameter slightly increased because sintering of support in carburization.

5.1.3 H_2-Temperature-programmed reduction (H_2-TPR)

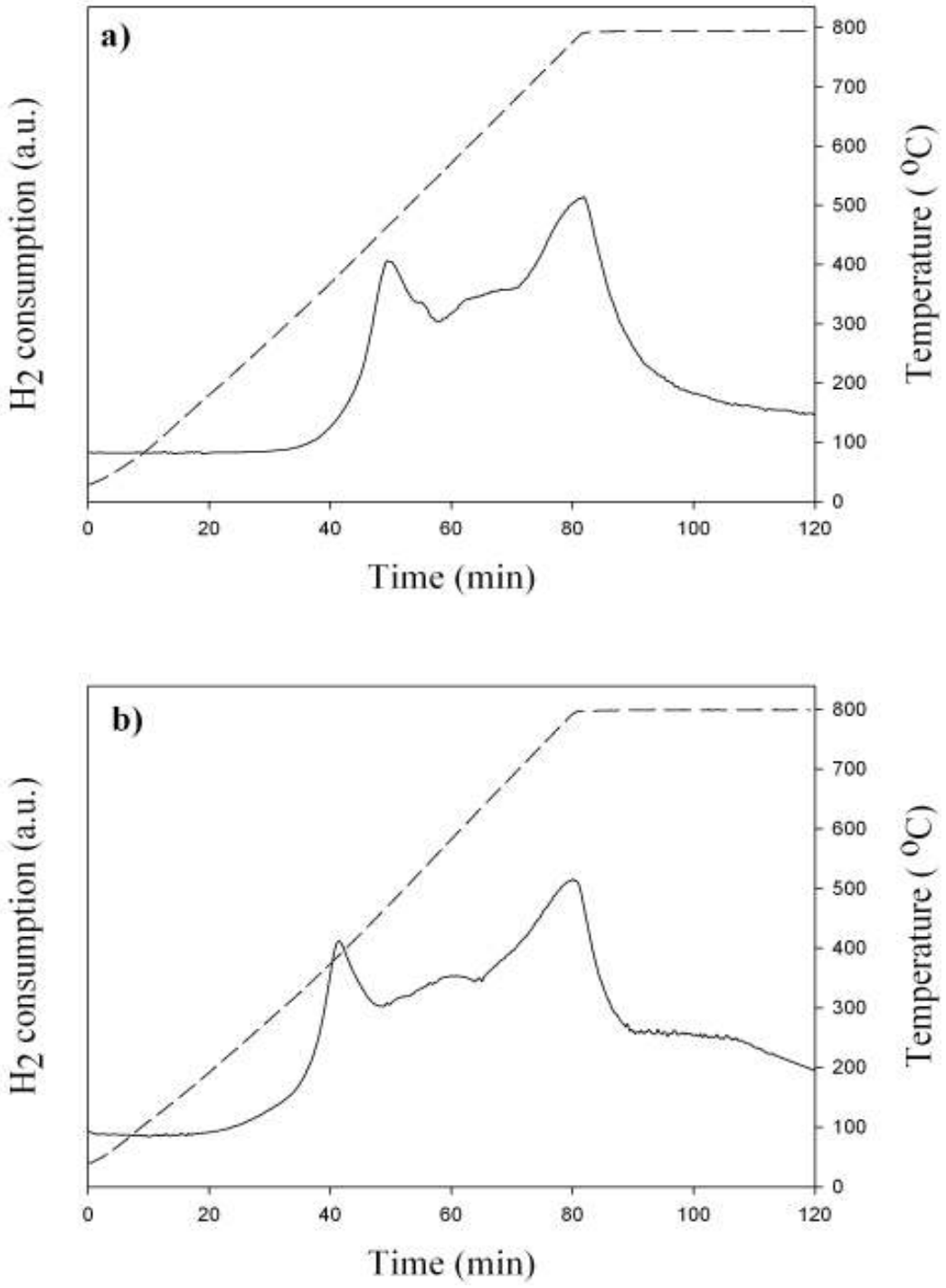

Figure 5.4 TPR profiles of a) $CoMo/Al_2O_3$ and b) $NiMo/Al_2O_3$ oxide catalysts.

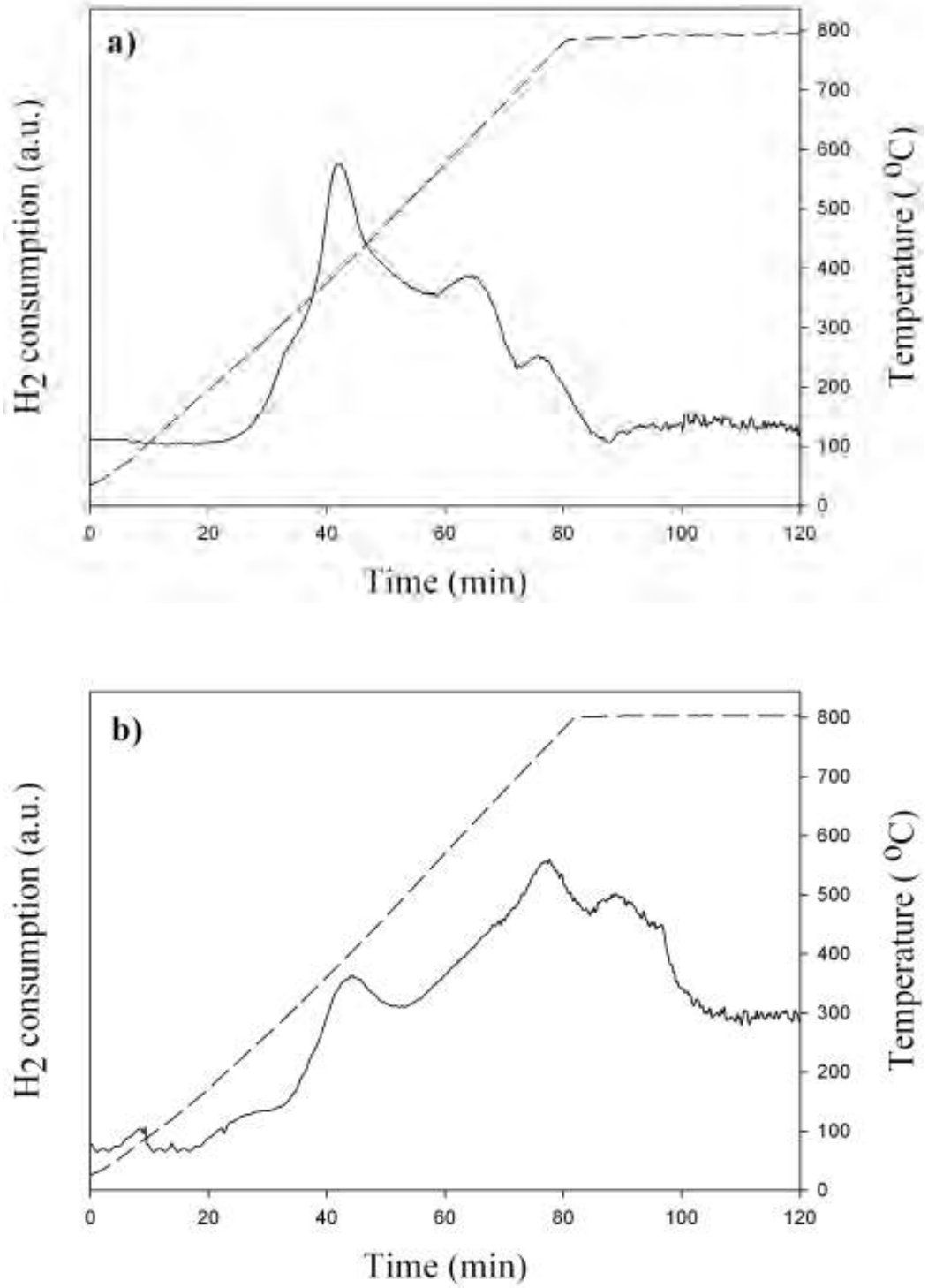

Figure 5.5 TPR profiles of a) $CoMo/Al_2O_3$ and b) $NiMo/Al_2O_3$ carbide catalysts.

Temperature-programmed reduction of hydrogen (H_2-TPR) was performed in order to determine the reduction behaviors. The H_2-TPR profiles of the $CoMo/Al_2O_3$ and $NiMo/Al_2O_3$ oxide catalysts are shown in Figure 5.4 a) and Figure 5.4 b) respectively. The TPR profile of $CoMo/Al_2O_3$ oxide catalyst contains three similar peak of reduction with $NiMo/Al_2O_3$ oxide catalyst at temperature from 200-800 ^oC. The results show the reduction of the $CoMo/Al_2O_3$ and $NiMo/Al_2O_3$ oxide catalysts were not completed until 800^oC. This can be suggested the presence of molybdenum species on the catalyst which is difficult to be reduced (Papadoupoulou et al., 2003).

The both peak of the $CoMo/Al_2O_3$ and $NiMo/Al_2O_3$ oxide catalysts reduction located at temperature lower than 400^oC could be assigned to the reduction of surface oxygen bonded of MoO_3 in the oxide precursor (Wei et al., 1997). The reduction temperature for $CoMo/Al_2O_3$ oxide was observed first peak at temperature 470 ^oC. The absence of any TPR peak to the reduction of Co oxide to Co^{2+} metal at temperature 350^oC that corresponding to the bulk cobalt oxide could be attributed to the well dispersed Co^{2+} species (Papadopoulou, 2004). While, the reduction temperature for $NiMo/Al_2O_3$ oxide was observed first peak at temperature 400^oC. Zielinski et al., 1997 reported the TPR profile of nickel supported on γ-Al_2O_3 has three ranges of the reduction process. Only reduction process of NiO (not interacted with γ-Al_2O_3) were located between temperature 240-260 ^oC and two ranges of NiO (interacted with γ-Al_2O_3) were located between temperature 420-440 ^oC and 520-540^oC.

The first peak of the TPR profile of $CoMo/Al_2O_3$ and $NiMo/Al_2O_3$ oxide catalysts are different because the promoter such as cobalt or nickel metal has different TPR profiles. Moreover, the TPR profiles of all catalysts have depend on molybdenum, which is based metal catalyst.

The TPR profiles were in accordance with the bulk MoO_3 also contains three reduction peaks at temperature range 400-490, 490-590 and 800^oC (Clark and Oyama, 2003), which correspond to the two-steps reduction of MoO_3 to MoO_2 and then to $Mo^{\delta+}$ metal (Zepeda et al., 2006). The peak of reduction at temperature 400 to 490 ^oC corresponding to the reduction of MoO_3 to MoO_2 was observed (Sundaramurthy et al., 2006). This behavior is typical of the reduction of bulk MoO_3 in hydrogen. After that, the reduction peak located about temperature range 490-590 and 800^oC indicated the reduction behavior of MoO_2 to $Mo^{\delta+}$ has been assigned to low oxidation state species ($0 \leq \delta \leq 2$) (Polo and Brito, 2008),which are strong interaction with the alumina support (Ramirez et al., 2000). Furthermore, the reduction of $CoMoO_4$, which was

reported to reduce in two steps, leading to two reduction peaks at temperature 517 and 707°C (Arnoldy et al., 1986).

In the Figure 5.5 a) and Figure 5.5 b) shows the H_2-TPR profiles of the $CoMo/Al_2O_3$ and $NiMo/Al_2O_3$ carbide catalysts. These TPR profiles clearly show a distinct behavior of catalysts towards hydrogen reduction. The $CoMo/Al_2O_3$ and $NiMo/Al_2O_3$ carbide catalysts have peak maximam at around 400 ^{o}C. This peak is due to the reduction of surface oxygen on passivated carbided Mo (Sundaramurthy et al., 2006) and promoter such as Co and Ni metal. The absence of above peak at lower temperature in carbide catalysts show that MoO_3 is completely converted into carbide during carburization.

Izhar et al., 2007 studied the spectra of the CH_4 desorption during the TPR were deconvoluted into α-MoC (487°C), β-Mo_2C (587°C), pyrolitic carbon (687°C), η-Mo_3C_2 (787°C), and graphitic carbon (876°C). The $CoMo/Al_2O_3$ and $NiMo/Al_2O_3$ carbide catalysts exhibited mainly η-Mo_3C_2 at peak 778 ^{o}C and the $CoMo/Al_2O_3$ and $NiMo/Al_2O_3$ carbide catalyst exhibited pyrolitic carbon at 667°C. The H_2-TPR profile of the both carbide catalysts can be overlap and very complex, which are difficult to specific for each peak. Due to the maximum operating temperature of the apparatus at 800°C, no presence of the final peak that graphitic carbon was observed at 876°C.

It should be note that the reduction temperature peak is shifted to low temperature on higher nickel addition. Furthermore, the higher cobalt compositions, CoMoC oxide tends to transform into CoMoC at lower carburization temperature (Sundaramurthy et al., 2006).

5.1.4 Carbon monoxide chemisorption

Table 5.2 Amount of carbon monoxide adsorbed on catalysts.

Catalysts	Total CO chemisorption µmol CO/g.cat	Active site, Molecule/g.cat ($*10^{18}$)	CO chemisorption/ BET surface area µmol CO/m^2
$NiMo/Al_2O_3$ sulphided	55.0	33.1	0.57
$CoMo/Al_2O_3$ sulphided	50.5	30.3	0.53
$NiMo/Al_2O_3$ carbide	43.4	26.1	0.61
$CoMo/Al_2O_3$ carbide	44.6	26.8	0.60

The amount of carbon monoxide adsorption on the catalysts was performed in order to determine the number of reduced metal surface atoms. The amount of adsorbed CO is directly proportional to the active site of catalyst. The results CO chemisorption for all catalysts was summarized in Table 5.2. The sulphided and carbide catalysts were activated with hydrogen at 400°C for 2 h in order to remove the inactive oxide layer.

The result showed that the total CO chemisorption decreased in the following order: $NiMo/Al_2O_3$ sulphided > $CoMo/Al_2O_3$ sulphided > $CoMo/Al_2O_3$ carbide > $NiMo/Al_2O_3$ carbide catalysts were 55.0, 50.5, 44.6 and 43.4 µmol CO/g.cat respectively. In addition, the CO chemisorption result was corresponding with Izhar et al., 2007 reveal that the number of active site was not depend on the BET surface area. Whereas, the CO chemisorption increased when compared surface of catalyst were 0.53, 0.57, 0.60 and 0.61 µmol CO/m^2 with $CoMo/Al_2O_3$ sulphided, $NiMo/Al_2O_3$ sulphided, $CoMo/Al_2O_3$ carbide and $NiMo/Al_2O_3$ carbide respectively. It can be concluded that, the active site of carbide catalysts are inferior to sulphided catalysts when the active site is compared on the basis of a unit of catalyst weight. Moreover, the active site of carbide catalysts expressed per unit of surface increases with decreasing surface and/or increasing particle size (Furimsky, 2003).

5.2 Reaction performance with corresponding product composition

5.2.1 Composition of WCPO

The WCPO was obtained from Sarmyarn restaurant in Bangkok. The WCPO contains some food particles, phospholipids, grease, and wax. The genaral process of pretreatment consists of two steps including filtration and dehydration (Meng et. al., 2008). The compositions of WCPO analyzed by gas chromatography with mass spectrometry (GC-MS) are presented in Table 5.3. From GC–MS analysis, it was found that WCPO contains mainly 47.15 wt% of palmitic acid.

Table 5.3 Chemical compositions of pretreated waste cooking palm feedstock (exclude triglycerides).

Fatty acid composition	Wt%
Palmitic acid (C16:0)	47.15
Stearic acid (C18:0)	13.01
Oleic acid (C18:1)	17.12
Others	
Octadecanol ($C_{18}H_{38}O$)	7.92
Hexanedioic ($C_{22}H_{42}O_4$)	14.8

Hydroprocessing of WCPO was performed in shaking batch reactor with a catalyst were chose as following: NiMo/Al_2O_3, CoMo/Al_2O_3 sulphided catalysts and NiMo/Al_2O_3, CoMo/Al_2O_3 carbides catalysts under operating temperatures of 360, 380, 400 and 420°C, hydrogen pressure of 50 bar and reaction times of 2, 4, 6 and 8 h. After reaction was performed for a desired period, the reactor was quenched in cooled water. Gas and organic liquid phase were physically separated and, analyzed using several gas-chromatography methods. Gas products (carbon monoxide, carbon dioxide, methane, propane) were analyzed by gas-chromatography with thermal conductivity detector. Organic liquid products were analyzed by gas-chromatography with flame ionization detector.

5.2.2 Organic liquid product

All organic liquid products were slightly yellowish or brownish liquids. At the temperature range 25-30°C they became solids. The fraction distillated from 250 to 380°C was the major distillated fraction, the diesel range (nC_{15}-C_{18}) were determined by program simulated distillation curve according to the ASTM-2887-D86 procedure. The reaction could not be taken place at reaction temperatures below 280°C as no desired product of n-C_{15}–C_{18} alkanes and no gas products can be detected. Simacek et al., 2010 reported that rapeseed oil can be completely converted by NiMo/Al_2O_3 catalyst with operating temperature of 360°C. Therefore, initial temperature of 360°C was first applied to our study.

The preparation of the correct material balance for the laboratory studies is a very difficult assignment (Walendziewski et al., 2009), therefore the reaction performance are defined in different approaches. Some researchers define reaction performance by using selectivities of nC_{15}-C_{18} alkanes products based on the total yield of organic liquid products (Kubicka and Kaluza, 2010; Immer et al., 2010; Guzman et al., 2010; Berzergianni et al., 2010). Berzergianni and Kalogianni, 2009 has defined the conversion and yields of nC_{15}-C_{18} alkanes products of base on a the total liquid products basis as shown in equation (1) and (2).

$$\text{Conversion (\%)} = \frac{\text{Feed}_{360+} - \text{Product}_{360+}}{\text{Feed}_{360+}}.100 \quad (1)$$

$$\text{Product selectivity (\%)} = \frac{\text{Product}_{A\text{-}B} - \text{Feed}_{A\text{-}B}}{\text{Feed}_{360+} - \text{Product}_{360+}}.100 \quad (2)$$

In equation (1), $Feed_{360+}$ and $Product_{360+}$ are wt% of the feed and product respectively, which have a boiling point higher than 360ºC. In equation (2), $Feed_{A\text{-}B}$ and $Product_{A\text{-}B}$ are the wt% of the feed and product respectively, which have a boiling point range between A and B degrees Celsius.

Huber et al., 2007 and Mikulec et al., 2010 used yield of diesel range instead of selectivity by assuming triglyceride and free fatty acid are completely converted. In our study, selectivity are defined selectivities of nC_{15}-C_{18} alkanes products (which corresponding to distillation temperature in the range of 250-380ºC) based on the total yield of organic liquid products. Yield can be used only complete conversion which no observe triglyceride and fatty acid in the products.

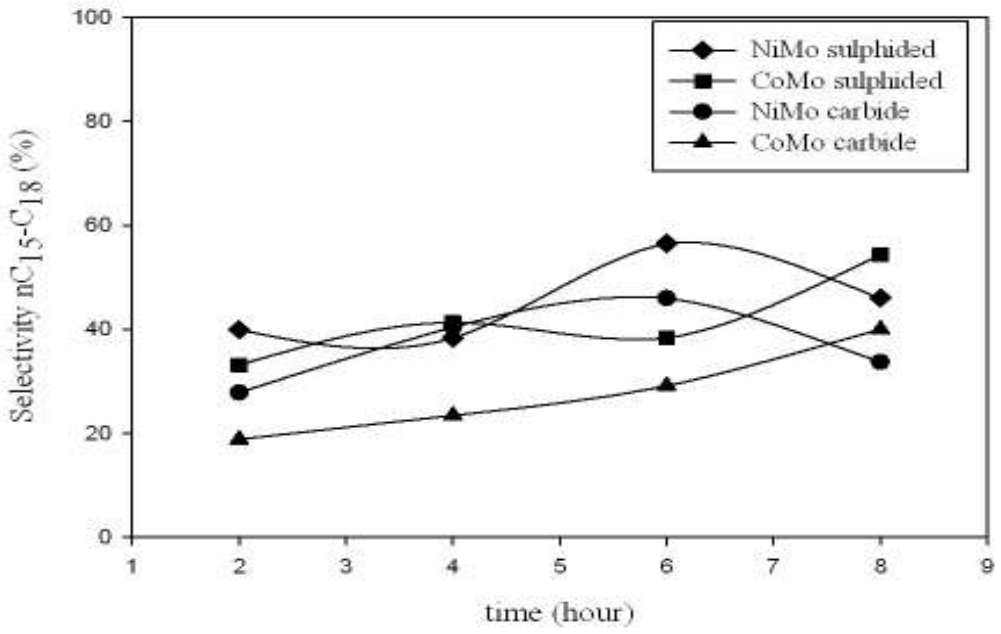

Figure 5.6 Effect of reaction time on selectivity of n-C_{15}-C_{18} alkanes products varying catalysts. (Operating temperature of 360°C and hydrogen pressure of 50 bar)

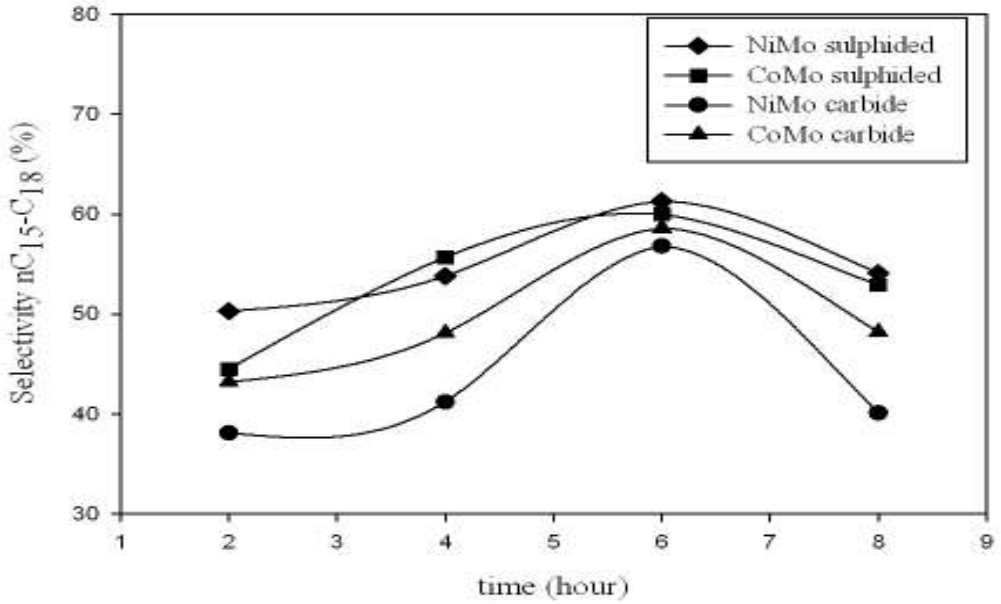

Figure 5.7 Effect of reaction time on selectivity of n-C_{15}-C_{18} alkanes products varying catalysts. (Operating temperature of 380°C and hydrogen pressure of 50 bar)

The selectivity of n-C_{15}-C_{18} alkanes tends to increase with increasing reaction time at operating temperature of 360°C in case of CoMo sulphided and CoMo carbide and showed optimum at 6 h in case of NiMo sulphided and NiMo carbide as shown in Figure 5.6. The increase of reaction time lead to increase in conversion of tri-glycerides and fatty acids to n-C_{15}-C_{18} alkanes. However to long of reaction time may leads to increase of lighter hydrocarbons (< C15 from cracking of n-alkanes). However it is worth to note that at temperature of 360°C, complete conversion of tri-glycerides and fatty acid can not to obtained within 8 h. Therfore, the reaction temperature was raised to 380°C. At temperature of 380°C is shown in Figure 5.7, all catalyst showed optimal time of 6 h in term of diesel range selectivity. The complete conversion can be obtained from all catalysts within 6 h. Therfore, the n-C_{15}-C_{18} products yield of 6 – 8 h of reactor time can be plotted as shown in Figure 5.8 The reactor of 6 h gave higher diesel yield than that of 8 h. Sulphided catalyst (both NiMo and CoMo) gave slightly higher diesel range yield than that od carbide catalysts. Among four catalysts. NiMo sulphided gave the highest diesel range yield of 61.3%.

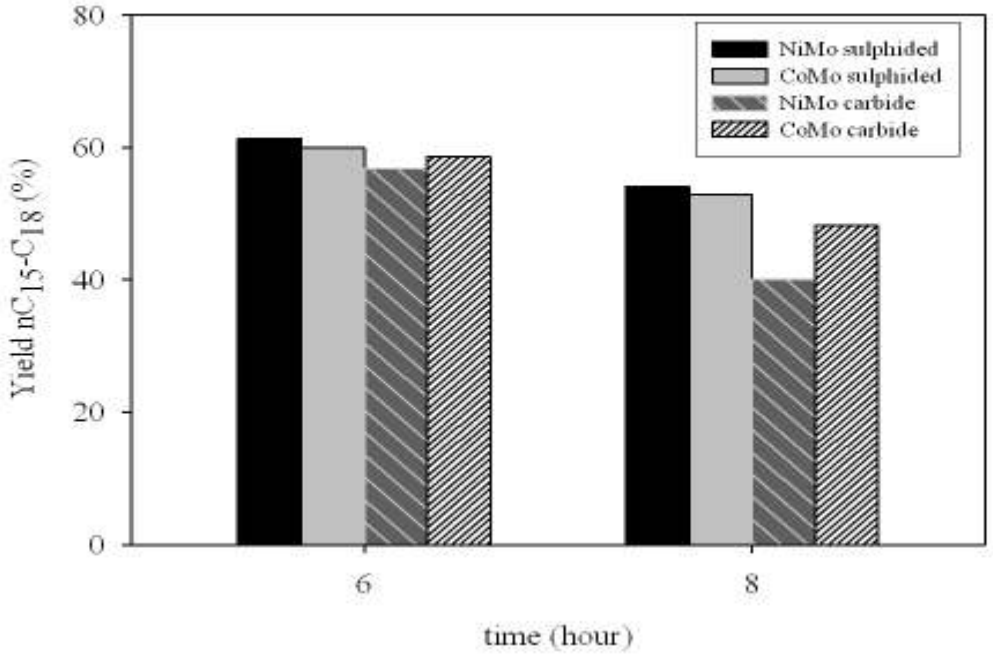

Figure 5.8 Effect of reaction time on yield of n-C_{15}-C_{18} alkanes products varying catalysts and reaction time 6-8 h. (Operating temperature of 380 ˚C and hydrogen pressure of 50 bar)

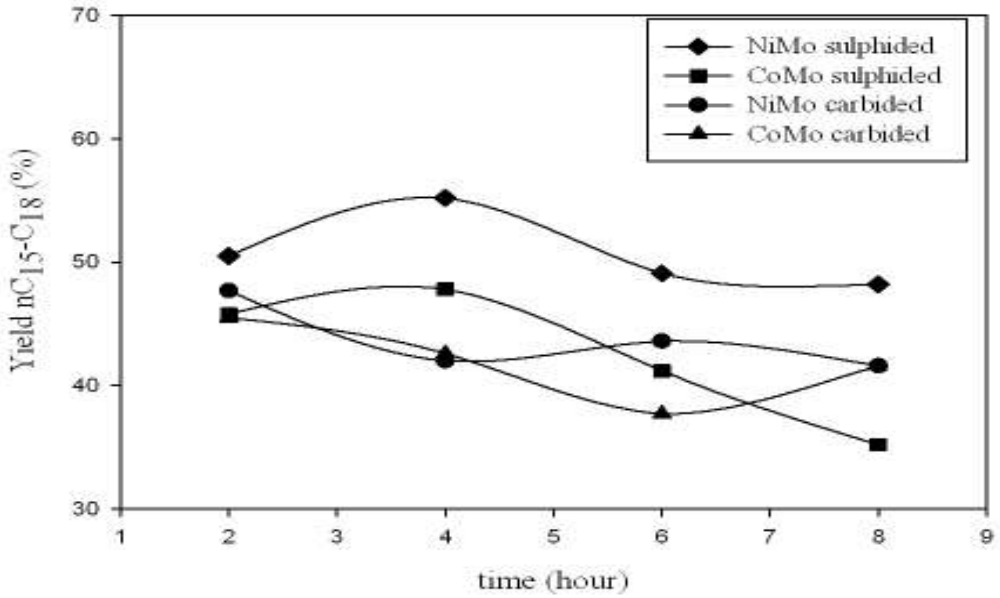

Figure 5.9 Effect of reaction time on yield of n-C_{15}-C_{18} alkanes products varying catalysts. (Operating temperature of 400°C and hydrogen pressure of 50 bar)

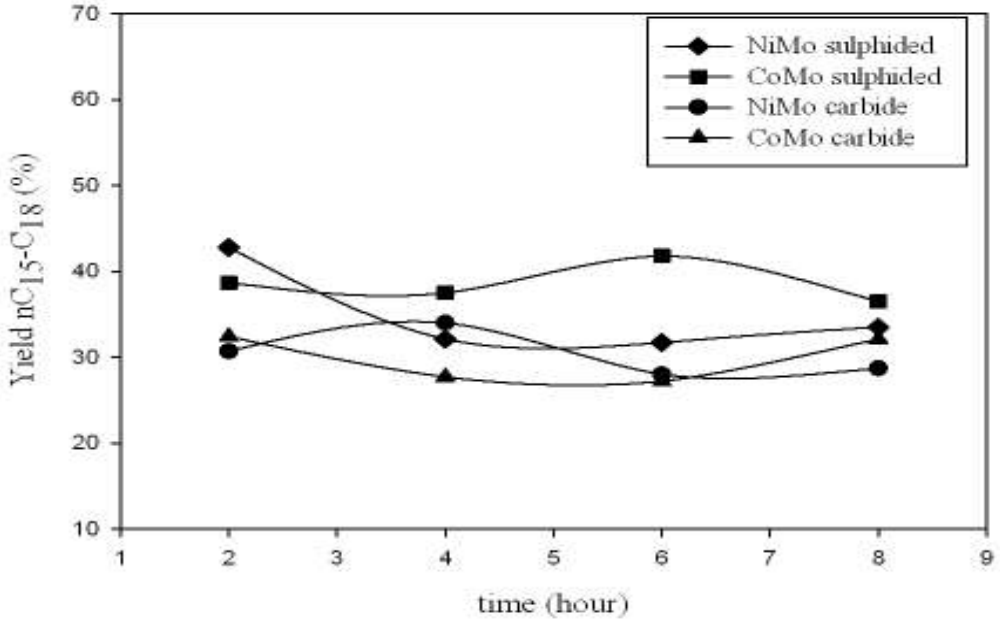

Figure 5.10 Effect of reaction time on yield of n-C_{15}-C_{18} alkanes products varying catalysts. (Operating temperature of 420°C and hydrogen pressure of 50 bar).

At higher operating temperature i.e. 400 and 420°C, the reaction time providing high yield of diesel range become shorter i.e. ca. 2 and 4 h respectively as shown in Figure 5.9 and 5.10 respectively. However, with increase operating temperature to 400 and 420°C, the mechanism obtained yield become lower as 50.5% and 42.8% NiMo/Al_2O_3 sulphided respectively.

The appropriated operating condition for biodiesel production via hydroprocessing of WCPO could be obtained with reaction temperature of 380°C, hydrogen pressure of 50 bar and reaction time of 6 h. The yield of n-C_{15}–C_{18} alkanes of 61.3, 60, 58.6 and 56.8% on a product basis with NiMo/Al_2O_3 sulphided, CoMo/Al_2O_3 sulphided, CoMo/Al_2O_3 carbide and NiMo/Al_2O_3 carbide catalysts respectively.

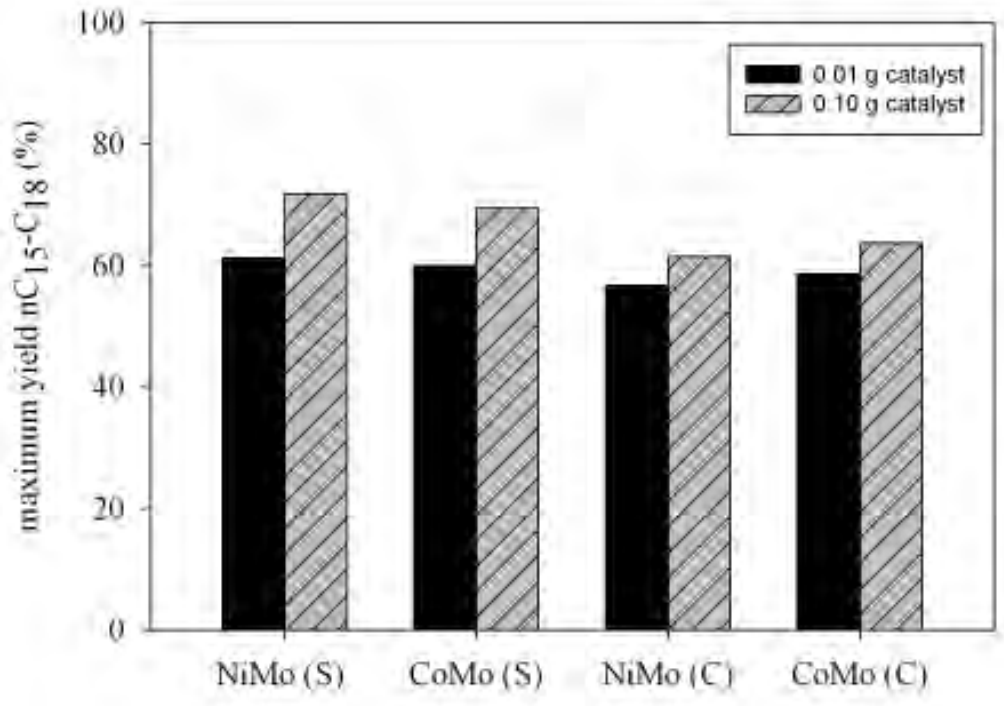

Figure 5.11 The maximum yield of n-C_{15}-C_{18} alkanes products varying weight of Catalysts (S and C can be subscript sulphided and carbide).

After that, increased the amount of catalyst from 0.01 to 0.1 g at the appropriated operating condition with reaction temperature from 380°C, hydrogen pressure of 50 bar and reaction time of 6 h as shown in Figure 5.10. With increasing amount of catalyst, the yield of n-C_{15}–C_{18} alkanes increases from 61.3, 60, 58.6 and 56.8% to 71.8, 69.5, 63.7 and 61.5% on a product basis with NiMo/Al_2O_3 sulphided, CoMo/Al_2O_3 sulphided, CoMo/Al_2O_3 carbide and NiMo/Al_2O_3 carbide catalyst respectively. Hydroprocessing reactions occur on the active sites of the catalysts. Also, a suitable pore size distribution is required to ensure the access of reactant molecules to the active sites (Furimsky et. al., 1999).

The NiMo/Al_2O_3 and CoMo/Al_2O_3 sulphided catalysts showed the yield of n-C_{15}–C_{18} alkanes was 71.8 and 69.5% higher than the NiMo/Al_2O_3 and CoMo/Al_2O_3 carbide catalysts was 61.5 and 63.7% because active site (basis on unit of catalyst weight) of the sulphided catalysts are higher than the carbide catalysts (data shown in Table 5.2). The yield of n-C_{15}-C_{18} alkanes increased with the activity of the catalysts increased in the order NiMo/Al_2O_3 sulphided, CoMo/Al_2O_3 sulphided, CoMo/Al_2O_3 carbide and NiMo/Al_2O_3 carbide catalysts respectively.

It can be concluded that the higher hydroprocessing activities of the sulphided catalysts can be traced to more active site but the carbide catalysts showed higher active site densities (Diaz et al., 2003). On the both sulphided catalysts, the hydrogenation reactions was inhibited on the NiMo/Al_2O_3 catalyst, but were not appreciably on the CoMo/Al_2O_3 catalyst (Senol et al., 2007). Similarly, sulfur compounds has been reported to inhibit the hydrogenation reactions in the case of NiMo/Al_2O_3 sulphided catalyst and to have an insignificant effect in the case of CoMo/Al_2O_3 sulphided catalyst (Rota and Prins, 2000; Egorova and Prins, 2004).

5.2.3 Gas products

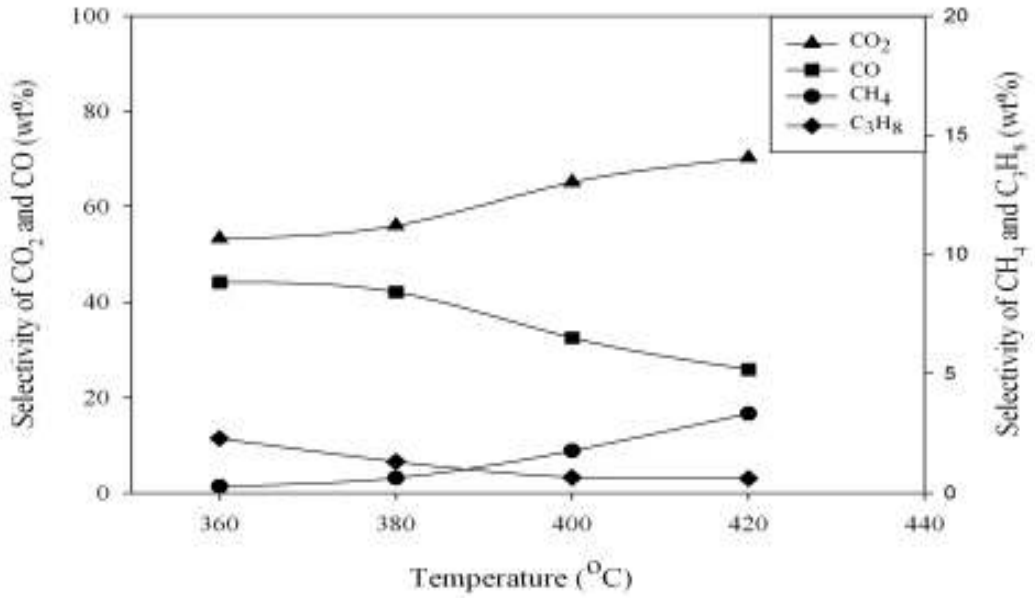

Figure 5.12 Effect of operating temperature on gas products. (Operating hydrogen pressure of 50 bar, reaction time of 6 hour and Ni-Mo/Al_2O_3 sulphided catalyst).

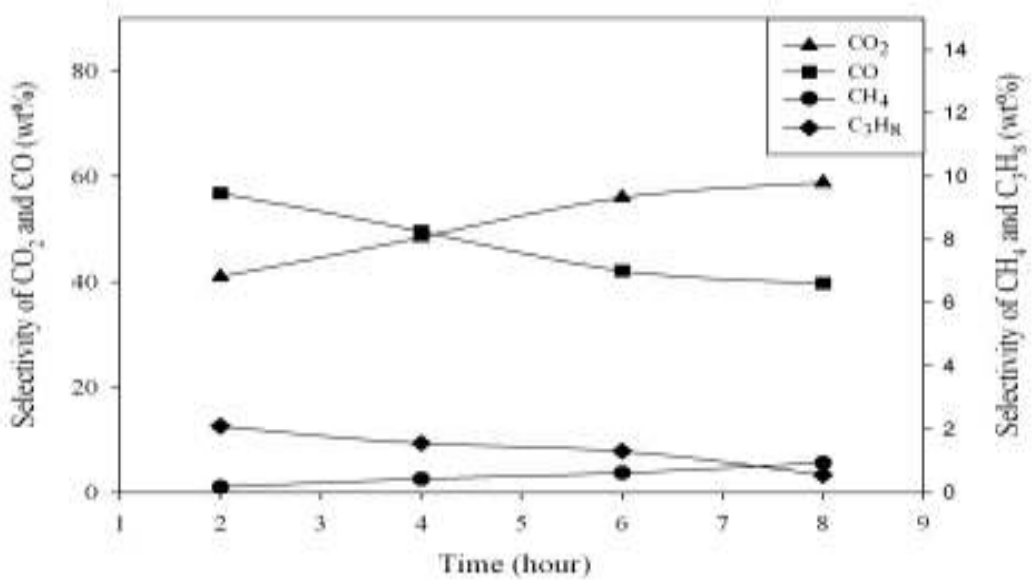

Figure 5.13 Effect of reaction time on gas products. (Operating temperature of 380°C, hydrogen pressure of 50 bar and NiMo/Al_2O_3 sulphided catalyst).

With increasing temperature at a constant hydrogen pressure, reaction towards the hydrodecarboxylation and hydrodecarbonylation were enhanced. These two yields are relatively equal, and both increase by approximately the same value with increasing tempurature. The rates of these two reactions are similar and these reactions could be occurring by a similar mechanism (data is not show here). Therefore, the relative rate of the decarboxylation plus the decarbonylation versus the hydrodeoxygenation increases with increasing temperature (Huber et. al., 2007).

The relative rates of the decarboxylation versus decarbonylation pathway can be compared by looking at the selectivity of carbon dioxide and carbon monoxide. As shown in Figure 5.12. Carbon dioxide formation from the decarboxylation reaction was slightly increased with increasing the temperature from 360 – 420°C. On the other hand, carbon monoxide formation from the decarbonylation reaction was slightly decreased by increasing the temperature. The straight chain alkanes can undergo isomerization and cracking to produce lighter and isomerized alkanes. Propane which obtained from the backbone of tri-glyceride was slightly decreased due to propane was cracked to lighter hydrocarbon (mostly methane), therfore lead to increase of metane at higher temperature. Moreover, metane is formed by side equilibrium reaction of hydrogen and carbon monoxide (Mikulec et. al., 2010)

As well, with increasing the reaction time from 2 – 8 h (Figure 5.13). Carbon dioxide formation was slightly increased with increasing the reaction time from 2 – 8 h. Whereas, carbon monoxide was slightly decreased by increasing the reaction time. Similarly, metane was slightly increased due to propane was cracked to lighter hydrocarbon (mostly methane) at higher time of reaction. The relative rate of the decarboxylation versus the decarbonylation increases with increasing the reaction time.

5.3 Coke formation of the spent catalysts

Thermogravimetric analysis of the spent catalysts was carried out to estimate coke deposit as revealed by the reduction in weight due to oxidation of coke in air. In general, coke samples exhibit four distinct temperature regions as shown in Table 5.4. Region I (T < 180 ˚C) can be ascribed to the loss of water, volatile species and Region II (180 ˚C $\leq$ T $\leq$ 330°C) can be ascribed to mobile carbonaceous residues or physisorbed products or side products in the samples (altogether can be termed as

'soft coke'). Furthermore, sulfur exiting as metal sulfides is removed before organic coke (Furimsky, 1991) and simultaneously replaced by oxygen; for example, MoS_2 and CO_9S_8 are converted into MoO_3 and CoO respectively. Therefore, the weight loss by the oxidation of metal sulfides is much smaller than that by carbon combustion (Oh et. al., 1997). At temperature range of 330 - 750^oC can be ascribed to desorption of coke as CO was major and CO_2 was minor produce. It is more bulky carbonaceous compounds (termed as 'hard coke'), which can be exhibited two distinct coke oxidation temperature regions corresponding to metal and support sites as observed (Barbier, 1987; Parera et al., 1983). Region III (330 $^\circ C \leq T \leq 450^oC$) consists of coke species deposited on metal sites and Region IV (450 $^\circ C \leq T \leq 750^oC$), coke on the support that contains more polymerized/condensed coke species. At temperature higher of 750^oC can be ascribed to the small weight loss when higher temperature (Sahoo et. al., 2004).

Table 5.4 Temperature range of coke formation in spent catalyst.

Temperature range (°C)	Type
< 180	Water, volatile species[a]
180 – 330	Mobile carbonaceous (sofe coke)[a]
330 - 750	Bulky carbonaceous (hard coke)[a]
330 - 450	Coke on metal sites[b,c]
450 - 750	Coke on support sites[b,c]

[a] Sahoo et. al., (2004); [b] Barbier, (1987); [c] Parera et al., (1983)

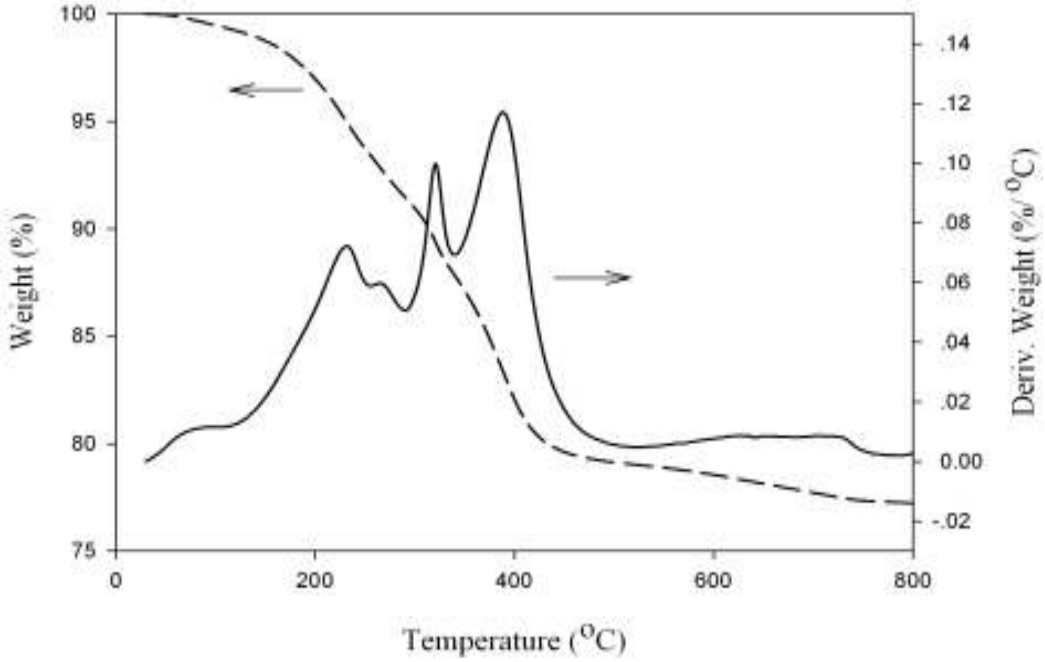

Figure 5.14 TGA/DTG diagram of the spent $NiMo/Al_2O_3$ sulphided catalyst.

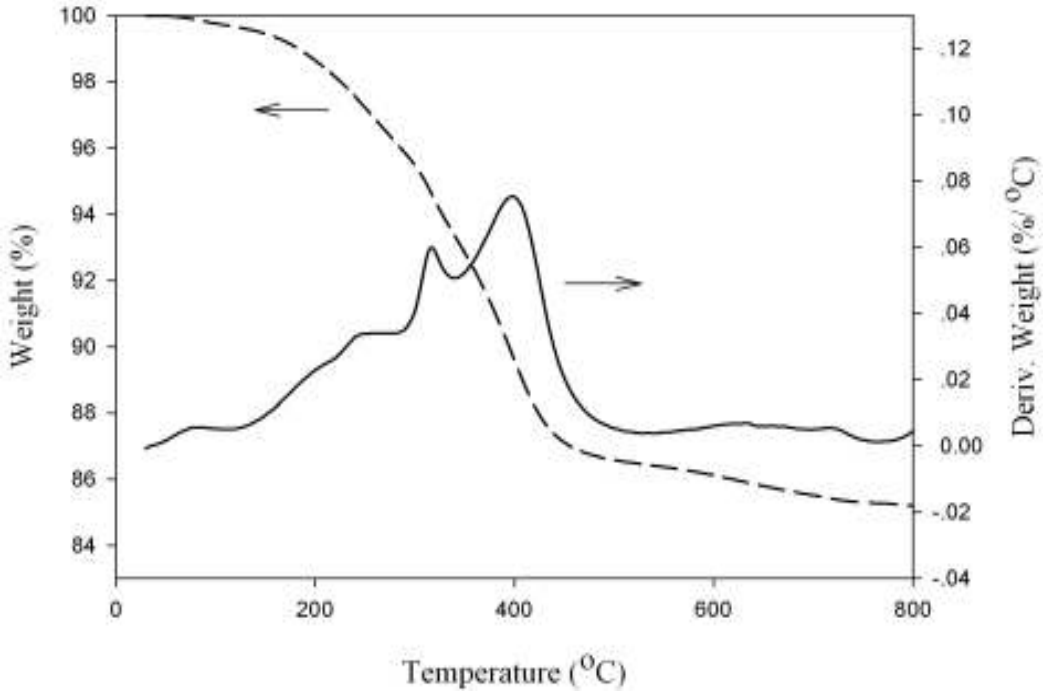

Figure 5.15 TGA/DTG diagram of the spent $CoMo/Al_2O_3$ sulphided catalyst.

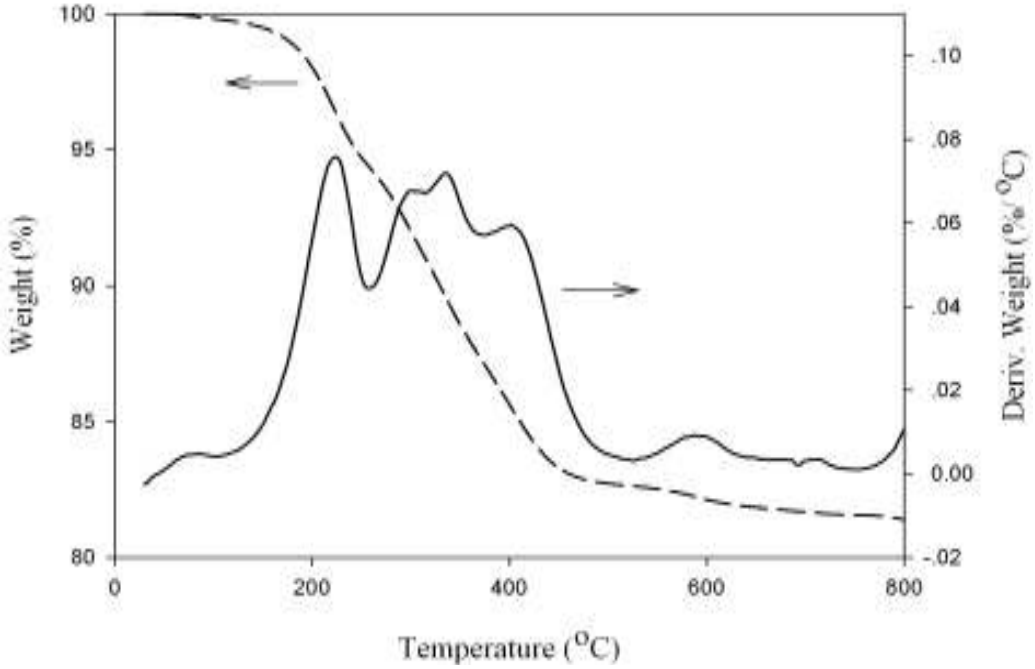

Figure 5.16 TGA/DTG diagram of the spent NiMo/Al_2O_3 carbide catalyst.

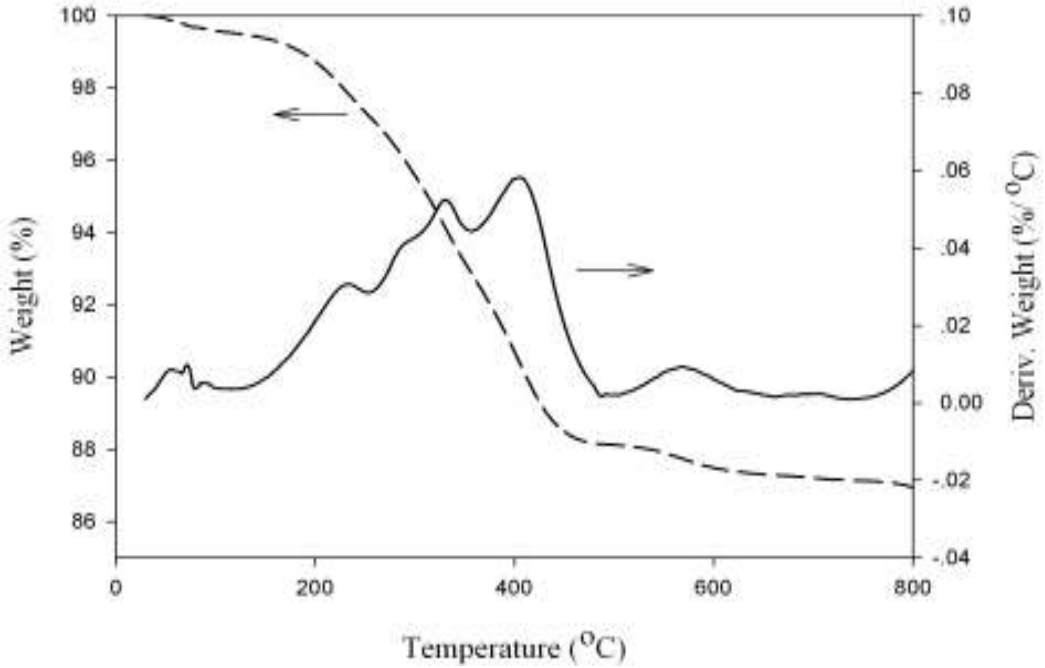

Figure 5.17 TGA/DTG diagram of the spent CoMo/Al_2O_3 carbide catalyst.

As the result, thermograms of four spent catalyst samples: $NiMo/Al_2O_3$, $CoMo/Al_2O_3$ sulphided catalysts and $NiMo/Al_2O_3$, $CoMo/Al_2O_3$ carbide catalysts are shown in Figure 5.14 - Figure 5.17.

Table 5.4 Coke formation of the spent catalysts (from TGA)

Catalyst	Coke on metal (%) at 330-450^oC	Coke on support (%) at 450-750^oC	Total coke (%) at 330-750^oC
Ni-Mo/Al_2O_3 sulphided	8.94	2.27	11.21
Co-Mo/Al_2O_3 sulphided	6.76	1.82	8.58
Ni-Mo/Al_2O_3 carbide	6.68	1.73	8.41
Co-Mo/Al_2O_3 carbide	5.68	1.36	7.04

The total coke content of the spent catalyst sample was calculated from weight loss (%) at 330-750^oC, which is shown in Table 5.4. It was found, the both $NiMo/Al_2O_3$ and $CoMo/Al_2O_3$ sulphided catalysts were containing 11.21 wt% and 8.58 wt% respectively as shown in Figure 5.14 and Figure 5.15. In both catalysts sample, peak coke show one major weight loss that consists of coke species deposited on metal sites 8.94% and 6.76%. Minor weight loss can be specified coke on the support 2.27% and 1.82%. On the other hand, the both $NiMo/Al_2O_3$ and $CoMo/Al_2O_3$ carbides catalysts were containing 8.41 wt% and 7.04 wt% respectively as shown in Figure 5.16 and Figure 5.17. In both catalysts sample, peak coke species deposited on metal sites show one major weight loss 6.68% and 5.68% at around 400^oC. Minor weight loss (coke on the support) was containing 1.73% and 1.37% at higher temperature at 575^oC.

It can be concluded that the both $NiMo/Al_2O_3$ and $CoMo/Al_2O_3$ sulphided catalysts were deactivated by coke from hydroprocessing process than both $NiMo/Al_2O_3$ and $CoMo/Al_2O_3$ carbide catalysts because the structure and properties are difference between carbide catalysts compared with sulphided catalyst (Sajkowski and Oyama, 1996).

5.4 Activity of fresh, spent and regenerated catalysts

In relatively light feeds, deactivation of the catalyst is minimal for the process can operate long periods of time before replacement of the new catalyst. However, in hydroprocessing heavy residues, catalyst deactivation can be severe, having an important commercial economic consideration with respect to catalyst lifetime. Degree of deactivation is depending on the feed source, operating conditions and catalyst activity (Furimsky and Massoth, 1999). The activity of the fresh, spent and regenerated catalysts at operating condition with reaction temperature from 380°C, hydrogen pressure of 50 bar and reaction time of 6 h with $NiMo/Al_2O_3$ sulphided, $CoMo/Al_2O_3$ sulphided, $NiMo/Al_2O_3$ carbide and $CoMo/Al_2O_3$ carbide catalysts respectively as shown in Figure 5.18.

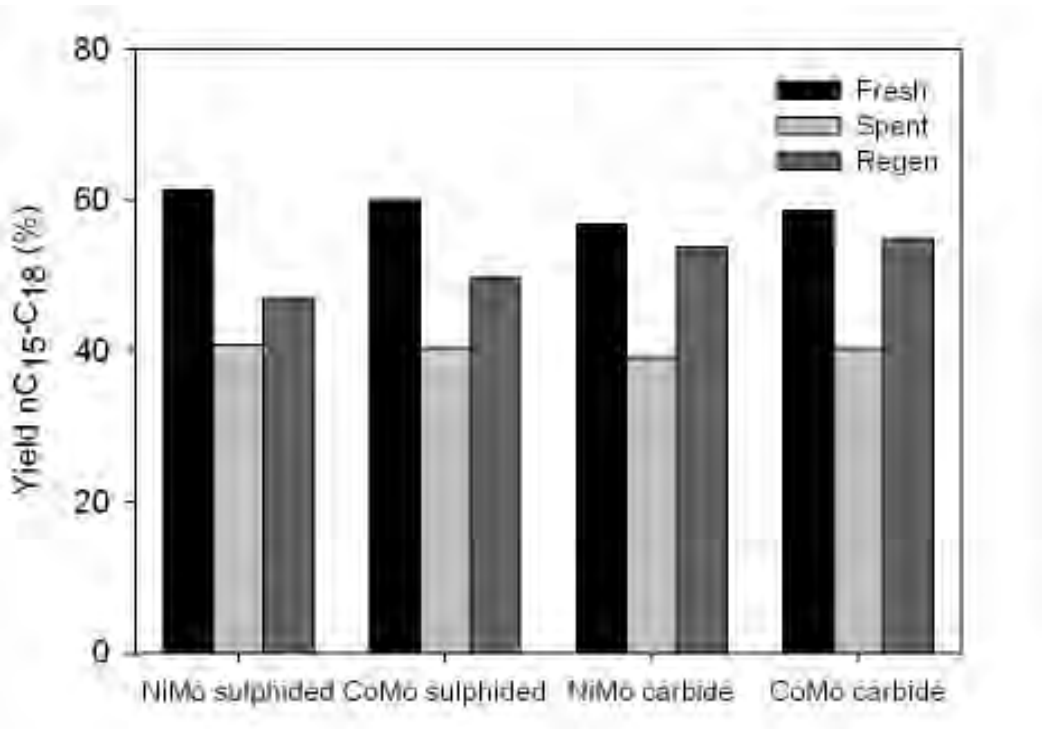

Figure 5.18 The yield of n-C_{15}-C_{18} with fresh, spent and regenerated catalysts in hydroprocessing.

The yield of n-C_{15}-C_{18} alkanes were less than the fresh catalysts from 61.3, 60, 56.8 and 58.6% to 40.8, 40.4 39.1 and 40.4% respectively with spent NiMo/Al_2O_3 sulphided, CoMo/Al_2O_3 sulphided, NiMo/Al_2O_3 carbide and CoMo/Al_2O_3 carbide catalysts. The activity of all spent catalysts dramatically decreased compared with the all fresh catalysts. As expected, the contamination of catalyst was insignificant. Deactivation is mainly caused by active site coverage by deposits by coke, pore mouth constriction and ultimate pore blockage as well as sintering of active phase (Furimsky and Yoshimura, 1989).

The spent catalysts were regenerated in fixed bed using air at temperature 400°C because the carbon deposited on the catalyst surface is almost completely removed at this temperature Moreover, the surface area and properties were similar with comparison to the fresh catalyst (Oh et. al., 1997). For catalyst combustion of inorganic sulfur dominated the initial stage of burn off and the coke burn off began only after amount of the sulfur was removed. Then, coke was burned on the external surface of the catalyst particles followed by the burn of coke in the pores. It believed that most of the carbon in the vicinity of metal Mo and Ni/Co species was removed as called “reversibly poison” (Furimsky et. al., 1999). As the result, the yield of n-C_{15}-C_{18} alkanes were less than the fresh catalysts from 61.3, 60, 56.8 and 58.6% to 47, 49.7 53.8 and 54.9% respectively with regenerated NiMo/Al_2O_3 sulphided, CoMo/Al_2O_3 sulphided, NiMo/Al_2O_3 carbide and CoMo/Al_2O_3 carbide catalysts. The activity loss may be the removal of the last amounts of carbon is the most difficult as called “quasi-irreversibly poison”. The activity of sulphided catalysts decreases over than the carbide catalysts because the effect of remaining carbon on metal as called “irreversibly poison” of sulphided catalysts were higher than carbide catalysts.

In addition, the regeneration in air resulted in a significant loss of surface area presumably due to sintering of the catalyst support. The pore size of catalysts shift to the small size was observed. This may be attributed to the presence of a skin of coke, which increased the size of the spent catalyst particles compared with the fresh catalyst particles (Furimsky et. al., 1999). Moreover, molybdenum sulfided is an active phase in hydroprocessing catalysts. After, regeneration in air is attributed to the presence of MoO_2. This species is an intermediate in the stepwise oxidation of MoS_2 to MoO_3. The formation of MoO_2 was not converted during sulfidation, may

contribute to loss in catalyst activity. There was no evidence of diffusion problems for H_2S (Furimsky and Yoshimura, 1989).

CHAPTER VI

CONCLUSIONS AND RECOMMENDATIONS

6.1 Conclusions

The hydroprocessing of WCPO is a prominent process for the biodiesel production. The reaction pathway involves hydrogenation of the double bonds followed by alkane production by three different pathways: hydrodeoxygenation, hydrodecarboxylation and hydrodecarbonylation.

The operating condition for biodiesel production via hydroprocessing of WCPO with reaction temperature of 380°C, hydrogen pressure of 50 bar and reaction time of 6 h was found suitable to maximize the diesel range yield. The highest yield of n-C_{15}–C_{18} alkanes were 71.8, 69.5, 63.7 and 61.5% on a product basis with NiMo/Al_2O_3 sulphided, CoMo/Al_2O_3 sulphided, CoMo/Al_2O_3 carbide and NiMo/Al_2O_3 carbide catalysts respectively. The gas product distribution shows a conform results which indicated that hydrodecarboxylation and hydrodecarbonylation reaction pathways are dominated over hydrodeoxygenation.

In conclusion, this work indicates that the performance of the catalysts activity. Sulphided catalyst shows slightly higher diesel yield than that of carbide catalyst. However, the strong beneficial of carbide catalyst over sulphided catalyst are higher reusability. After pretreatment the used carbide catalyst, the catalytic performance becomes comparable to the fresh carbide catalyst while the regenerated sulphided catalysts are still suffered from activity loss.

6.2 Recommendations

1. Develop and perform the experiment in a continuous flow operation which more suitable for industrial scale.
2. The properties of bimetallic catalysts should be studied by ICP (Inductive Coupled Plasma Optical Emission Spectrometer) technique in order to investigate the actual amount of the metals loading in support.
3. As suggested by Furimsky, (1990). O_2 diffusion limitation becomes important because attributed to reopening of pores which increases the availability of O_2, using air oxidizing gas for regeneration of hydroprocessing catalysts should be avoided. Therefore, low O_2 content gas should be used to compare the regeneration performance.

REFERNCES

Arnoldy, P., Franken, M.C., Scheffer, B., and Moulijn, J.A. Temperature-programmed reduction of $CoO-MoO_3/Al_2O_3$ catalysts. Journal of Catalysis 96 (1985): 381.

Banerjee, A., and Chakraborty, R. Parametric sensitivity in trans-esterification of waste cooking oil for biodiesel production-A review. Resources Conservation and Recycling 53 (2009): 490-497.

Barbier, J. Coking of reforming catalysts. Studies in Surface Science and Catalysis 34 (1987): 1-19.

Bezergianni, S., and Kalogianni, A. Hydroprocessing of used cooking oil for biofuels production. Bioresource Technology 100 (2009): 3927-3932.

Bezergianni, S., Dimitriadis, A., Kalogianni, A., and Pilavachi, P.A. Hydrotreating of waste cooking oil for biodiesel production Part I: Effect of temperature on product yields and heteroatom removal. Bioresource Technology 101 (2010): 6651–6656.

Bezergianni, S., Dimitriadis, A., Sfetsas, T., and Kalogianni, A. Hydrotreating of waste cooking oil for biodiesel production Part II: Effect of temperature on hydrocarbon composition. Bioresource Technology 101 (2010): 7658–7660.

Bozenko, J.S., and Mushrush, G.W. Analytical Profile of organo-nitrogen compounds in gulf coast refined fuels by GC/MS. Petroleum Science and Technology 26 (2008): 674–689.

Brungs, A.J., York, A.P.E., and Green, M.L.H. Comparison of the group V and VI transition metal carbides for methane dry reforming and thermodynamic prediction of their relative stabilities. Catalysis Letters 57 (1999): 65.

Collier, A.R., Rhead, M.M., Trier, C.J., and Bell, M.A. Polycyclic aromatic compound profiles from a light- duty direct-injection diesel engine. Fuel 74 (1995): 62-367.

Colling, C.W., and Thompson, L.T. The structure and function of supported molybdenum nitride hydrodenitrogenation catalysts. Journal of Catalysis 146 (1994): 193-203.

Cvengros, J., and Cvengrosova, Z. Used frying oils and fats and their utilization in the production of methyl esters of higher fatty acids. Biomass and Bioenergy 27 (2004): 173–181.

Diaz, B., et al. Hydrodesulfurization over supported monometallic, bimetallic and promoted carbide and nitride catalysts. Catalysis Today 86 (2003): 191-209.

Donnis, B., Egeberg, R.G., Blom, P., and Knudsen, K.G. Hydroprocessing of Bio-Oils and Oxygenates to Hydrocarbons Understanding the Reaction Routes, Topics in Catalysis (2009) 52: 229-240.

Egorova, M., and Prins, R. Hydrodesulfurization of dibenzothiophene and 4, 6-dimethyldibenzothiophene over sulfide NiMo/γ-Al_2O_3, CoMo/γ-Al_2O_3, and Mo/γ-Al_2O_3 catalysts. Journal of catalysis 225 (2004): 417-427.

Filho, G.N., Brodzki, D., and Djega-Mariadassou, G. Formation of alkanes alkylcycloalkanes and alkylbenzenes during the catalytic hydrocracking of vegetable oils. Fuel 72 (1993): 4.

Furimsky, E., and Massoth, F.E. Deactivation of hydroprocessing catalysts. Catalysis today 52 (1999): 381-495.

Furimsky, E., and Yoshimura, Y. N.P. Cheremissinoff (Ed), and Mass Transfer, Vol. 3, Kinetic, Catalysis and Reactor Engineering Houston, TX. 1989.

Furimsky, E. Effect of coke and catalyst structure on oxidative regeneration of hydroprocessing catalyst. Fuel Processing Technology 27 (1991): 131-147.

Furimsky, E. Metal carbides and nitrides as potential catalysts for hydroprocessing. Applied Catalysis A: General 240 (2003): 1–28.

Gates, B.C., Katzer, J.R., and Chuit, G.C.A. Chemistry of Catalytic Processes. New York: McGraw-Hill, 1979.

Grzechowiak, J.R., Szyszka, I., and Masalska, A. Effect of TiO_2 content and method of titania-silica preparation on the nature of oxidic nickel phases and their activity in aromatic hydrogenation. Catalysis Today 137 (2008): 433–438.

Guzman, A., Torres, J.E., Prada, L.P., and Nunez, M.L. Hydroprocessing of crude palm oil at pilot plant scale. Catalysis Today 156 (2010): 38-43.

Huber, G.W., O'Connor, P., and Corma, A. Processing biomass in conventional oil refineries: Production of high quality diesel by hydrotreating vegetable oils in heavy vacuum oil. Applied Catalysis A: Genaral 329 (2007): 120-129.

Immer, J.G., Kelly M.J., and Lamb, H.H. Catalytic reaction pathways in liquid-phase deoxygenation of C18 free fatty acids. Applied Catalysis A: General 375 (2010): 134–139.

Isidoro, G.C., et al. Proton affinity of S-containing aromatic compounds: Implications for crude oil hydrodesulfurization. Journal of Molecular Catalysis A: Chemical 281 (2008): 79–84.

Izhar, S., Kanesugi, H., Tominaga, H., and Nagai, M. Cobalt molybdenum carbides: Surface properties and reactivity for methane decomposition. Applied Catalysis A: General 317 (2007): 82–90.

Kabe, T., Ishihara, A., and Qian, W. Hydrodesulfurization and Hydrodenitrogenetion. Wiley-VCH, Weinhein. Chemistry and Engineering. (1999)

Kiatkittipong, W., Suwanmanee, S., Laosiripojana, N., Praserthdam P., and Assabumrungrat, S. Cleaner gasoline production by using glycerol as fuel extender. Fuel Processing Technology 91 (2010): 456–460.

Knothe, G. Biodiesel and renewable diesel: A comparison. Progress in Energy and Combustion Science 36 (2010): 364–373.

Knowledge Management on Air Quality: Case studies. Asian Development and CAI-Asia Center. 2010.

Krylov, I.F., Emel'Yanov, V.E. Nikitina, E.A. Vizhgorodskii, B.N. and Rudyak., K.B. Low-sulfur diesel fuels: Pluses and minuses. Chemistry and Technology of Fuels and Oils 41 (2005): 423-428.

Kubicka, D., and Kaluza, L. Deoxygenation of vegetable oils over sulfided Ni, Mo and NiMo catalysts. Applied Catalysis A: General 372 (2010): 199–208.

Macrae, J.C. An Introduction to the Study of Fuel. New York: Elsevier Publishing company. (1966): 173-175.

Macrae, J.C. An Introduction to the Study of Fuel. New York: Elsevier Publishing company. (1966): 696.

Meng, X., Chen, G., and Wang, Y. Biodiesel production from waste cooking oil via alkali catalyst and its engine test. Fuel Processing Technology 89 (2008): 851-857.

Mikulec, J., Cvengros, J., Jorikova, L., Banic, M., and Kleinova, A. Second generation diesel fuel from renewable sources. Journal of Cleaner Production 18 (2010): 917-926.

Oh, E.K., Park, Y.C., Lee, I.C., and Rhee, H.K. Physicochemical change in hydrodesulfurization catalysts during oxidative regeneration. Journal of Catalysis 172 (1997): 314-321.

Othmer, K. Encyclopedia of chemical technology. Volume 6. 4th edition. New York: A Wiley Interscience Publication John Wiley&Son. 1991.

Oyama, S.T., Ertl, G. Knozinger, H., Wcitkamp, Journal Handbook of Heterogeneous Catalysis, vol. 1, VCH, Verlagsgesellschaft mbH. Weinheim Germany. 1997.

Papadoupoulou, C., Vakros, J., Matralis, H.K., Kordulis, C., and Lycourghiotis, A. On the relationship between the preparation method and the physicochemical and catalytic properties of the CoMo/γ-Al_2O_3 hydrodesulfurization catalysts. Journal of Colloid and Interface Science 261 (2003): 146.

Papadopoulou, C., Vakros, J., Matralis, H.K., Voyiatzis, G.A., and Kordulis, C. Preparation, characterization, and catalytic activity of CoMo/γ -Al2O3 catalysts prepared by equilibrium deposition filtration and conventional impregnation techniques. Journal of Colloid and Interface Science 274 (2004): 159–166.

Parera, J.M., Figoli, N.S., and Traffano, E.M. Catalytic naphtha reforming: science and technology. Journal of Catalysis 79 (1983): 484.

Patil, P. Deng, S., Isaac Rhodes, J., and Lammers, P.J. Conversion of waste cooking oil to biodiesel using ferric sulfate and supercritical methanol processes. Fuel 89 (2010): 360-364.

Pierson, H.O. Handbook of Refractory Carbides and Nitrides. Noyes Public Library, Westwood, Newjersey, USA 1996.

Piqueras, C.M., Costilla, I.O., Belelli, P.G. Castellani, N.J., and Damiani, D.E. Pd-γAl_2O_3 applied to triglycerides hydrogenation with supercritical propane Experimental and theoretical catalysts characterization. Applied Catalysis A: General 347 (2008): 1–10.

Radich, A. Biodiesel performance, costs, and use. Energy Information Administration. 1998.

Ramanathan, S., and Oyama, S.T. New catalysts for hydroprocessing: Transition metal carbides and nitrides. The Journal of Physical Chemistry (1995): 99 16365-16372.

Ramirez, J., Contreras, R., Castillo, P., Klimova, T., Zarate, R., and Luna, R. Characterization and catalytic activity of CoMo HDS catalysts supported on alumina-MCM-41. Applied Catalysis A: General 197 (2000) 69–78.

Rantanen, L., Linnaila, R., Aakko, P., and Harju, T. NExBTL-Biodiesel fuel of the second generation. Neste Oil Corporation. Technical Research Centre of Finland 1 (2005): 3771.

Rojanapipatkul, S., and Jongsomjit, B. Synthesis of cobalt on cobalt aluminate via solvothermal method and its catalytic properties for carbon monoxide hydrogenation. Catalysis Communications. 10 (2008): 232-236.

Rota, F., and Prins, R. Mechanism of the C-N bond breaking in the hydrodenitrogenation of methylcyclohexylamine over sulfide NiMo/γ-Al_2O_3. Journal of Molecular Catalysis A: Chemical. 162 (2000): 367.

Sahoo, S.K., Rao, P.V.C., Rajeshwer, D., Krishnamurthy, K.R., and Singh, I.D. Structural characterization of coke deposits on industrial spent paraffin dehydrogenation catalysts. Applied Catalysis A: General 244 (2003): 311–321.

Sahoo, S.K., Ray, S.S., and Singh, I.D. Structural characterization of coke spent hydroprocessing catalysts used for processing of vacuum gas oils. Applied Catalysis A: General 278 (2004): 83–91.

Sajkowski, D.J., and Oyama, S.T. Catalytic hydrotreating by molybdenum carbide and nitride: unsupported Mo_2N and Mo_2C/Al_2O_3. Applied Catalysis A: 134 (1996): 399-349.

Santana, R.C., et al. Evaluation of different reaction strategies for the improvement of cetane number in diesel fuels. Fuel 85 (2006): 643-656.

Santillán-Vallejo, L.A., et al. Supported (NiMo, CoMo)-carbide, -nitride phases: Effect of atomic ratios and phosphoruconcentration on the HDS of thiophene and dibenzothiophene. Catalysis Today 109 (2005): 33-41.

Santos, S.P., Santos, S.H., and Toledo, S.P. Standard transition aluminas electron microscopy studies. Materials Research 3, 4 (2000): 104-114.

Schwartz, V., Oyama, S.T., and Chen, J. G. Supported Bimetallic Nb-Mo Carbide: Synthesis, Characterization, and Reactivity. The Journal of Physical Chemistry B (2000): 104 8800-8006.

Sebos, I., Matsoukas, A., Apostolopoulos, V., and Papayannakos., N. Catalytic hydroprocessing of cottonseed oil in petroleum diesel mixtures for production of renewable diesel. Fuel 88 (2009): 145-149.

Shemer, H., and Linden, K.G. Aqueous photodegradation and toxicity of the polycyclic aromatic hydrocarbons fluorene, dibenzofuran, and dibenzothiophene. Water Research 41 (2007): 853-861

Simacek, P. and Kubicka, D. Hydrocracking of petroleum vacuum distillate containing rapeseed oil: Evaluation of diesel fuel. Fuel 89 (2010): 1508–1513.

Simacek, P., Kubicka, D., Sebor, G., and Pospisil, M. Fuel properties of hydroprocessed rapeseed oil. Fuel 89 (2010): 611–615.

Simacek, P., Kubicka, D., Sebor, G., and Pospisil, M. Hydroprocessed rapeseed oil as a source of hydrocarbon-based biodiesel. Fuel 88 (2009): 456–460.

Simakova, I., Simakova, O., Arvela, P.M., Simakov, A., Estrada, M., and Murzin, D.Y. Deoxygenation of palmitic and stearic acid over supported Pd catalysts: Effect of metal dispersion. Applied Catalysis A: General 355 (2009): 100–108.

Smejkal, Q. Smejkalova, L. and Kubicka, D. Thermodynamic balance in reaction system of total vegetable oil hydrogenation. Chemical Engineering Journal 146 (2009): 155–160.

Standard Test Method for Boiling Range Distribution of Petroleum Chromatography. Designation: D 2887-01. American Society for Testing and Materials.

Sundaramurthy, V., Dalai, A.K., and Adjaye, J. Comparison of P-containing γ-Al_2O_3 supported Ni-Mo bimetallic carbide, nitride and sulfide catalysts for HDN and HDS of gas oils derived from Athabasca bitumen. Applied Catalyst A: General 311 (2006): 155.

Sundaramurthy, V., Dalai, A.K., and Adjaye, J. Effect of phosphorus addition on the hydrotreating activity of NiMo/Al_2O_3 carbide catalyst. Catalysis Today 125 (2007): 239-247.

Sundaramurthy, V., Dalai, A.K., and Adjaye, J. Tetraalklthiomolybdates-derived Co(Ni)Mo/γ-Al_2O_3 sulfide catalysts for gas oil hydrotreating. Journal of Molecular Catalysis A: Chemical. 294 (2008): 20-26.

Supple, B., Howard-Hildige, R., Gonzalez-Gomez, E., and Leahy, J.J. The Effect of Steam Treating Waste Cooking Oil on the Yield of Methyl Ester. Journal of the American oil Chemists' Society 79 (2002): 175-178.

Tailleur, R. G. Diesel upgrading into a low emissions fuel. Fuel Processing Technology 87 (2006): 759–767.

Tomasevic, A.V., and Siler-Marinkovic, S.S. Methanolysis of used frying oil. Fuel Process Technology 81 (2003): 1-6.

Villalanti, D.C., Raia, J.C., and Maynard, J.B. High-temperature simulated distillation applications in petroleum characterization. Encyclopedia Analytical Chemistry R.A. Meyers (Ed.) pp. 6726-6741@John Wiley&Sons Ltd, Chicherter, 2000.

Walendziewski, J., Stolarski, M., Luzny, R., and Klimek, B. Hydroprocesssing of light gas oil-rape oil mixtures. Fuel Processing Technology 90 (2009): 686–691.

Wei, Z., Xin, Q., Grange, P., and Delmon, B. TPD and TPR studies of molybdenum Nitride. Journal of Catalysis 168 (1997): 176.

Williams, P.T., Bartle, K.D., and Andrews, G.E. The relation between polycyclic aromatic compounds in diesel fuels and exhaust particulates. Fuel 65 (1986): 1150-1158.

Yang, X., and Edison, N.J. Stabilized flash calcined gibbsite as a catalyst support. United States: Patent Application Publication 2007.

Yanik, P.J., O' Donnell, T.H., Macko, S.A., Qian, Y., and Kennicutt, M.C. The isotopic compositions of selected crude oil PAHs during biodegradation. Organic Geochemistry 34 (2003): 291-304.

Young, R.S. Cobalt: Its Chemistry, Metallurgy, and Uses. New York: Reinhold Publishing Corporation. 1960.

Zepeda, T.A. Hydrodesulfurization of dibenzothiophene over CoMo/HMS and CoMo/Ti-HMS catalysts. Catalysis Communications 7 (2006): 33–41.

Zielinski, J. Morphology of nickel/alumina catalysts. Journal of Catalysis 76 (1982): 157.

APPENDICES

APPENDIX A

CALCULATION FOR CATALYST PREPARATION

Preparation of 2.45Ni9.4Mo/γ-Al_2O_3 is shown as follows:

Calculation for the preparation of Nickel and Molybdenum loading catalyst for 2.45Ni9.4Mo

Example calculation for the preparation of 2.45Ni9.4Mo/γ-Al_2O_3

Based on 100 g of catalyst used, the composition of the catalyst will be as follows:

Nickel	=	2.45 g		
Molybdenum	=	9.4 g		
Al_2O_3	=	100 - (2.45 + 9.4)	=	88.15 g

For 2 g of Al_2O_3

Weight of catalyst	=	2 × (100/88.15)	=	2.2689 g
Nickel required	=	2.2689 × (2.45/100)	=	0.0559 g

Nickel 0.0554 g was prepared from $Ni(NO_3)_2{\cdot}6H_2O$ and molecular weight of Ni is 58.6934 g/mol

$$Ni(NO_3)_2{\cdot}6H_2O \text{ required} = \frac{\text{MW of } Ni(NO3)2{\cdot}6H2O \times \text{Nickel required}}{\text{MW of Nickel}}$$

$$= (290.79/58.6934) \times 0.0559 = 0.2932 \text{ g}$$

$$\text{Molybdenum required} = 2.2689 \times (9.4/100) = 0.2133 \text{ g}$$

Molybdenum 0.2133 g was prepared from $(NH_4)_6Mo_7O_{24}{\cdot}4H_2O$ and molecular weight of Mo is 95.94 g/mol

$$(NH_4)_6Mo_7O_{24}{\cdot}4H_2O \text{ required} = \frac{\text{MW of } (NH_4)_6Mo_7O_{24}{\cdot}4H_2O) \times \text{Molybdenum required}}{\text{MW of Molybdenum}}$$

$$= (1234.58/95.94 \times 7) \times 0.2133 = 0.3924 \text{ g}$$

Preparation of 2.54Co9.71Mo/γ-Al_2O_3 is shown as follows:

Calculation for the preparation of Cobalt and Molybdenum loading catalyst for 2.54Co9.71Mo

Example calculation for the preparation of 2.54Co9.71Mo/γ-Al_2O_3

Based on 100 g of catalyst used, the composition of the catalyst will be as follows:

Cobalt	=	2.54 g		
Molybdenum	=	9.71 g		
Al_2O_3	=	100 - (2.54 + 9.71)	=	87.75 g

For 2 g of Al_2O_3

Weight of catalyst	=	2 × (100/87.75)	=	2.2792 g
Cobalt required	=	2.2689 × (2.54/100)	=	0.0579 g

Cobalt 0.0579 g was prepared from $Co(NO_3)_2{\cdot}6H_2O$ and molecular weight of Co is 58.93 g/mol

$$Co(NO_3)_2{\cdot}6H_2O \text{ required} = \frac{\text{MW of } Co(NO_3)_2{\cdot}6H_2O \times \text{Cobalt required}}{\text{MW of Cobalt}}$$

$$= (291.03/58.93) \times 0.0579 = 0.2859 \text{ g}$$

Molybdenum required= 2.279 × (9.71/100) = 0.2213 g

Molybdenum 0.2213 g was prepared from $(NH_4)_6Mo_7O_{24}{\cdot}4H_2O$ and molecular weight of Mo is 95.94 g/mol

$$(NH_4)_6Mo_7O_{24}{\cdot}4H_2O \text{ required} = \frac{\text{MW of } (NH_4)_6Mo_7O_{24}{\cdot}4H_2O) \times \text{Molybdenum required}}{\text{MW of Molybdenum}}$$

$$= (1234.58/95.94 \times 7) \times 0.2213 = 0.4071 \text{ g}$$

APPENDIX B

CALCULATION FOR TOTAL CO-CHEMISORPTION

Calculation of the total CO chemisorption of the catalyst, a stoischiometry of CO/Co = 1, is assumed. The calculation procedure is as follows:

Let the weight of catalyst used	=	W	g
Integral area of CO peak (i) after adsorption	=	A_i	unit
Integral area of 30 µl of standard CO peak	=	B	unit
Total amounts of CO adsorbed on catalyst	=	$\sum(B-A_i)$	unit
Volume of CO adsorbed on catalyst	=	$30\times[\sum(B-A_i)/B]$	µl
Volume of 1 mole of CO at 30 °C	=	24.86×10^{6}	µl
Mole of CO adsorbed on catalyst	=	$[\sum(B-A_i)/B]\times[30/24.86]$	µmole
Total CO chemisorption	=	$[\sum(B-A_i)/B]\times[30/24.86]\times[1/W]$	$\mu mole/g_{catalyst}$
	=	N	$\mu mole/g_{catalyst}$
Active site	=	$N\times6.02$	Moleculeper gram ($*10^{-23}$)

APPENDIX C

CALIBRATION CURVES OF GAS CHROMATOGRAPHY WITH THERMAL CONDUCTIVITY DETECTOR

This appendix showed the calibration curves for calculation of composition of gaseous products in hydroprocessing of WCPO. The reactant is hydrogen and the main product is carbon monoxide, carbon dioxide, methane and propane.

The thermal conductivity detector, gas chromatography Shimadzu model 8A was used to analyze the concentration of carbon monoxide and methane by using Molecular sieve 5A column.

The thermal conductivity detector (TCD), gas chromatography Shimadzu model 8A was used to analyze the concentration of carbon dioxide and propane by using porapack Q column. Conditions uses in both column are illustrated in Table D.1.

Mass of reagent in y-axis and area reported by gas chromatography in x-axis are exhibited in the curves. The calibration curves of carbon monoxide, carbon dioxide, methane and propane are illustrated in the following figures.

Table C.1 Conditions use in Shimadzu modal GC-8A by using Molecular sieve 5A and Porapack Q column.

Parameters	Condition	
	Molecular sieve 5A	Porapack Q
Width	5	5
Slope	50	50
Drift	0	0
Min. area	10	10
T.DBL	0	0
Stop time	15	20
Atten	0	0
Speed	2	2
Method	41	41
Format	1	1
SPL.WT	100	100
IS.WT	1	1

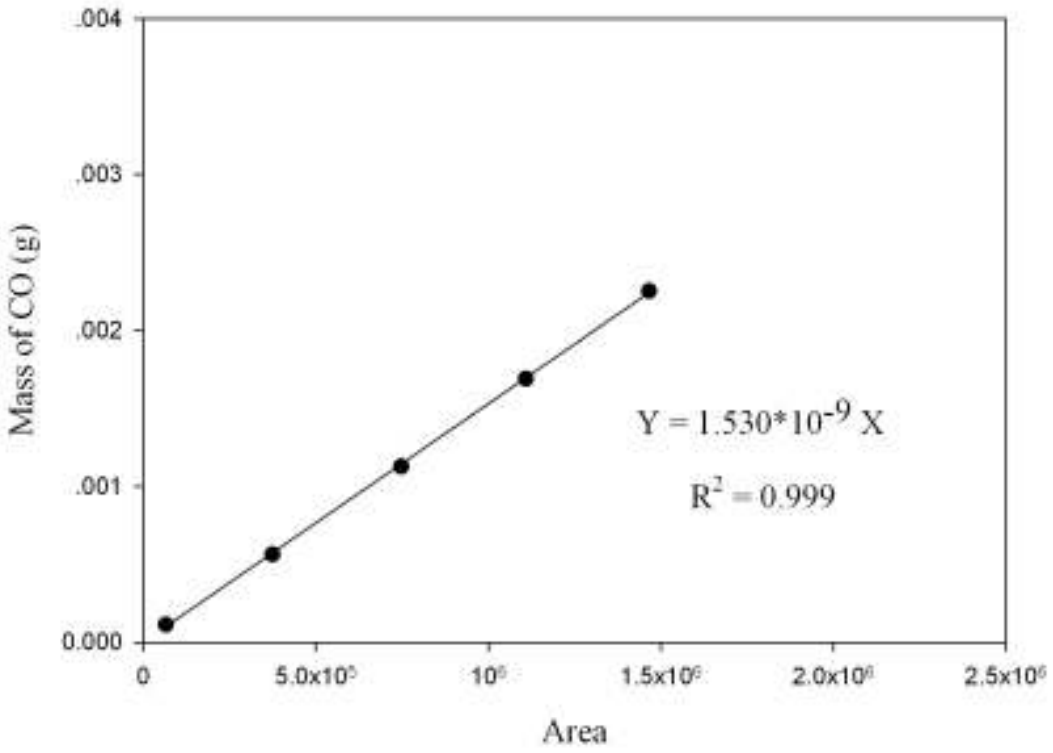

Figure C.1 The calibration curve of carbon monoxide.

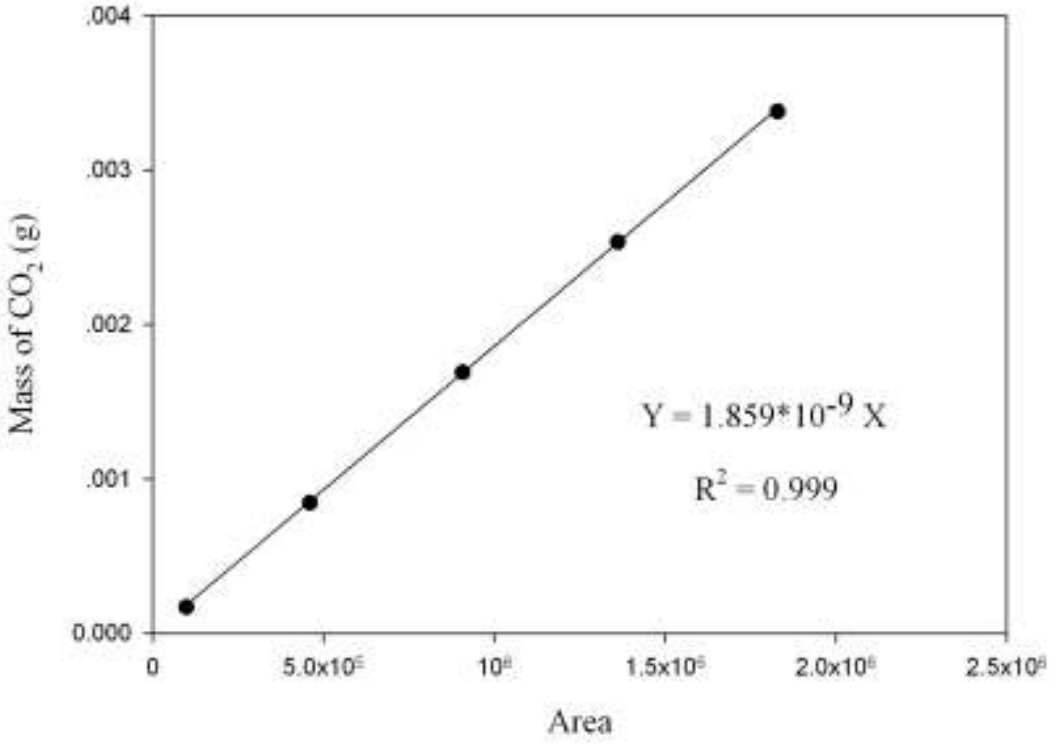

Figure C.2 The calibration curve of carbon dioxide.

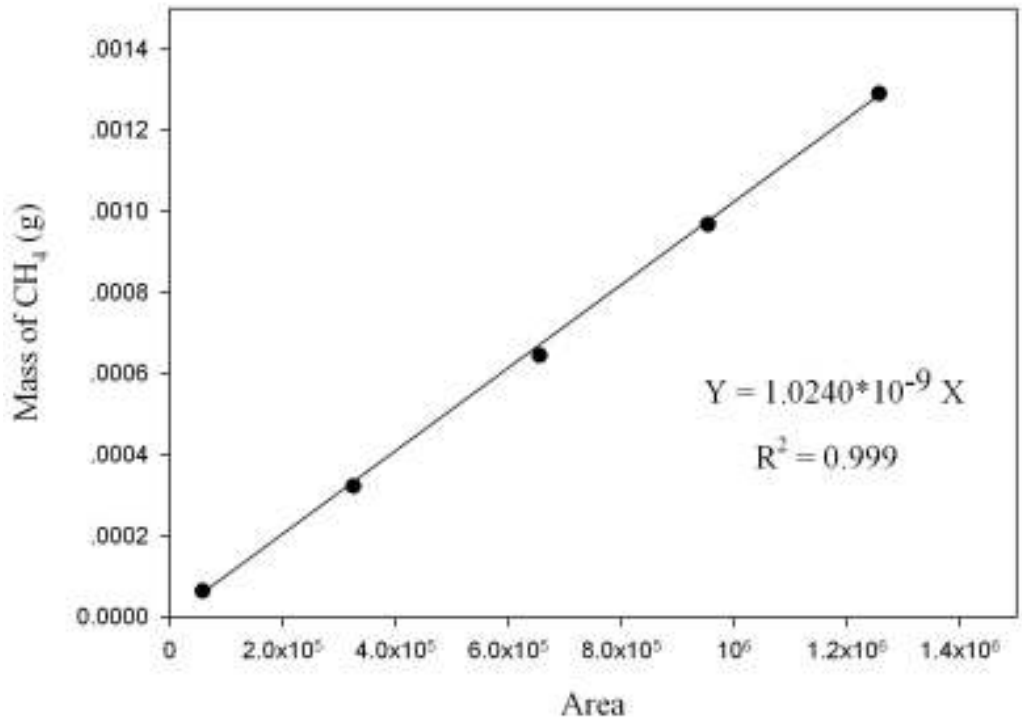

Figure C.3 The calibration curve of methane.

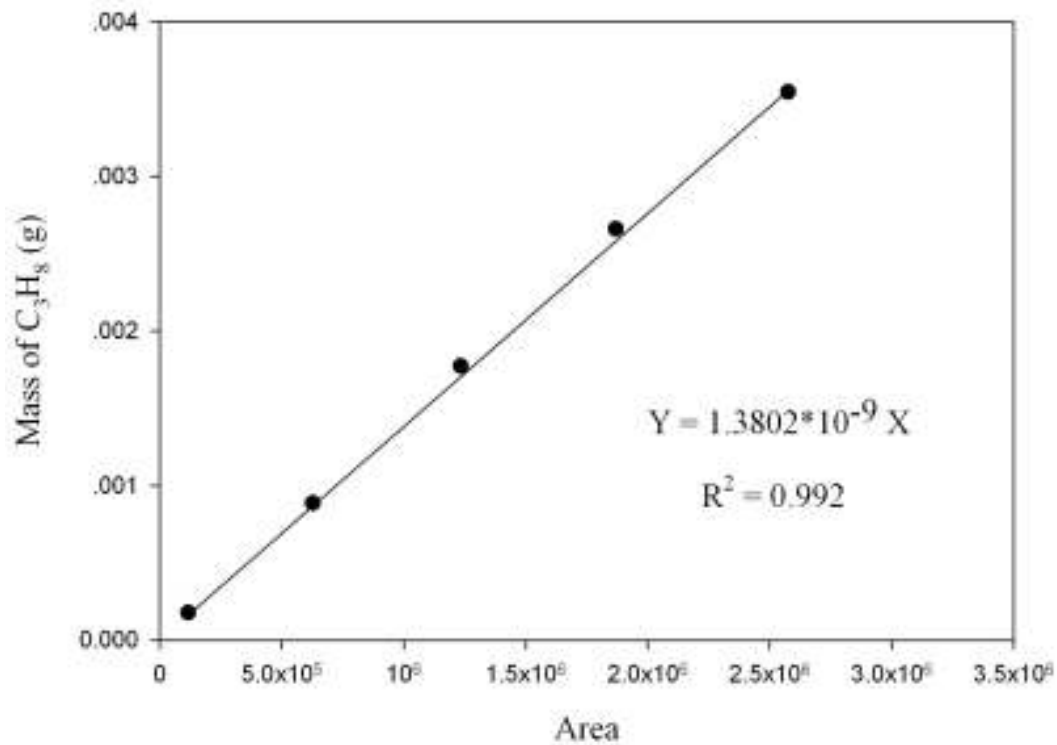

Figure C.4 The calibration curve of propane.

APPENDIX D

PROGRAM SIMULATED DISTILLATION OF GAS CHROMATOGRAPHY WITH FLAME IONIZATION DETECTOR

This appendix showed the program Simulated distillation (SimDist) for calculation of composition of hydrocarbon components in hydroprocessing reaction.

A flame ionization detector (FID) is used for detection and measurement of the hydrocarbon analytes. The result of SimDist analysis provides a quantitative percent mass yield as a function of boiling point of the hydrocarbon components of the sample. The chromatographic elution times of the hydrocarbons are calibrated to the atmospheric equivalent boiling point (AEBP) of the paraffins reference material. The SimDist method ASTM (American Society for Testing and Materials) D2887 covers the boiling range 55–538°C (100–1000°F) which covers the n-alkanes (n-paraffins) of chain length about C_5–C_{44}.

In this study, we used simulated distillation to analyze the temperature range of products following by ASTM-2887-D86 procedure. It was found, at temperature range of 250-380°C is a suitable for diesel range (n-C_{15}-n-C_{18}). Table D.1 – Table D.3 and Figure D.1 – Figure D.2 are shown conditions use in gas chromatography with flame ionization detector, chromatogram of calibration mixture reference and data analysis.

Table D.1 Conditions use in gas chromatography with flame ionization detector.

Parameters	Condition
Width	5 sec
Slope	2,000 uV/min
Drift	0 uV/min
T.DBL	1,000 min
Min.Area/Hight	10,000 counts
Quantitation	
Quantitative Method	Corrected Area Normalization
	External Standard
Calculated by	Area
# of Calib. Levels	1
Curve Fit Type	Liner
Unit	%(w/w)
X Axis of Calib. Curve	Conc.
Identification	
Window	5 %
Default Band Time	0.01 min
Identification Method	Absolute Rt
Peack Select	Closest Peak
Grouping	Not Used
Correction of RT	No Change

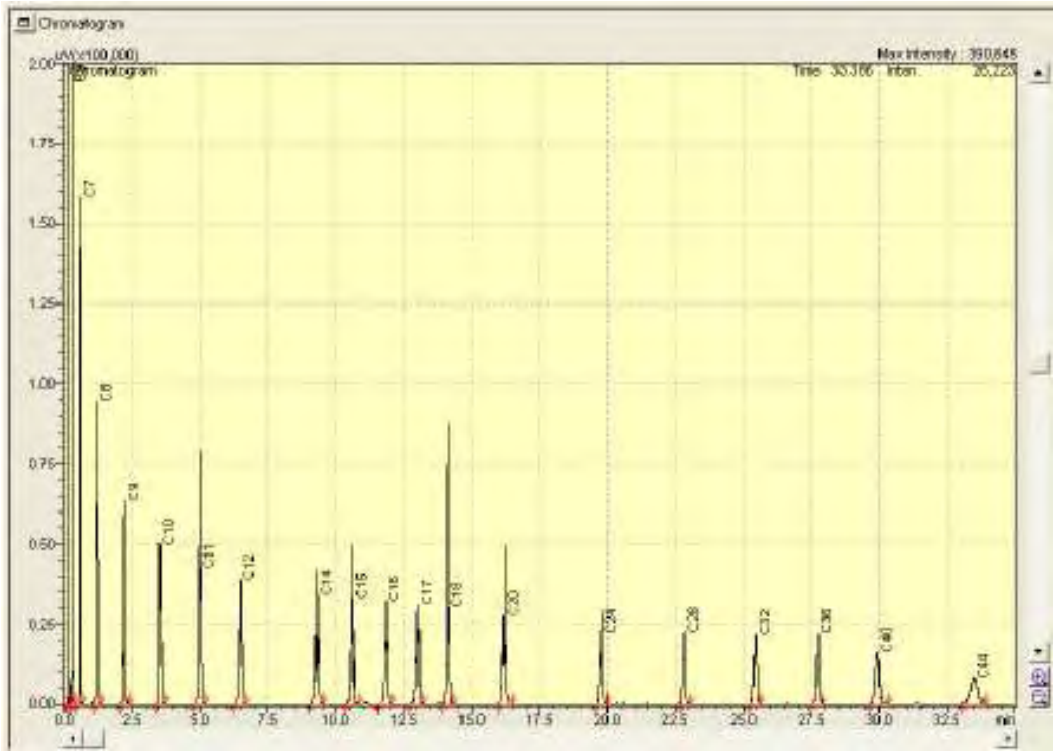

Figure D.1 Chromatogram of calibration mixture reference.

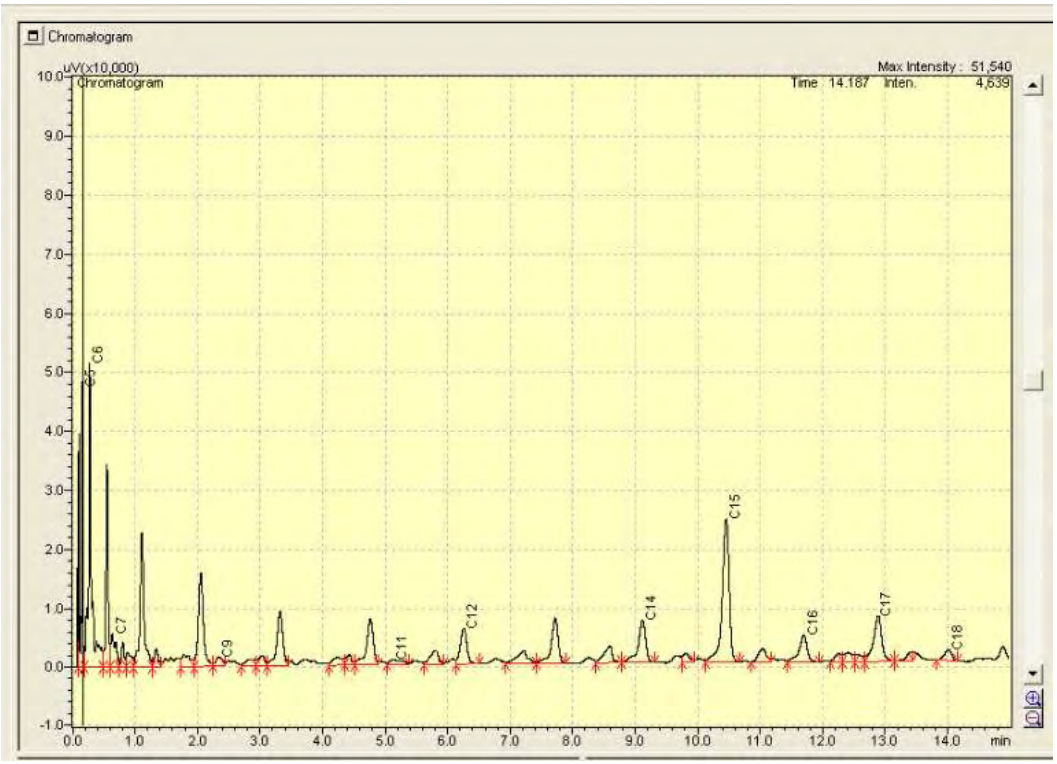

Figure D.2 Chromatogram of data analysis.

Table D.2 Results from chromatogram of calibration mixture reference.

Peak	Component	Rt (min)	Area	Conc.	Conc. (100%)	Units
1	C_5H_{12}	0.163	316798.1	0.9995	5.00033	%(w/w)
2	C_6H_{14}	0.3	345611.2	0.9995	5.00033	%(w/w)
3	C_7H_{16}	0.61	330865.1	0.9995	5.00033	%(w/w)
4	C_8H_{18}	1.22	63212.1	0.9995	5.00033	%(w/w)
5	C_9H_{20}	2.23	300457.4	0.9995	5.00033	%(w/w)
6	$C_{10}H_{22}$	3.55	291602.6	0.9995	5.00033	%(w/w)
7	$C_{11}H_{24}$	5.01	273183.5	0.9995	5.00033	%(w/w)
8	$C_{12}H_{26}$	6.5	262581.8	0.9995	5.00033	%(w/w)
9	$C_{14}H_{30}$	9.32	239842.9	0.9995	5.00033	%(w/w)
10	$C_{15}H_{32}$	10.62	233431.4	0.9995	5.00033	%(w/w)
11	$C_{16}H_{34}$	11.85	225150.5	0.9995	5.00033	%(w/w)
12	$C_{17}H_{36}$	13.02	216383.8	0.9995	5.00033	%(w/w)
13	$C_{18}H_{38}$	14.13	205113.8	0.9995	5.00033	%(w/w)
14	$C_{20}H_{42}$	16.19	187065.4	0.9995	5.00033	%(w/w)
15	$C_{24}H_{50}$	19.76	160614.5	0.9995	5.00033	%(w/w)
16	$C_{28}H_{58}$	22.83	160561.9	0.9995	5.00033	%(w/w)
17	$C_{32}H_{66}$	25.45	157273.7	0.9991	4.99832	%(w/w)
18	$C_{36}H_{74}$	27.76	153387.5	0.9995	5.00033	%(w/w)
19	$C_{40}H_{82}$	29.94	158740	0.9986	4.99582	%(w/w)
20	$C_{44}H_{90}$	33.52	146186.8	0.9995	5.00033	%(w/w)

Table D.3 Distillation GC calibration initial setting.

ID	Component	Rt (min)	Boiling point (˚C)
1	C_5H_{12}	0.163	36
2	C_6H_{14}	0.3	69
3	C_7H_{16}	0.61	98
4	C_8H_{18}	1.22	126
5	C_9H_{20}	2.23	151
6	$C_{10}H_{22}$	3.55	174
7	$C_{11}H_{24}$	5.01	196
8	$C_{12}H_{26}$	6.5	216
9	$C_{14}H_{30}$	9.32	254
10	$C_{15}H_{32}$	10.62	271
11	$C_{16}H_{34}$	11.85	287
12	$C_{17}H_{36}$	13.02	302
13	$C_{18}H_{38}$	14.13	316
14	$C_{20}H_{42}$	16.19	344
15	$C_{24}H_{50}$	19.76	391
16	$C_{28}H_{58}$	22.83	431
17	$C_{32}H_{66}$	25.45	466
18	$C_{36}H_{74}$	27.76	496
19	$C_{40}H_{82}$	29.94	522
20	$C_{44}H_{90}$	33.52	545

Data analysis can be converted from GC postrun to program GC distillation data calibration by batch table for calculated distillation data, distillation curve, distillation data in specified temperature range and ASTM D-86. Result analysis form program simulated distillation are shown in Figure D.3 – Figure D.6 respectively.

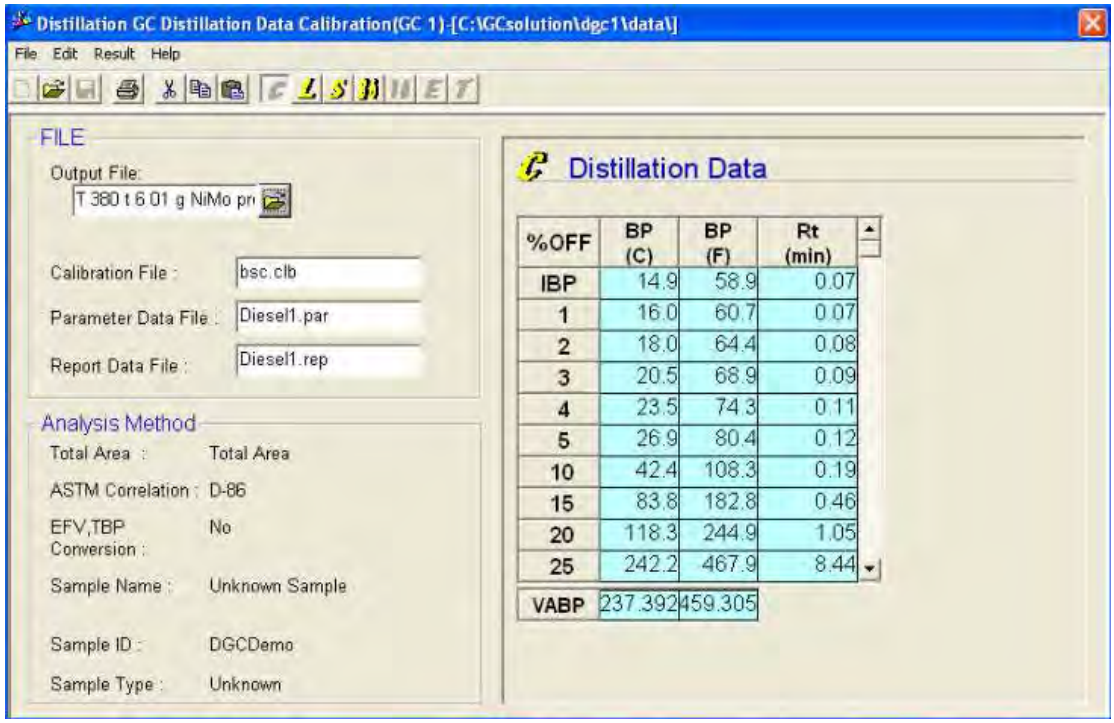

Figure D.3 Calculated distillation data.

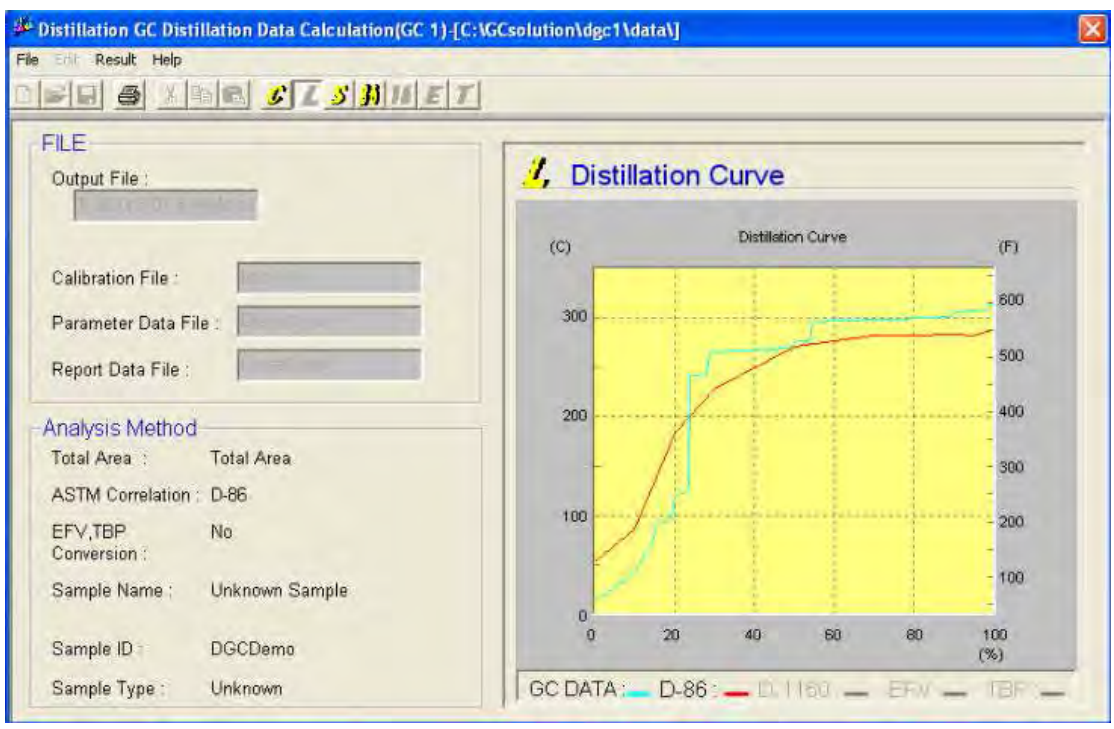

Figure D.4 Distillation curve.

Distillation GC Distillation Data Calculation(GC 1)-[C:\GCsolution\dgc1\data\]

File Edit Result Help

FILE

Output File:

Calibration File :

Parameter Data File :

Report Data File :

Analysis Method

Total Area : Total Area

ASTM Correlation : D-86

EFV,TBP Conversion : No

Sample Name : Unknown Sample

Sample ID : DGCDemo

Sample Type : Unknown

Distillation Data in Specified Temperature Range

Number of Specified Temperature Range : 5

Range	IBP (C)	FBP (C)	%
1	40	65	3.8
2	65	150	10.3
3	150	250	4.6
4	250	380	71.8
5	380	520	0.0
6			
7			
8			
9			
10			

Figure D.5 Distillation data in specified temperature range.

Distillation GC Distillation Data Calculation(GC 1)-[C:\GCsolution\dgc1\data\]

File Edit Result Help

FILE

Output File :

Calibration File :

Parameter Data File :

Report Data File :

Analysis Method

Total Area : Total Area

ASTM Correlation : D-86

EFV,TBP Conversion : No

Sample Name : Unknown Sample

Sample ID : DGCDemo

Sample Type : Unknown

ASTM D-86

%OFF	BP (C)	BP (F)
IBP	54.5	130.2
10	85.5	185.9
20	183.6	362.5
30	228.8	443.8
50	271.2	520.1
70	281.6	538.9
80	282.2	540.0
90	283.3	541.9
95	-	-
FBP	287.3	549.1
VABP(F)	446.132	

Figure D.6 ASTM D-86.

VITA

Mr. Chaiyod Kongwattanakul was born on 1st September 1986, in Ratchaburi, Thailand. He studied high school from Suankularb wittayalai. He received his Bachelor degree of Chemical Engineering from Kasetsart University, Thailand in March 2009. Since May 27, 2009, he has been studying for his Master degree of Engineering from the department of Chemical Engineering, Chulalongkorn University.

List of plublication:

Chaiyod Kongwattanakul, Worapon Kiatkittipong, and Suttichai Assabumrungrat, "HYDROPROCESSING OF WASTE COOKING PALM OIL OVER Pd/C CATALYST', Proceedings of Pure and Applied Chemistry International Conference 2011, Bangkok, Thailand, Jan. 5-7, 2011.